

**Development and characterisation of
silsesquioxane-polycaprolactone
nanocomposite scaffolds for use in small
intestinal tissue engineering**

A thesis submitted for the degree of Doctor of Medicine (M.D)

at the

University College London

by

Ashish Gupta MBBS, MRCS

2010

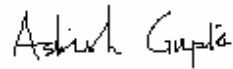
**Supervised by Professor A Seifalian
& Professor M Winslet**

Centre for Nanotechnology & Regenerative Medicine/ Division of Surgery and Interventional
Science/ University College London

Declaration

I, Ashish Gupta confirm that the work presented in this thesis is my own.
Where information has been derived from other sources, I confirm that this
has been indicated in the thesis.

Candidate's signature

Handwritten signature of Ashish Gupta in black ink.

Date

21st December 2009

Abstract

Tissue engineering of small intestine aims to provide a cure to patients suffering from short bowel syndrome by increasing the absorptive surface through neo-intestinal mucosal tissue. So far, preliminary *in vivo* attempts by a research team in the USA have shown regeneration of neo-intestinal mucosa in rat models with some success; however experiments in this complex field of tissue engineering still remain in infancy and far from clinical use. A fresh perspective is required to further investigate all the three aspects of tissue engineering, namely, the polymer scaffold, the cell supply, and the biomolecules. The concept of nanocomposite polymer is rapidly emerging and has generated a lot of enthusiasm in tissue engineering due to their high surface to volume ratio and hence enhanced performance. This work was focussed to develop and characterise scaffolds for small intestinal tissue engineering using a new nanocomposite polymer of polycaprolactone and silsesquioxane, developed in our laboratory. An *in vitro* study was also performed to test the scaffolds for cell viability and proliferation using rat's intestinal epithelial cells. Our results have shown that biodegradable polycaprolactone-silsesquioxane nanocomposite can be fabricated in desired scaffold morphology using simple techniques like particulate leaching, and that it supports intestinal cell growth and proliferation. Future studies incorporating these scaffolds for *in vivo* use in animal models need to be carried out in order to investigate further about their ability to withstand

natural forces within the abdomen, and whether they support cell growth based on principles of cell migration, before a more definitive and continuous cell supply is available in form of stem cells cued specifically to intestinal lineage.

Table of Contents

| | |
|--|-----------|
| TITLE PAGE..... | 1 |
| SIGNED DECLARATION..... | 2 |
| ABSTRACT..... | 3 |
| TABLE OF CONTENTS..... | 5 |
| DEDICATION..... | 13 |
| ACKNOWLEDGEMENTS..... | 14 |
| HYPOTHESIS..... | 16 |
| ABBREVIATIONS..... | 17 |
| CHAPTER 1: INTRODUCTION..... | 19 |
| 1.1 Clinical Problem..... | 20 |
| 1.2 Current solutions to the problem of Short Bowel Syndrome..... | 21 |
| 1.2.1 Parenteral Nutrition..... | 21 |
| 1.2.2 Sequential intestinal lengthening procedures for Short Bowel Syndrome..... | 22 |
| 1.2.3 Small Bowel Transplantation..... | 24 |
| 1.3 Problems with current solutions to Short Bowel Syndrome..... | 25 |
| 1.4 The need for small intestine tissue engineering..... | 26 |
| 1.5 Aim of this study..... | 28 |
| 1.6 Layout of thesis..... | 29 |

| | |
|---|-----------|
| CHAPTER 2: CRITICAL REVIEW OF LITERATURE – CELL SOURCE..... | 31 |
| 2.1 Introduction..... | 32 |
| 2.2 Search Methodology..... | 34 |
| 2.3 Tissue engineering of small intestine..... | 34 |
| 2.4 Cell source..... | 35 |
| 2.4.1 From Bone Marrow - Hematopoietic stem cells..... | 35 |
| 2.4.2 From peripheral blood..... | 39 |
| 2.4.3 Gastrointestinal stem cells (tissue specific cells)..... | 39 |
| 2.4.4 Enterocyte Isolation..... | 43 |
| 2.4.5 Intestinal Epithelial Organoid Units..... | 44 |
| 2.4.6 Organoid unit-polymer construct implantation..... | 45 |
| 2.5 Extracellular Matrix (ECM)..... | 48 |
| 2.6 Role of trophic factors after massive bowel resection..... | 54 |
| 2.7 Discussion..... | 55 |
| CHAPTER 3: CRITICAL REVIEW OF LITERATURE - SCAFFOLDS..... | 62 |
| 3.1 Natural scaffold..... | 64 |
| 3.1.1 Small Intestinal Submucosa (SIS)..... | 64 |
| 3.1.2 Collagen Scaffold..... | 66 |
| 3.2 Synthetic scaffold..... | 67 |
| 3.2.1 Scaffold fabrication..... | 68 |
| 3.2.2 Nanocomposites..... | 69 |
| 3.3 Scaffold Properties..... | 71 |
| 3.3.1 Biodegradable vs Nonbiodegradable..... | 72 |
| 3.3.2 Hydrophobic versus Hydrophilic and Surface Modification..... | 76 |
| 3.3.3 Biocompatibility..... | 77 |
| 3.3.4 Porosity..... | 78 |
| 3.3.5 Mechanical Strength..... | 79 |

| | |
|---|------------|
| 3.4 Fabrication Methods..... | 80 |
| 3.4.1 Particulate Leaching..... | 80 |
| 3.4.2 Electrospinning..... | 83 |
| 3.4.3 Compression Molding..... | 84 |
| 3.4.4 Gas Foaming..... | 84 |
| 3.4.5 Fibre meshes with fibre bonding..... | 85 |
| 3.4.6 Freeze Drying..... | 86 |
| 3.4.7 Phase separation..... | 86 |
| 3.4.8 Solid Free-Form fabrication (SFF)/ Rapid Prototyping (RP)..... | 87 |
| 3.5 Surface modification of scaffolds..... | 89 |
| 3.6 Discussion..... | 92 |
| CHAPTER 4: MATERIALS AND METHODS..... | 98 |
| 4.1 Introduction..... | 99 |
| 4.2 Synthesis of POSS-PCL nanocomposite..... | 101 |
| 4.3 Characterisation of polymer solutions..... | 101 |
| 4.4 Preparation of scaffolds using particulate leaching/ solvent..... | 102 |
| 4.5 Extrusion-coagulation combined with solvent casting/ particulate leaching..... | 103 |
| 4.6 Characterisation of Scaffolds..... | 104 |
| 4.6.1 Porosity of Scaffolds..... | 105 |
| 4.6.2 Scanning Electron Microscopy (SEM)..... | 106 |
| 4.6.3 Micro-CT..... | 106 |
| 4.6.4 Mechanical Properties..... | 108 |
| 4.6.5. Fourier transform infrared spectroscopy (FTIR)..... | 108 |
| 4.7 Electrohydrodynamic print-patterning..... | 109 |
| 4.8 Cell Work..... | 113 |
| 4.8.1 Optimising seeding density for IEC-6 cells on tissue culture plastic without scaffolds..... | 114 |
| 4.8.2 Optimising seeding time for IEC-6 cells on tissue culture plastic without | |

| | |
|--|-----|
| scaffolds..... | 114 |
| 4.8.3 Scaffold preparation for cell seeding..... | 115 |
| 4.8.4 Trial seeding of scaffold samples with lower density of 0.25×10^5 cells..... | 115 |
| 4.8.5 Trial seeding of scaffold samples with higher density of 0.25×10^6 cells..... | 115 |
| 4.8.6 Higher seeding density experiment on scaffolds..... | 116 |
| 4.8.7 Assessment of Initial Cell Damage by LDH analysis..... | 117 |
| 4.8.8 Assessment of Cell Growth and Metabolism by Alamar blue™ assay..... | 118 |
| 4.8.9 Statistical analysis..... | 119 |

CHAPTER 5: DEVELOPMENT AND CHARACTERISATION OF HIGHLY POROUS SCAFFOLDS BY SOLVENT CASTING AND PARTICULATE-LEACHING.....120

| | |
|--|------------|
| 5.1 Experimental details..... | 121 |
| 5.2 Characterisation of the scaffolds..... | 123 |
| 5.3 Results..... | 123 |
| 5.3.1 Properties of polymer..... | 123 |
| 5.3.2 Porosity of scaffolds..... | 124 |
| 5.3.3. Scanning Electron Microscopy (SEM)..... | 125 |
| 5.3.4 Extrusion-Coagulation combined with salt leaching..... | 130 |
| 5.3.5 Micro CT..... | 132 |
| 5.3.6 Stress-Strain values..... | 133 |
| 5.3.7 Fourier transform infrared spectroscopy (FTIR)..... | 136 |
| 5.4 Discussion..... | 137 |

CHAPTER 6: ELECTROHYDRODYNAMIC ATOMISATION – NOVEL USE FOR PRINT PATTERNING OF BIOPOLYMER SCAFFOLDS.....143

| | |
|--------------------------------------|------------|
| 6.1 Introduction..... | 143 |
| 6.2 Experimental Details..... | 145 |
| 6.3 Results..... | 146 |
| 6.3.1 Scaffold characteristics..... | 147 |
| 6.4 Discussion..... | 150 |

| | |
|--|------------|
| 6.5 Conclusions..... | 153 |
| CHAPTER 7: IN VITRO SMALL INTESTINAL EPITHELIAL CELL GROWTH ON A NANOCOMPOSITE POLYCAPROLACTONE SCAFFOLD..... | 154 |
| 7.1 Introduction..... | 155 |
| 7.2 Experimental details..... | 155 |
| 7.3 Results..... | 156 |
| 7.3.1 Optimising seeding density on tissue culture plastic..... | 156 |
| 7.3.2 Optimising seeding time on tissue culture plastic..... | 158 |
| 7.3.3 Trial Seeding of graft segments with lower cell density..... | 159 |
| 7.3.4 Trial seeding of scaffolds with higher cell density..... | 160 |
| 7.3.5 Higher cell density seeding of scaffolds washed with stringent washing regime... | 162 |
| 7.3.6 Assessment of Initial Cell Damage by LDH analysis..... | 163 |
| 7.1.7 Assessment of Cell Seeding by Scanning Electron Microscopy..... | 165 |
| 7.4 Discussion..... | 167 |
| CHAPTER 8: DISCUSSION..... | 172 |
| CONCLUSION AND FUTURE RECOMMENDATIONS..... | 188 |
| REFERENCES..... | 190 |
| PUBLICATIONS..... | 205 |

List of Figures

| | |
|--|-----|
| Figure 1.1: Schematic diagram of the intestinal lengthening device..... | 23 |
| Figure 2.1: Schematic diagram of overview of small intestinal tissue engineering..... | 35 |
| Figure 2.2: Intestinal epithelial cell generation..... | 40 |
| Figure 2.3: Tissue engineered intestine..... | 47 |
| Figure 3.1: Schematic drawings of the operative procedure using collagen sponge..... | 67 |
| Figure 3.2: Optimal relationship between matrix formation and scaffold degradation..... | 73 |
| Figure 4.1: Molecular structure of trans-cyclohexane diol isobutyl-POSS..... | 100 |
| Figure 4.2: Schematic illustration of the electrohydrodynamic process..... | 109 |
| Figure 4.3: Schematic representation of electrohydrodynamic printing..... | 111 |
| Figure 4.4: An overview of cell culture experiments..... | 113 |
| Figure 5.1: Porous scaffold prepared with solvent casting/ particulate leaching..... | 122 |
| Figure 5.2: SEM of Sample 1; magnification x 10..... | 126 |
| Figure 5.3: SEM of Sample 1; magnification x 20..... | 126 |
| Figure 5.4: SEM of cross section of sample 1..... | 127 |
| Figure 5.5: SEM of sample 1; magnification x 80..... | 127 |
| Figure 5.6: SEM of sample 2 and 4; magnification x 80..... | 128 |
| Figure 5.7: SEM of sample 3; magnification x 160..... | 129 |
| Figure 5.8: SEM of sample 5 (non-porous)..... | 130 |
| Figure 5.9: SEM of tubular scaffold (sample with NaCl)..... | 131 |
| Figure 5.10: SEM of tubular scaffold (sample with NaHCO ₃)..... | 132 |
| Figure 5.11: Micro CT images of sample 1..... | 133 |
| Figure 5.12: Stress-strain graphs | 134 |
| Figure 5.13: FTIR..... | 136 |
| Figure 6.1: Stable electrically forced microthreading of the biopolymer..... | 147 |

| | |
|--|-----|
| Figure 6.2: Optical micrographs showing discontinuous printing..... | 148 |
| Figure 6.3: Optical micrographs showing continuous printing..... | 149 |
| Figure 6.4: Scanning electron micrograph of a single layer of scaffold printed from polymer, showing coiling..... | 149 |
| Figure 6.5: Scanning electron micrograph of a scaffold printed from polymer and subsequently peeled off the glass substrate..... | 150 |
| Figure 7.1: Optimal seeding density..... | 157 |
| Figure 7.2: Optimal seeding time..... | 159 |
| Figure 7.3: Trial seeding of the scaffolds with 0.25×10^5 cells per ml..... | 160 |
| Figure 7.4: Trial seeding of the scaffolds with 0.25×10^6 cells per ml | 161 |
| Figure 7.5: Alamar blue assay on IEC seeded POSS-PCL samples over 21 days..... | 163 |
| Figure 7.6: LDH assay test | 164 |
| Figure 7.7: SEM of IEC cells seeded on nanocomposite at day 21..... | 166 |
| Figure 7.8: SEM showing cell in-growth..... | 167 |

List of Tables

| | |
|---|-----|
| Table 2.1: Review of published studies on small bowel tissue engineering..... | 51 |
| Table 3.1: Main scaffold fabrication techniques..... | 81 |
| Table 5.1: Scaffold samples with different salt concentrations and size..... | 122 |
| Table 5.2: Physical properties of the POSS-PCL polymer used in this study..... | 124 |
| Table 5.3: Porosity of POSS-PCL scaffolds using varying salt concentrations..... | 125 |
| Table 5.4: Stress strain values of scaffolds..... | 135 |
| Table 6.1: Properties of the nanocomposite polymer, DMAC and ethanol..... | 146 |

Dedication

I would like to dedicate this thesis to my parents who taught me the meaning of diligence and sincerity, for their unconditional love and support throughout my career progression.

Acknowledgements

I would sincerely like to thank Professor Alexander Seifalian, my research supervisor, for his enormous support and faith in me, without which this work would not have been possible. His clear vision in the evolving subject of tissue engineering and scientific knowledge base was always the main driving force to accomplish this project. He was always there to guide me as a father figure especially in difficult times.

I also thank Professor Marc Winslet, my clinical supervisor, who taught me the importance of research in clinical medicine, and was always there to support and boost my morale.

I would also like to thank Geoffrey Punshon, Dina Vara, Arnold Derbyshire and Ramesh Bala for their continuous support and guidance whilst in the lab for taking me through most of the procedures which as a clinician I would never have understood.

I also thank Professor Mohan Edirisinghe and his faculty in mechanical engineering department at the University College London, to help me carry out an experimental project using their expertise and machines in their lab.

Last but not least, I would like to take this opportunity to thank my wife

Angela and kids Parth and Dhruv for their immense patience, cooperation and love throughout the project.

Hypothesis

Polycaprolactone-Silsesquixane nanocomposites can be fabricated in scaffolds with desired pore morphology and the scaffolds should support intestinal cell growth and proliferation when tested *in vitro*.

Abbreviations

| | |
|------|---|
| AB | Alamar Blue |
| bFGF | Basic Fibroblast Growth Factor |
| BM | Basement Membrane |
| BM | Bone Marrow |
| CT | Computed Tomography |
| DMAC | Dimethylacetamide |
| DMEM | Dulbecco's Modified Eagle Medium |
| EC | Enterocytes |
| ECM | Extra Cellular Matrix |
| EGF | Epidermal Growth Factor |
| EN | Enteral Nutrition |
| FDM | Fused Deposition Modelling |
| FGF | Fibroblast Growth Factor |
| FTIR | Fourier Transform Infrared Spectroscopy |
| GF | Growth Factor |
| GLP | Glucagon Like Peptide |
| HBSS | Hank's balanced salt solution |
| HPN | Home Parenteral Nutrition |
| HSC | Haematopoietic Stem Cell |
| IAP | Intestinal Alkaline Phosphatase |
| IEC | Intestinal Epithelial Cell |
| LDH | Lactate Dehydrogenase |
| MAPC | Multipotent Adult Progenitor Cell |
| MDI | Methylene Diphenyl Isocyanate |
| MIP | Mercury Intrusion Porosimetry |
| MJS | Multiphase Jet Solidification |
| MSC | Mesenchymal Stem Cell |
| PB | Peripheral Blood |
| PBS | Phosphate Buffer Solution |
| PCL | Polycaprolactone |
| PCU | Poly Carbonate Urea |
| PEG | Poly Ethylene Glycol |

| | |
|-------|---|
| PEM | Precise Extrusion Manufacturing |
| PGA | Polyglycolic Acid |
| PLGA | Poly(D,L-lactic-co-glycolic acid) |
| PLLA | Poly-L-lactic Acid |
| PN | Parenteral Nutrition |
| POSS | Polyhedral Oligomeric Silsesquioxane |
| PSC | Pluripotent Stem Cell |
| PVA | Polyvinyl Alcohol |
| RP | Rapid Prototyping |
| SBR | Small Bowel Resection |
| SD | Standard Deviation |
| SEM | Scanning Electron Microscopy |
| SFF | Solid Freeform Fabrication |
| SiEP | Small intestinal epithelial progenitors |
| SIS | Small Intestinal Submucosa |
| SGLT1 | Sodium Glucose CoTransporter |
| SLA | Stereo Lithography Apparatus |
| SLS | Selective Laser Sintering |
| TCP | Tissue Culture Plastic |
| TESI | Tissue Engineered Small Intestine |
| TGF | Transforming Growth Factor |
| VEGF | Vascular Endothelial Growth Factor |

Chapter 1: Introduction

1.1 Clinical Problem

Short-bowel syndrome (SBS) has always posed a difficult clinical problem in children as well as adults. Short bowel syndrome (SBS) is condition of nutritional malabsorption related to the surgical removal or disease of a large portion of the small intestine. In neonates small intestine measures around 250 cm in length and it grows to around 750 cm in adults. In adult patients, small bowel length of < 100 cm is highly predictive of permanent intestinal failure (Messing et al. 1999). It is generally believed that a loss of more than 70% small intestine causes SBS, which is characterised by diarrhoea, steatorrhoea, severe weight loss, malnutrition, and eventually failure to thrive resulting in a high incidence of mortality both in children and adults. The amount of bowel that must be lost to produce malabsorption is variable and depends on which section(s) is/are lost, and whether the ileocecal valve is preserved. It is known that patients with short bowel syndrome do better who have an intact ileocaecal valve and where all the colon is preserved (Mayr et al. 1999).

The most common cause for SBS remains extensive surgical resection of the small intestine. Necrotising enterocolitis in neonates and Crohn's disease in adults remain the most common cause for extensive surgical resection. Other causes include abdominal wall defects, jejunoileal atresia, midgut volvulus, and Hirschsprung's disease in children. Other causes in adults

include mesenteric ischemia, neoplasms, trauma and radiation enteritis. Although uncommon, SBS in adults can potentially result from even commonly performed surgical procedures like intestinal obstruction, colectomy, hysterectomy and gastric bypass (Thompson et al. 2005).

1.2 Current solutions to the problem of SBS

The mainstay of treatment of SBS remains to improve the nutritional status of the patients by enteral (EN) or parenteral (PN) feeding. Home parenteral nutrition (HPN) has been used as a life-saving treatment for patients with intestinal failure. Other surgical procedures like sequential intestinal loop lengthening have been attempted to treat SBS but only with limited success. For patients dependent on PN, intestinal transplantation is the last hope in the present medical field.

1.2.1 Parenteral Nutrition

Approximately 500 patients in the U.K are treated with HPN at one time (British Association for Parenteral and Enteral Nutrition 2003). The estimated annual cost in the U.K (1995) for HPN is about £ 55 000 per patient year (Puntis 1998). Overall survival at one year is 92%. Some patients survive ten years or more with good quality of life. Less than 1% of time is spent in hospital once on HPN although underlying disease states often demand

complex care. Some patients cease to require HPN as they become able to return to enteral or oral nutrition due to intestinal adaptation or reconstructive surgery (British Association for Parenteral and Enteral Nutrition 2003). However, in most patients with remaining small intestine length of < 100 cm, dependence on PN is highly likely. The goal of treatment remains to wean off from this dependence. The degree of adaptation is vital in decreasing the dependence on parenteral nutrition and for improving patient quality of life and long-term outcome.

Despite advancements in managing SBS such as the use of trophic factors to stimulate intestinal adaptation and enhance intestinal absorption, intestinal transplantation remains the only option for those who have developed life-threatening complications from PN and cannot be managed using more conservative techniques (Jackson and Buchman 2005). Due to high morbidity and mortality associated with PN and intestinal transplantation, alternative treatment strategies have been employed in form of intestinal loop lengthening thus facilitating better intestinal absorption.

1.2.2 Sequential intestinal lengthening procedures for SBS

Techniques have been employed in the past with little success where a small bowel nipple valve is constructed distally to provide temporary partial obstruction and thereby induce dilatation and lengthening of the proximal

small intestine (Bianchi 1980;Georgeson et al. 1994).

A recent publication describes the first successful application of tension to induce length and growth in rat intestine as illustrated in **figure 1.1** (Jackson & Buchman 2005;Safford et al. 2005).

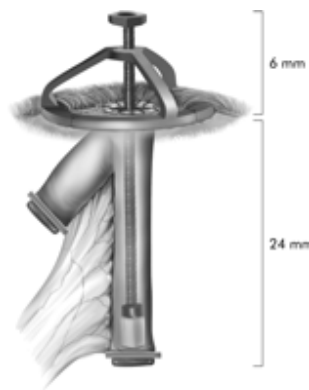


Figure 1.1: Schematic diagram of the intestinal lengthening device (adapted with permission from (Chen et al. 1997;Safford et al. 2005)

Chen Y et al have described a similar procedure in 1997 but they did not measure all the parameters of intestinal growth (Chen et al. 1997). With the use of an intestinal lengthening device to apply longitudinal mechanical tension, they have demonstrated growth of intestine in form of increased length by 149 %, total weight by 218 %, mucosal weight by 122 %, and protein mass by 164 % as compared to the controlled limb of the bowel. Histologically, there was a markedly increased thickness of the muscularis propria in the lengthened bowel (200% increase compared with the control limb) and functionally, increased intestinal length corresponded with

increased disaccharidase activity, thus implying potential increased absorptive capacity of the lengthened bowel. This experimental study has a potential to be used as an alternative treatment for SBS, but has not been investigated by many researchers.

1.2.3 Small Bowel Transplantation

Despite some success offered by surgical techniques to lengthen small intestine, the most promising treatment for SBS, to date, remains intestinal transplantation. As of 1999, 474 cases including isolated intestinal transplant, liver/intestinal transplant, and multivisceral transplant have been performed worldwide, as per the International Transplantation Registry, with 1-year graft and patient survival rates of 66% and 54% respectively (Kato et al. 2002). Small bowel transplantation should be considered for all children with proven irreversible intestinal failure who are dependent on parenteral nutrition for survival (Kelly and Buckels 1995). It is important to refer children for small bowel transplantation as soon as hepatic dysfunction occurs or as soon as there are any difficulties for vascular access (Brook 1998). It is estimated that around 40% of patients with complete intestinal failure will develop liver disease by 2 years (Brook 1998). Decision to do an isolated intestinal transplant or combined with liver depends on the extent of liver damage (Beath et al. 1997). Rejection rate was significantly decreased by the introduction of new immunosuppressant Tacrolimus (FK506) in 1989.

Overall worldwide survival for isolated small bowel transplantation is around 50% at 5 years, and for combined small bowel and liver transplantation 40% (Brook 1998). A study on 43 patients who received intestinal transplantation, showed better long-term results in those who had intestinal and multivisceral transplantation rather than intestinal transplantation alone (Janson 2002).

1.3 Problems with current solutions to SBS

There is a high mortality and morbidity associated with SBS. Most of the neonates with SBS die of sepsis or liver failure secondary to PN. Other complications include electrolyte-imbalances, bone metabolic disorders, catheter occlusion; catheter induced central vein thrombosis and pulmonary embolism. In a recent cohort study, mortality rates were as high as 37.5% in neonates with SBS who were on PN (Wales et al. 2005) and a recent study in Spain showed mortality figures in patients using HPN as high as 50% (Moreno et al. 2005).

There are major restrictions to the rapid development of intestinal transplant programs due to high incidence of rejection and limited availability of donor-organs. Many patients die while waiting for the intestinal transplant. Another problem is the size of the donor. A donor graft size smaller than the recipient is preferable especially if the recipient has undergone previous abdominal surgery for resection resulting in the contraction of the abdominal cavity.

Significant complications remain to be rejection, sepsis, and lymphoproliferative disease.

1.4 The need for small intestine tissue engineering

Like any other organ, the idea to generate an artificial small intestine would obviously emerge from the constant need to replace small intestine that is either functionally impaired or massively resected. SBS patients depend on a meticulous regime of nutrition for their survival. Remaining length of < 100 cm of small intestine in adults almost inevitably results in a permanent intestinal failure, requiring institution of PN. Incidence of sepsis and liver failure from PN is significantly high. Patients who develop PN dependence are the best candidates for intestinal transplantation. However, high mortality rates of about 50% as well as shortage of donor organs limits intestinal transplantation to progress rapidly. The constant drive to develop tissue engineering has flourished because of the limitations associated with the alternative therapies such as Organ Transplantation or Reconstructive Surgery in form of limited availability of the donor organs, graft rejection and high costs. The availability of off-the-shelf tissues and organs would mean a substantial savings, being less expensive than donor organs, and would allow physicians to begin treatment before patients are critically ill. An off-the-shelf artificial intestine can potentially prove to be a novel therapy for patients with SBS.

Tissue engineering is a rapidly emerging multidisciplinary area in biotechnology, which combines various aspects of medicine, cell and molecular biology, materials science and engineering, for the purpose of regenerating, repairing or replacing diseased tissues.

Tissue engineering principles are based on the utilization of three primary components, namely the cell, the scaffold (whether biological or synthetic), and the biomolecules, which serve to integrate and to functionally regulate the behavior of the first two. Bioreactors play an important role in providing optimum *in vitro* physiochemical environment mimicking *in vivo* conditions for growth of tissue.

Since early 1990s, almost every human tissue has been targeted for engineering, including parts of cardiovascular and nervous system, skin, eyes, liver, pancreas, muscle and intestine. To date, Bioartificial Skin is the most common commercially available tissue engineered biological substitute. Different forms of cartilage replacement have been implanted into humans with success, as well as bone and blood vessels.

Tissue engineering of small intestine is a complex field in regenerative medicine. Attempts to generate neo-intestinal mucosa started in 1988 and some success was demonstrated by research groups in University of

Massachusetts, when rats' intestinal epitheloid units were implanted in syngenic juvenile rats' omentum. The scaffold used was fabricated from polyglycolic acid or its copolymer with polylactic acid. This generated a lot of enthusiasm worldwide, however due to reasons described in the next chapter, tissue engineered intestine remains far from clinical use.

Recently the emergence of nanotechnology and concept of stem cells have given the field of tissue engineering a significant boost. A fresh perspective is required to restart investigating small intestinal tissue engineering. Although investigations still remain experimental, continued attempts worldwide especially with evolving nanotechnology, offer hope to provide an off-the-shelf artificial intestine as a novel therapy for patients with Short Bowel Syndrome.

1.5 Aim of this study

1. To analytically review published studies for small bowel tissue engineering and discuss methods adopted by different groups using different cell sources and polymers.
2. To develop and characterise porous biodegradable scaffolds from nanocomposite POSS-PCL (Polyhedral oligomeric silsesquioxane-Polycaprolactone) manufactured in our laboratory.

3. To grow rats' intestinal epithelial cells onto developed scaffolds to study *in vitro* characteristics of the scaffold for future small intestinal tissue engineering.

1.6 Layout of thesis

In chapter 2, published studies on small intestinal tissue engineering are analytically reviewed with particular emphasis on cell source. Achievements so far by researchers aimed to generate tissue engineered small intestine (TESI) are highlighted. Simultaneously, limitations and pitfalls are discussed which prevent TESI far from clinical use. In chapter 3, polymer source including role of nanocomposites, their properties and different methods to fabricate scaffolds are reviewed. Main advantages and disadvantages of fabricating techniques are addressed. Based on the review of literature, our nanocomposite polymer (POSS-PCL) is subjected to two chosen fabrication methods, as described in experimental chapters 5 and 6.

Chapter 4 describes materials and methods used for all experiments.

Results of these experiments are described in chapters 5, 6 and 7. Chapter 5 describes formation of porous scaffolds by particulate leaching/ solvent casting using NaCl as the particulate. Scaffolds are characterised for their

porosity and pore morphology using scanning electron microscopy and micro CT. They are also tested for mechanical strength and chemical bond structure. Scaffolds made using this technique are later used for *in vitro* cell culture as described in chapter 7.

In chapter 6, scaffolds developed by electrohydrodynamic atomisation using the same polymer (POSS-PCL) are characterised. This chapter addresses unsuccessful role of electrohydrodynamic spraying or spinning to form macro-porous scaffolds, whereas electrohydrodynamic printing to be a useful and potentially novel technique for obtaining pre-designed pore morphology.

In chapter 7, cell work is described where scaffolds developed are tested for cell viability and proliferation. *In vitro* cell growth of rats' intestinal epithelial cells is studied using Alamar Blue and LDH assays.

Chapter 8 concludes the thesis by summarising the main achievements and limitations of the project. It addresses the issues associated with lack of progress in this complex field of tissue engineering and discusses possible future work.

Chapter 2: Critical Review of Literature – Cell Source

2.1 Introduction

The term “tissue engineering” was officially coined at a National Science Foundation workshop in the United States (Georgia Tech/Emory Centre for the Engineering of Living Tissues) in 1988 to mean “the application of principles and methods of engineering and life sciences toward fundamental understanding of structure-function relationships in normal and pathological mammalian tissues and the development of biological substitutes to restore, maintain or improve tissue function.” (McIntire et al. 2002).

Human tissue engineering is a rapidly emerging multidisciplinary area in biotechnology, which combines various aspects of medicine, cell and molecular biology, materials science and engineering, for the purpose of regenerating, repairing or replacing diseased tissues. Tissue engineering principles are based on the utilization of three primary components, namely the cell, the biomaterial (whether biological or synthetic), and the biomolecules, which serve to integrate and to functionally regulate the behavior of the first two.

Since early 1990s, almost every human tissue has been targeted for engineering, including parts of the nervous system, skin, eyes, liver, pancreas, muscle and intestine. To date, Bioartificial Skin is the most common commercially available tissue engineered biological substitute.

Different forms of cartilage replacement have been implanted into humans with success, as well as bone and blood vessels.

It was the same time when concept of tissue engineering was first introduced in 1988, that Joseph P Vacanti et al reported the generation of intestine from minced pieces of foetal intestine, in form of a visible 6 mm cyst, when a cell-polymer construct was implanted into rat's omentum (Vacanti et al. 1988). These results generated a lot of enthusiasm amongst researchers and an off the shelf intestine as a cure to short bowel syndrome could be seen as a viable clinical option.

In our work described later in the chapters, we have aimed to address the biomaterial aspect of tissue engineering using a relatively new concept of nanotechnology. We used biodegradable nanocomposite POSS-PCL developed and patented in our laboratory to fabricate porous scaffolds, and characterized them for their suitability to be used as scaffolds for soft tissue engineering of structures like small intestine.

As a preliminary step, we reviewed published literature to understand the evolution of small intestinal engineering and critically analysed the advancements done in this field so far against the obstacles which are expected in this complex field before a clinical use is likely.

2.2 Search Methodology

A literature search was performed using keywords 'tissue engineering', 'small intestine', 'scaffold', 'stem cells', 'regenerative medicine', and 'polymer' in the following databases between 1966 – 2009: Pubmed, Embase, Athens, Ovid online, ISI web of science, Ingenita select, Elsevier texts and Blackwell-Synergy.

2.3 Tissue engineering of small intestine

It was in 1988 when the most initial attempts were made to engineer small intestine. This pioneering work was done by a research group in the USA (Vacanti et al. 1988) where a cell-polymer construct was implanted in an animal model (rat) to generate cyst like structures having neo-intestinal mucosa.

An overview of tissue engineering principles is described below in **figure 2.1**. As mentioned earlier, they are based on the utilization of three primary components, namely the cell, the biomaterial (whether biological or synthetic), and the biomolecules, which serve to integrate and to functionally regulate the behavior of the first two.

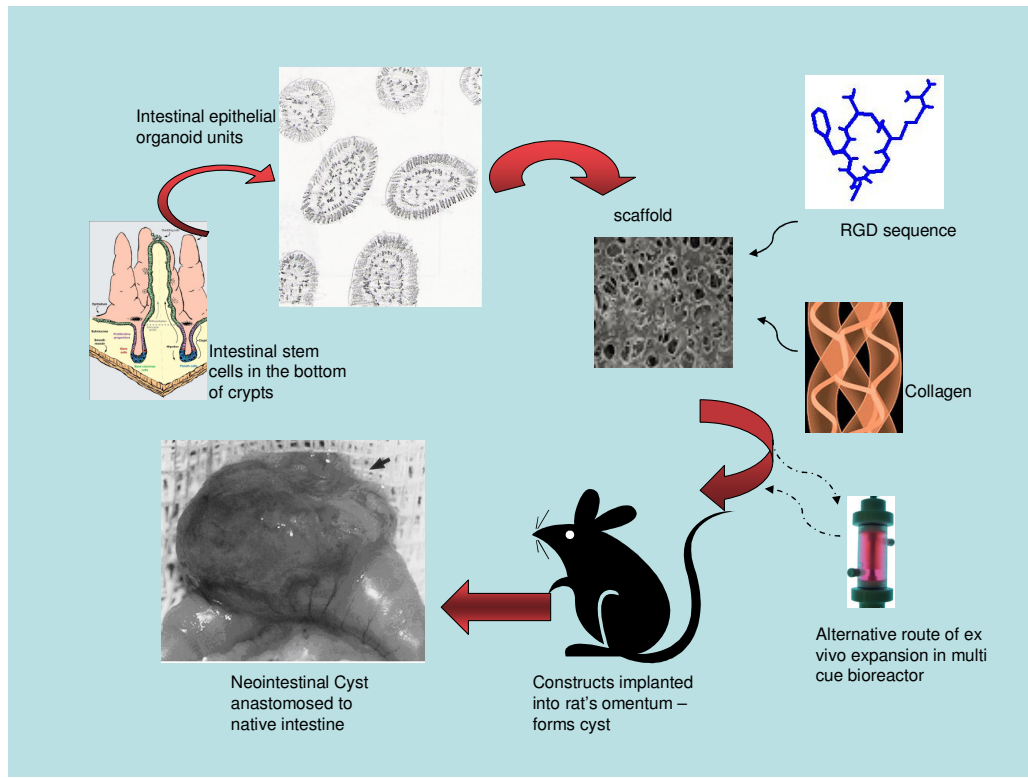


Figure 2.1: Schematic diagram of overview of small intestinal tissue engineering.

2.4 Cell source

Cells can be differentiated or progenitor cells, adult or embryonic stem cells, or tissue or organ specific cells. They can be autologous, allogenic, or xenogenic. Attempts have been made to isolate intestinal cells from all the above sources, which are described below.

2.4.1 From Bone Marrow - Hematopoietic stem cells

Although, embryonic stem cells which are totipotent and parent all types of

tissue would be considered most demanding in the field of tissue engineering, sensitive issues like ethical and legislative issues and scarcity of the available embryonic cells have always driven research to continuous attempts finding an adult source of totipotent cells. It is believed traditionally that the adult stem cell differentiates only to the tissue in which it resides. For example, hematopoietic stem cell (HSC) would generate blood cells, liver progenitor cells (oval cells) would produce hepatocytes and stem cells in the crypts of intestinal mucosa would lead to generate intestinal cells. The process by which an adult stem cell can jump lineage barriers to differentiate into cells outside their own tissue is called *Stem Cell Transdifferentiation*. In other words this is also called *lineage plasticity* of adult stem cells (Korbling et al. 2003). The concept of transdifferentiation is one of the explanations why transplanted bone marrow (BM) or peripheral blood (PB) cells are detected in recipient solid organ specific tissues. However, the stem cell transdifferentiation model has also been challenged. Cell fusion has been postulated to be the alternative mechanism to explain the presence of BM-derived cells in solid organ specific tissue (Korbling, Estrov, & Champlin 2003). Apart from the HSCs that renew circulating blood cells, the adult bone marrow also contains mesenchymal stem cells (MSCs), which contribute to the regeneration of mesenchymal tissues such as bone, cartilage, muscle, ligament, tendon, adipose, and stroma (Pittenger et al. 1999). Bone marrow contains pluripotent stem cells with the potential to differentiate into mature cells of various organs like hepatic oval cells, hepatocytes, cholangiocytes

(Alison et al. 2000; Petersen et al. 1999; Theise et al. 2000), skeletal muscle cells (Alison et al. 2000; Ferrari et al. 1998), astrocytes, neurons (Alison et al. 2000) and even renal tubular epithelial cells (Poulsom et al. 2001).

To determine whether circulating stem cells have a similar potential Korbly et al. concluded from a study on the biopsy specimen from liver, skin and gastrointestinal tract from patients with leukaemia who had undergone transplantation of hematopoietic stem cells from peripheral blood or bone marrow that circulating stem cells can differentiate into mature hepatocytes and epithelial cells of the skin and gastrointestinal tract (Korbly et al. 2002). However the exact mechanism of origin and physiological role of these cells is unknown. A study demonstrated a quantitative analysis of the donor engraftment of nonhematopoietic tissues eleven months post transplant of single bone marrow stem cell in mice (Krause et al. 2001). In addition to engraftment of columnar epithelial cells in the small bowel, donor-derived epithelial cells were identified throughout much of the GI tract, including the lining of the oesophagus, stomach, and large bowel. They demonstrated two patterns of epithelial engraftment of marrow-derived cells: large-scale repopulation in response to injury as demonstrated in liver and lung, and low level engraftment as individual scattered cells in the absence of marked injury as in liver, skin, and G.I tract. These randomly inserted single cells may not be fully functional since they did not appear to proliferate. Although little is known about how these cells obtain the degree of differentiative

potential, tissue-injury, local environmental signals, and recombinant human granulocyte colony-stimulating factor may have a significant role in the above process (Korbling et al. 2002; Krause et al. 2001).

In the human bone marrow, the sialomucin CD34 is a hematopoietic cell surface antigen that has been extensively exploited for the selection of long-term repopulating cells with multi-lineage potential, though not all HSCs express this marker.

A study demonstrated that bone marrow cells could differentiate into human GI tract epithelia, and that the increase of these bone-marrow derived cells was closely related to the recovery from epithelial damage (Okamoto et al. 2002). They were the first to conclude that cells derived from transplanted bone marrow could 'repopulate' every part of the human GI tract epithelia and contribute to the regeneration of damaged epithelial tissues.

A study (Alison et al. 2000; Jiang et al. 2002) on rodent bone marrow, has indicated that certain mesenchymal stem cells - termed multipotent adult progenitor cells (MAPCs) – differentiate, at the single cell level, not only into mesenchymal cells, but also cells with visceral mesoderm, neuroectoderm and endoderm characteristics *in vitro*. When injected into an early blastocyst, MAPCs contribute to most, if not all, somatic cell types. On transplantation into a non-irradiated host, MAPCs engraft and differentiate to the

haematopoietic lineage, in addition to the epithelium of liver, lung and gut, depending on the environmental cues provided by different organs. This technique of expansion of MAPCs *in vitro* and when transplanted, differentiation *in vivo* into cells of different lineages, can have a potential to be used into tissue engineering of small intestine in future. However, Hori Y and group's attempts to generate a muscle layer failed when they seeded autologous mesenchymal cells onto the 5 cm tubular collagen scaffold and replaced it into the defect in the small intestine (Alison et al. 2000;Hori et al. 2002).

2.4.2 From peripheral blood

Zhao Y et al have identified, cultured, characterised, and propagated adult pluripotent stem cells (PSCs) *in vitro* from a subset of human peripheral blood monocytes. They induced these cells to differentiate into mature macrophages by lipopolysaccharide, T lymphocytes by IL-2, epithelial cells by epidermal growth factor, endothelial cells by vascular endothelial cell growth factor, neuronal cells by nerve growth factor, and liver cells by hepatocyte growth factor. The pluripotent nature of these individual PSC was further confirmed by a clonal analysis (Zhao et al. 2003).

2.4.3 Gastrointestinal stem cells (tissue specific cells)

Intestinal stem cells are believed to reside in the base of the crypts of Lieberkuhn in the small intestine as shown in **figure 2.2**.

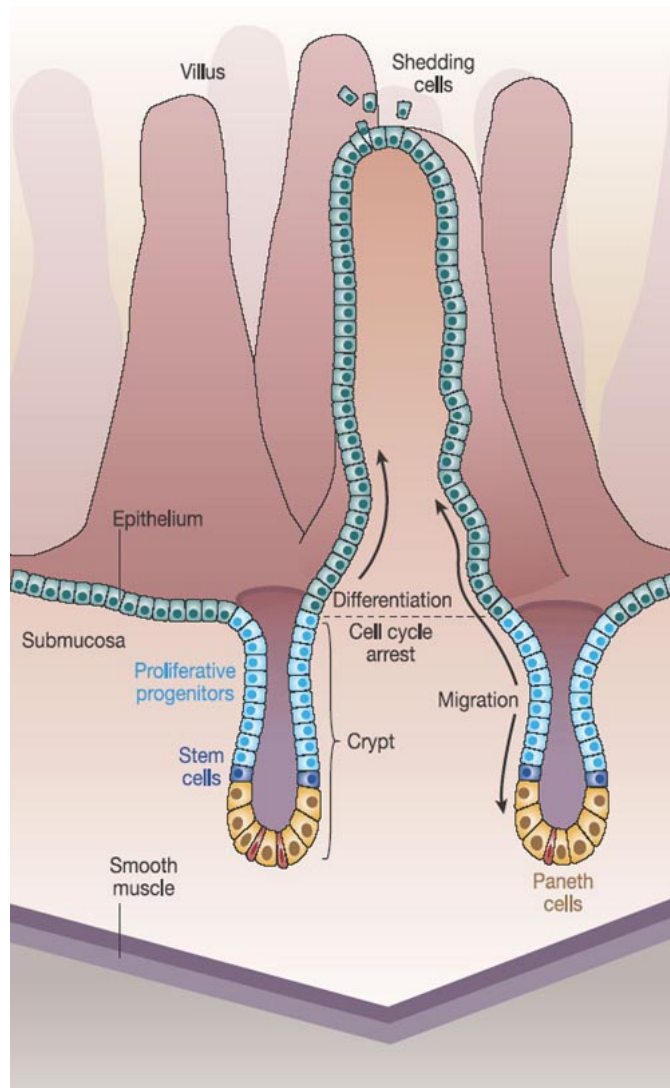


Figure 2.2: Intestinal epithelial cell generation. Putative stem cells (dark blue) reside immediately above the Paneth cells (yellow) near the crypt bottom. Proliferating progenitor cells occupy the remainder of the crypt. Differentiated cells (green) populate the villus, and include goblet cells, enterocytes and entero-endocrine cells. [Adapted with permission from (Reya and Clevers 2005)].

They lie just superior to the Paneth cells (approximately the fourth or fifth cell position in mice) within a 'niche' and studies suggest that a single stem cell undergoes asymmetrical division to produce an identical daughter cell, and thus replicate itself, and a committed progenitor cell which further differentiates into an adult epithelial cell (Reya & Clevers 2005).

There is a constant turnover of the epithelial cell lineages in the GI tract, increased especially in tissue injury. This process is regulated by multipotent stem cells, which give rise to all gastrointestinal epithelial cell lineages (Paneth, goblet, absorptive columnar and enteroendocrine) and can regenerate whole intestinal crypts (Brittan and Wright 2002).

Little is known of the location and fate of the stem cells within the gastrointestinal tract, due to the lack of distinct stem cell markers, but they are usually said to appear histologically primitive and can be identified functionally by their ability to repopulate crypts and glands after damage (Brittan & Wright 2002). There are no reliable specific means to identify these stem cells. Musashi 1, a neural stem cell marker, is expressed in immature cells in the lower crypt and may prove useful as an intestinal stem cell marker (Kayahara et al. 2003). Recent success in identification of stem cells in small intestine and colon by marker gene Lgr5 may prove to be a vital step in isolating intestinal specific stem cells from the crypts of small intestine (Barker et al. 2007). Lgr5 (leucine-rich-repeat-containing G-protein-

coupled receptor 5) is a gene selected from intestinal Wnt target genes. In this study, *Lgr5* is found to be expressed in cycling columnar cells at the crypt base and when lineage-tracing experiments were performed in adult mice, the *Lgr5* –positive crypt cell generated all epithelial lineages over a 60-day period, suggesting that it represents the stem cell of the small intestine and colon.

Evans et al (Evans et al. 1992) have described a reproducible method for growing small intestinal epithelium (from suckling rat intestine) in short-term cultures. Isolation of the epithelia and, significantly, preservation of its three-dimensional integrity was achieved using a collagenase/dispase digestion technique. They suggested that proliferation in vitro is also critically dependent upon the quality of the medium and constituents used.

Although the morphologic features of small intestinal epithelial progenitors (SiEPs) are known, their molecular features are poorly defined. Previous impediments to purification and molecular characterization of SiEPs include lack of *ex vivo* clonogenic assays and the difficulty of physically retrieving them from their niche where they are interspersed between their numerous differentiated Paneth cell daughters (Stappenbeck et al. 2003). In the study by Stappenbeck et al these cells were harvested by laser capture microdissection.

Stem cells are a small percentage of the total cellularity. In the mouse small intestine, there are perhaps 4-5 stem cells in a ring near the bottom of the crypt (Bjerknes and Cheng 1999) out of a total crypt population of about 250 cells.

2.4.4 Enterocyte Isolation

Organ et al in 1992 have reported transplantation of enterocytes (small intestinal epithelial cells) using cell-polymer constructs to produce neointestine (Organ et al. 1992). They isolated enterocytes from rat small intestine by using the method of Weiser (Weiser 1973) where they dissociated cells using citrate and obtained sequential fractions of epithelial cells in a villus to crypt gradient by a series of incubations and washings of gut loops avoiding over-manipulation. The isolated cells were seeded onto biodegradable polymer of PGA and enterocyte-polymer constructs were implanted in rats' omentum or mesentery and also in subcutaneous plane. They had an overall successful engraftment in 67% cases. Their study indicated that enterocytes attach to synthetic biodegradable polymeric scaffolds, and the transplanted constructs become vascularised and remain viable over at least a 2-week period. This study required long-term histological and immunocytochemical evaluation of morphogenesis and function of the implants. Use of isolated enterocytes to engineer neointestine cannot be seen in other studies after this preliminary attempt.

2.4.5 Intestinal Epithelial Organoid Units

After the attempted use of the enterocytes, Vacanti J.P and group moved on to use intestinal epithelial organoid units as the cell source to be seeded onto synthetic biodegradable polymer scaffolds and achieved considerable success in regenerating neointestinal tissue. Their laboratory was the first to report in 1997 making tissue engineered small intestine by the transplantation of organoid units on a polymer scaffold into the omentum of the Lewis rat (Choi and Vacanti 1997). These intestinal epithelial organoid units were isolated from neonatal rats as per the method first developed by Evans et al in 1992 for the preparation of rat intestinal epithelial cell primary cultures. Intestinal epithelial organoid units are multicellular units derived from neonatal rat intestine, containing a mesenchymal core surrounded by a polarized intestinal epithelium, and contain all of the cells of a full-thickness intestinal section (Evans et al. 1992;Weiser 1973). In this method Evans et al used enzymatic solution of dispase and collagenase to digest the supportive connective tissue thus allowing clusters of crypts and villi to be released after gentle pipetting. To date this method because of its surety to isolate intestinal stem cells has been extensively used by Vacanti JP and colleagues in their various experiments.

In this method, the entire length of the small intestine from 6-7 days old

neonatal Lewis rats is harvested, stripped of its mesentery, and placed in HBSS (Hank's balanced salt solution) on ice. The intestines are lavaged with HBSS, split open, and cut into 2-3 mm fragments. Intestinal fragments are further washed with HBSS, sharply minced into $< 1 \text{ mm}^3$ pieces, and then enzymatically digested by a solution of dispase and collagenase at room temperature on an orbital shaking platform at 80 rpm for 25 minutes. Three rounds of serial agitation, sedimentation and discarding of supernatant are performed. The intestinal organoid units are further purified by centrifugation in a solution of Dulbecco's serum, and 2% sorbitol at 300 rpm for 2 minutes. The resulting pellet is resuspended in medium and counted. The intestinal epithelial organoid units are then seeded statically onto the inner luminal surface of each polymer tube at a density of $4-6 \times 10^4$ organoid units per polymer. The organoid units are allowed to attach to the polymer for 1 hour before implantation (Kim et al. 1999b).

2.4.6 Organoid unit-polymer construct implantation

The unit-polymer constructs were wrapped with omentum after laparotomy and placed back in the abdominal cavity of rats. 2-3 weeks later they were found to develop cyst like structures and the cysts were histologically analysed for the characteristics of the intestinal tissue regeneration like presence or absence of villi, crypt width, and the thickness of the layers. The neointestine was also subjected to immunohistochemistry. Some studies by

Vacanti et al in Boston, U.S.A have shown successful formation of cysts between 1-8 weeks post-implantation of the organoid unit-polymer constructs.

In most of their studies, intestinal epithelial organoid units harvested from neonatal Lewis rats were seeded onto biodegradable polymer tubes and implanted into the omentum of adult Lewis rats either implantation alone (group 1), implantation followed by anastomosis to native small bowel at 3 weeks (group 2) and implantation after small bowel resection and anastomosis to native small bowel at 3 weeks (group 3). All constructs were harvested at 10 weeks and examined by histology. Morphometric analysis of the neomucosa was obtained using a computer image analysis program.

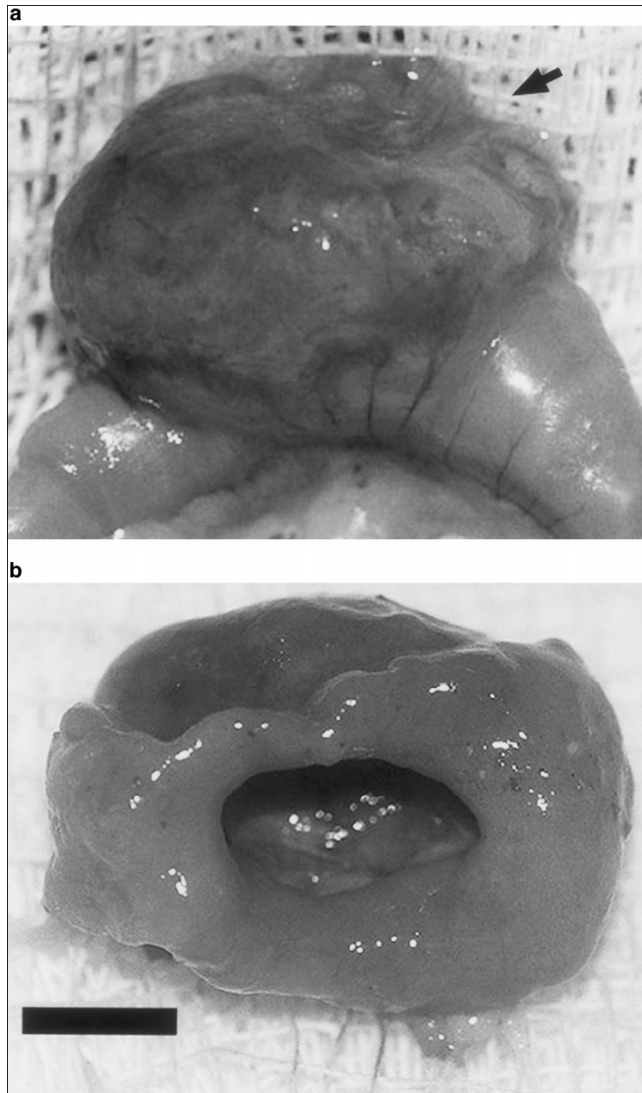


Figure 2.3 Tissue engineered intestine[(adapted from (Kim et al. 1999c)] (a) Photomicrograph of the tissue-engineered neointestine after anastomosis to native small intestine at the time of harvest (arrow indicates tissue-engineered neointestine). (b) Photomicrograph of the patent anastomosis between the tissue-engineered construct and native small intestine (bar 5.5 mm).

Cyst development was noted in all animals as shown in **figure 2.3**. All anastomoses were patent at 10 weeks. Histology revealed the development of a vascularized tissue with a neomucosa lining the lumen of the cyst with invaginations resembling crypt–villus structures.

Morphometric analysis demonstrated significantly greater villus number, villus height, crypt number, crypt area, and mucosal surface length in groups 2 and 3 compared with group 1, and significantly greater villus number, villus height, crypt area, and mucosal surface length in group 3 compared with group 2 (Kim et al. 1999c).

Lymphangiogenesis in TESI was shown to develop within 8 weeks of implantation of organoid unit-polymer constructs by demonstration of increased proportion of neointestinal VEGFR-3 –positive cells and ultimately formation of tubular structures which resembled lymphatics architecturally, were distinct from CD34-positive blood vessels, and lacked luminal erythrocytes (Duxbury et al. 2004;Kim et al. 1999c).

Kim et al in their studies have demonstrated that massive small bowel resection contributes significant regenerative stimuli for the heterotropically transplanted tissue-engineered intestine (Kim et al. 1999a;Kim et al. 1999b). They have also demonstrated that anastomosis between the TESI and native small bowel contributes significant trophic effects on neomucosal morphogenesis.

2.5 Extracellular Matrix (ECM)

The extracellular matrix (ECM) consists of a complex mixture of structural and functional macromolecules and serves an important role in tissue and organ morphogenesis and in the maintenance of cell and tissue structure and function. It is the noncellular part of a tissue and consists of protein and carbohydrate structures secreted by the resident cells (Hodde 2002). The great diversity observed in the morphology and composition of the ECM contributes enormously to the properties and function of each organ and tissue. The ECM is also important during growth, development, and wound repair: its own dynamic composition acts as a reservoir for soluble signalling molecules and mediates signals from other sources to migrating, proliferating, and differentiating cells. Tissue engineering is mainly based on the need to provide signals to cell populations in order to promote cell proliferation and differentiation. These “external signals” are generated from growth factors, cell-ECM, and cell-cell interactions, as well as from physical-chemical and mechanical stimuli (Rosso et al. 2004). For tissue engineering strategies it is essential to know how cells can interact with ECM and transduce the information received by the extracellular molecules into an intracellular event. The cell surface possesses two kinds of receptors: non integrin and integrin receptors. There are at least two main ways by which the ECM can affect cell behaviour. One of these is the cell-ECM interaction which may directly regulate cell functions through receptor-mediated signalling. The other is that ECM can control the mobilization of growth or differentiation factors, thus modulating cell proliferation and controlling cell

phenotype (Taipale and Keski-Oja 1997). Tissue-engineering approaches typically employ exogenous three-dimensional ECMs to engineer new natural tissues from natural cells. The exogenous ECMs are designed to bring the desired cell types into contact in an appropriate three-dimensional environment, and also to provide mechanical support until the newly formed tissues are structurally stabilized and specific signals occur to guide the gene expression of cells forming the tissue (Putnam and Mooney 1996). In other terms, the template made from exogenous material to serve as ECM is also called a 'scaffold'. The types of scaffolds, their fabrication methods, their characterisation methods and surface modification are reviewed in next chapter.

Table 2.1: Review of published studies on small bowel tissue engineering

In all studies the animal model was rats except *dogs and **rabbits

| Study | Cell Source | Polymer | Procedure | Outcome | Pitfalls |
|-----------------------|----------------------|--|---|--|--|
| (Vacanti et al. 1988) | Isolated enterocytes | Polyglactin 910, polyanhydrides, polyortho ester | Cell preparations cultured on biodegradable polymers prior to implantation into rat omentum and mesentery | 3 of 23 implantations successful (max 6mm cyst) | Preliminary study |
| (Organ et al. 1992) | EC | PGA | EC-polymer constructs in omentum, mesentery or subcutaneously for 2 weeks | Engraftment in omental and mesenteric but not subcutaneous. Stratified endothelium seen in one only | Preliminary study using EC. Only mucosal cells regenerated |
| (Organ et al. 1993) | Isolated enterocytes | PGA | As above compared with animals who had 75% SBR | Engraftment lower in SBR than non-resected group. Constructs vascularised and viable over a 1-month period | Lower engraftment in SBR group |
| (Choi et al. 1998) | Organoid units | PGA with PLLA +/- collagen | Studied brush border enzymes, basement membrane components, and electrophysiology of TESI | Maturation of the neointestine (2-6 weeks). Increased villi and crypts, more mature columnar epithelium and epithelial cells with collagen | Good results but requires long term studies |
| (Kim et al. 1999b) | Organoid units | PLLA coated PGA | Small bowel resection, partial hepatectomy, and portacaval shunt compared | Neointestinal cyst size was significantly greater in SBR group | Absorption and anastomosis to native bowel not tested |
| (Kim et al. 1999c) | Organoid units | PLLA coated PGA | Effects of anastomosis of TESI to native small bowel | Anastomosis contributed significant regenerative stimuli for morphogenesis and differentiation of TESI | Good results but requires long term studies |

| | | | | | |
|------------------------------|-----------------|-------------------|---|--|--|
| (Kaihara et al. 1999) | Organoid units | PLLA coated PGA | End-to-end anastomosis of TESI and native small bowel | Patency rate of 78% with a trophic effect on cyst size and neomucosa | Lower patency than side-to-side (90%) with higher mortality |
| (Chen and Badylak 2001)* | None | Porcine SIS patch | Defect on small bowel repaired with a SIS patch. Or resection interposed with tubular SIS | Patch regenerated mucosal epithelial layer, some smooth muscle. Tubular group died due to leakage | Layers not well organised and not feasible in longer resected segments |
| (Perez et al. 2002) | Organoid units | PLLA coated PGA | Studied the immune system of TESI | TESI developed an immune cells; dependent on exposure to the luminal stimuli and duration | No evidence for source of cells (donor or host) |
| (Hori et al. 2002)* | Autologous MSCs | Collagen Sponge | MSC seeded scaffold around silicone stent | Mucosal layer was created | Failed to generate muscle layer |
| (Demirbilek et al. 2003)** | None | Porcine SIS | SIS patch on 6cm jejunal defect | Well organised mucosa and submucosa in 6 weeks | Some graft contraction. Anastomosis not tested |
| (Gardner-Thorpe et al. 2003) | Organoid units | PLLA coated PGA | Angiogenesis in TESI | VEGF and bFGF delivery may prove useful for TESI | Further studies required to elucidate mechanism |
| (Ramsanahie et al. 2003) | Organoid units | PLLA coated PGA | Effects of GLP-2 on mucosal morphology and SGLT1 expression | GLP-2 increased villus height and crypt depth and enhanced SGLT1 expression | Further studies required to elucidate mechanism |
| (Tavakkolizadeh et al. 2003) | Organoid units | PLLA coated PGA | Impact of luminal contents on epithelium, morphology, cellular dynamics and nutrient transporter tested | Anastomosed neomucosa regenerated the SGLT1 mRNA expression topography of the native jejunum and epithelial proliferation higher | Mechanism not studied |
| (Wang et al. 2003) | | Rat SIS | Tubular SIS (2-cm)with bilateral anastomosis in isolated ileal loop | Mucosa showed smooth muscle and serosa (24 weeks). SIS biocompatible, resistant to infection, induced neovascularisation, and remodelled | Small length of the tubular segment. No re-innervation |

| | | | | | |
|--------------------------|---|---------------------|---|--|---|
| (Grikscheit et al. 2004) | Organoid units | PLLA coated PGA | Studied the effect of TESI anastomosis on recovery after MSBR | TESI anastomosis (side-to-side) improved postoperative weight and B12 absorption after MSBR | Villin mRNA and IAP levels suggestive of differentiation were found to be in contrast |
| (Duxbury et al. 2004) | Organoid units | PLLA coated PGA | Studied lymphangiogenesis in TESI | Lymphangiogenesis in submucosa and lamina propria by 8 weeks, stain positive for VEGFR-3 | Further studies required to elucidate mechanism |
| (Viney et al. 2009) | Co-culture of established intestinal epithelial cell lines with fibroblasts | Collagen based gels | Studied in vitro generation of intestinal epithelium | Epithelial growth achieved using one combination of vimentin expressing stromal and cytokeratin expressing intestinal epithelial cells grown on collagen gels. | Needs trials on polymer constructs. |
| (Gupta et al. 2009) | IEC-6 intestinal epithelial cells | POSS-PCL | Studied in vitro cell growth on nanocomposite scaffolds | Achieved confluence of cell growth by day 21. Nanocomposite POSS-PCL supports intestinal cell growth in vitro | Mainly polymer scaffold based study. Needs in vivo trials. |

MSC-mesenchymal stem cell, EC-enterocytes, PGA-polyglycolic acid, PLLA-poly-L-lactic acid, SIS-small intestine submucosa, SBR-small bowel resection, MSBR-massive SBR, TESI-tissue engineered small intestine, VEGF-vascular endothelial growth factor, bFGF-basic fibroblast growth factor, GLP-2-glucagon-like peptide, SGLT1-Na⁺ -glucose cotransporter, IAP-intestinal alkaline phosphatase, VEGFR-vascular endothelial growth factor receptor.

2.6 Role of trophic factors after massive bowel resection

Ray et al have studied the enterocyte nutrient transport after massive bowel resection when the intestine is in adaptation. They concluded from their study that parenteral growth hormone (GH) and epidermal growth factor (EGF) when given in combination for 2 weeks immediately after massive enterectomy synergistically enhance Na^+ - dependent glutamine (GLN) uptake. This study emphasises the importance of the need of the growth factors to be considered after implantation of tissue engineered small intestine (Ray et al. 2003).

Regulation of epithelial cell proliferation, migration and differentiation under physiological conditions is poorly understood. A better understanding of how the intestinal epithelial cells interact with their underlying basement membrane is required. A likely mechanism of this interaction as suggested through integrins, a specific subset of cell surface binding proteins (Beaulieu 1992). It is now recognized that the basement membrane composition defines the necessary microenvironment required for multiple cellular functions during development and at maturity such as adhesion, proliferation, migration and cell survival as well as tissue-specific gene expression. These functions are themselves mediated by various cell receptors, many of which are members of the integrin superfamily. Integrins are transmembrane heterodimeric glycoproteins composed of an alpha and a beta subunit.

Seventeen alpha and eight beta subunits have been identified to date that associate to form at least twenty two different receptors. It is mainly the integrins belonging to the beta1 and beta4 classes that bind to basement membrane molecules such as the laminins and the type IV collagens (Beaulieu 1992).

2.7 Discussion

Stem cells have played a pivotal role in tissue engineering of small intestine. Out of the three main sources - haematopoietic stem cells from the peripheral blood, mesenchymal stem cells from the bone marrow, and tissue specific stem cells from intestinal crypts, the later has proved to be the only successful cell source in generating near-normal intestinal tissue. Unlike the MSCs and HSCs, intestinal stem cells almost guarantee the regeneration of all types of intestinal cells (absorptive-columnar, goblet, Paneth and autoendocrine cells), including muscle cells. Although HSCs from the peripheral blood have been shown to engraft in the gut lining when leukaemia patients received transplantation of haematopoietic stem cells from peripheral blood, the exact mechanism of origin and physiological role of these cells is unknown (Korbling, Estrov, & Champlin 2003). A low level engraftment was seen as individual scattered cells. These randomly inserted single cells may not be fully functional since they did not appear to proliferate. Although little is known about how these cells obtain the degree of

differentiative potential, tissue-injury, local environmental signals, and recombinant human granulocyte colony-stimulating factor may have a significant role in the above process (Korbling, Estrov, & Champlin 2003; Krause et al. 2001). In another study Zhao et al successfully demonstrated fibroblasts like macrophages (f-M ϕ) derived from monocyte-rich samples of peripheral blood to show their ability to mature into epithelial cells when treated with Epidermal Growth Factor (EGF), and cells of other lineages when exposed to the respective growth factors. These cells have a potential for tissue repair and regeneration but their use in small intestinal tissue engineering has not been attempted so far. Can these PSCs be used *in vitro* to seed the polymer, will it generate all the layers of bowel wall, are there enough and appropriate growth factors available, these are some of the questions which remain unanswered. More knowledge about growth factors, cell markers, optimum culture medium, and their exact function is required before they can be experimented in tissue engineering of small intestine.

Adult bone marrow stem cells have many characteristics which make them suitable for their potential use in tissue engineering of small intestine, like they can replicate as undifferentiated cells that have the potential to differentiate into lineages of mesenchymal tissues, they display a stable phenotype, they are immunocompatible, and they have no ethical issues. However, there are a number of technical obstacles, such as how to isolate

stem cell preparations without contamination by other cells, how to control the permanent differentiation to the desired cell types, and how to increase the production of the large number of cells needed to create tissues (Shieh and Vacanti 2005). Bone marrow-derived cells or the cells from circulating stem cells (peripheral blood) although have a great potential to be used as a source for organ reconstitution and repair, to date no one has successfully used them in the field of small intestine tissue engineering. Lack of mechanism of differentiation, paucity of these cells (Krause et al found an extremely small number of bone marrow-derived epithelial cells in the lung, bile duct and G.I tract of mice transplanted with a single bone marrow hematopoietic stem cell) and lack of recognised function of these cells have restricted their use in tissue engineering of small intestine.

Hori et al in 2001 did succeed in regenerating intestinal tissue on the luminal surface of the collagen scaffold seeded by autologous MSCs which they applied to replace a 5 cm defect in the dog jejunum. However they failed to generate a muscle layer, which is essential for functional peristalsis. Presence of mucosal layer was evident in the neointestinal tissue as also described in their previous study on dogs where they replaced an intrathoracic oesophageal segment of 5 cm by collagen scaffold alone wrapped around a silicone tube without being seeded by MSCs (Yamamoto et al. 1999). Clearly, the presence of mucosal layer in both their studies appears to come from migration of epithelial cells from the surrounding

healthy intestinal mucosa. But the mechanism of cell-migration to generate a mucosal layer cannot be relied upon where a much longer intestinal scaffold is required to replace small intestine with an aim to treat short bowel syndrome. As suggested by them, the failure of muscle layer regeneration might be due to various reasons. First, the number of seeded cells could be inadequate, or expansion of MSCs on the scaffold *ex vivo* might be required before implantation, second possibility is that preconditioning of MSCs by some additional directional stimulus for differentiation into muscle might be necessary before implantation. Hence, as suggested by them, advancement in use of trophic factors with the MSCs like basic fibroblast growth factor or vascular endothelial growth factor may be effective in regenerating highly differentiated and organised intestinal tissue including muscle layer. It might be necessary to supplement the neointestinal implantation with the parenteral administration of trophic growth factors to improve the enterocyte nutrient transport as suggested by studies.

Clearly, intestinal stem cells remain the most valid option as the cell-source because of their ability to differentiate in all types of intestinal cells. Isolation of only stem cells from intestinal crypts poses a great difficulty due to lack of specific stem cell markers and also difficulty in physically retrieving them from their niche where they are interspersed between their numerous differentiated Paneth cell daughters. Laser capture microdissection technique has been used with little success to harvest these cells. Another

priority should be the development of robust in vitro culture systems for the intestinal epithelium (Bjerknes and Cheng 2005).

Use of intestinal epithelial organoid units by Vacanti and group since 1997 has proved to be a successful method in providing the cell source. These units of $< 1 \text{ mm}^3$ pieces of minced neonatal rat intestine are prepared by enzymatic digestion (as described earlier in this article) containing all of the cells of a full thickness intestinal section.

Regulation of epithelial cell proliferation, migration and differentiation under physiological conditions is poorly understood. A better understanding of how the intestinal epithelial cells interact with their underlying basement membrane is required. A likely mechanism of this interaction, as discussed before, is through integrins, a specific subset of cell surface binding proteins.

Apparently, much work is needed in the field of cell-ECM interactions, specific stem cell markers, and trophic growth factors. Advancements in developing larger absorptive surface area of the TESI with formation of a better muscular layer would prove to be a very successful step forward.

Tissue engineering of small bowel remains at an early stage. The absorptive capacity is yet to be adequately tested in any constructs and current methods would provide insufficient cells for clinical applications. The use of

organoid units suggests that mucosal stem cells are useful in the generation of mature mucosa in TESI. Studies on rats have shown that large numbers of such units are needed to produce short lengths of TE construct. The isolation of the stem cells from these units or the use of stem cells from other sources, such as the MSC from the bone marrow, may provide a clinical alternative to the organoid units. In vitro culture of these cells is likely to be necessary to obtain clinically useful numbers of such cells.

The use of cultured stem cells and improved polymer technology provide the most likely future for TESI. Peptides other than collagen like fibronectin or self assembling hydrogels bound to the polymers have been shown to be useful in bone, cartilage, and cardiovascular tissue engineering and provide further hope for tissue engineered small intestine.

A more definitive and continuous cell supply will be needed to maintain the generated absorptive surface in form of neo-intestine. Stem cells cued specifically to intestinal lineage offer promise to fulfil the high demand of continuous cell source. While awaiting the specific cell markers available which can be targeted for small intestinal lineage, an ideal scaffold needs to be prepared incorporating vital features of appropriate physical and chemical characteristics. Recently nanocomposite scaffolds have shown many advantages in tissue engineering due to their high surface to volume ratio. Our aim in this study has been to develop and characterise scaffolds for

small intestinal tissue engineering using a new nanocomposite of polycaprolactone and silsesquixane, developed in our laboratory. An *in vitro* study was also performed to test the scaffolds for cell viability and proliferation using rat's intestinal epithelial cells. Future studies incorporating these scaffolds for *in vivo* use in animal models will need to be carried out in order to investigate further about their ability to withstand natural forces within the abdomen, and whether they support cell growth based on principles of cell migration.

Chapter 3: Critical Review of Literature - Scaffolds

Scaffolds design is complex, and various parameters need to be addressed when fabricating a scaffold such as the material used, the fabrication technique, pore morphology and porosity, mechanical strength, biocompatibility, surface properties, degradation rate, and degradation products. There is not a 'universal' ideal scaffold, and design of a particular scaffold needs to be tailored according to the specific application in question. Scaffolds' main function is to provide support to the growing cells until the extra cellular matrix produced by cells take over the degrading scaffold material. An ideal scaffold should be easy to fabricate and mould in the desired shape. It should be strong enough to withstand forces in vivo and in vitro until the tissue has grown. It should not provoke inflammatory response, and should be sterilizable. It should have a controlled porous structure, and should be resorbable.

In this chapter, we review physical and chemical properties required in development of a scaffolds. We also review advantages and disadvantages of different methods used in literature to develop scaffolds.

Based on the source of material, a scaffold can be classified as:

- Natural
 - Small intestinal submucosa (SIS)
 - Collagen
 - Acellular dermis

- Amniotic membrane tissue
- Cadaveric fascia
- Bladder acellular matrix
- Synthetic – Polymers
 - Polyglycolic acid (PGA)
 - Poly(L-lactic acid) (PLLA)
 - Copolymer poly(D,L-lactic co-glycolic acid) (PLGA)
 - Polycaprolactone (PCL)

3.1 Natural scaffold

The naturally occurring scaffolds can be processed in such a way as to retain growth factors, such as basic fibroblast growth factor (FGF-2) and transforming growth factor-beta (TGF- β) (Voytik-Harbin et al. 1997), glycosaminoglycans, such as heparin and dermatan sulphate and structural elements, such as fibronectin, elastin and collagen. These material prevent many of the complications associated with foreign material implants because they provide a natural environment onto which cells can attach and migrate, within which they can proliferate and differentiate (Hodde 2002).

3.1.1 Small Intestinal Submucosa (SIS)

Small intestinal submucosa (SIS) is a naturally occurring, acellular

xenogenic biomaterial that has been used extensively as a soft tissue replacement, as a scaffold for tissue engineering, and as a substrate for the study of cells in 3D culture. It is mainly derived from porcine small intestine but other mammals like rats and dogs have also been used. The presence of above mentioned properties of a natural scaffold made it available to be used in a variety of clinical conditions including vascular grafts like inferior vena cava grafts, duodenal patches, tendon repair, repair of meniscal defects, as bladder neck strings for urinary incontinence, abdominal wall defect repair, in ophthalmic surgery and as a scaffold for experimental tissue regeneration like intestinal cells and dermal fibroblasts. SIS consists of three distinct layers: the lamina propria and muscularis mucosae of the intestinal mucosa, and the tunica submucosa (Hodde 2002). The tunica submucosa is the layer of connective tissue arranged immediately under the mucosal layer of the intestine and is a 100-200 μm thick interstitial ECM; it makes up the bulk of the SIS biopolymer scaffold (Hodde 2002). SIS is harvested from the mammalian small intestine by mechanically separating it from its outer muscular layers and internal mucosal layers. The biopolymer is thoroughly rinsed in water, treated with an aqueous solution of 0.1% peracetic acid, and rinsed in sequential exchanges of water phosphate buffered saline to yield a neutral pH. It is then either stored in an antibiotic solution containing 0.05% gentamicin sulphate, or sterilized using 2.5-mRad gamma irradiation (Badyalak et al. 2000). When SIS is implanted as a naturally occurring biopolymer scaffold, it stimulates angiogenesis, connective and epithelial

tissue growth and differentiation, as well as deposition, organisation, and maturation of ECM components that are functionally and histologically appropriate to the site of implantation (Badylak et al. 2000). SIS comprises primarily of fibrillar collagens and adhesive glycoproteins which serve as a scaffold into which cells can migrate and multiply. In the whole, unprocessed intestine, the SIS layers also contain potent regulatory factors, such as glycosaminoglycans, proteoglycans, and growth factors, which regulate cellular processes that maintain tissue homeostasis and respond to injury and infection. Many of these components are retained in the biopolymer scaffold following processing (Hodde 2002).

Demirbilek et al (Demirbilek et al. 2003) studied the effect of porcine SIS as a xenogenic material used in intestinal regeneration when used to repair the created jejunal defect in rabbits. They demonstrated a remarkable regeneration of complete intestinal mucosa at 6 weeks with evidence of fibroplasias, angiogenesis, and mild mononuclear cell infiltration.

3.1.2 Collagen Scaffold

Hori Y et al reported successful tissue engineering of small intestine in a study on dogs when they used 'acellular' collagen sponge scaffold grafting with a silicon tube stent (Hori et al. 2001) (**figure 3.1**).

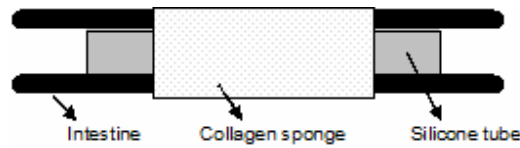


Figure 3.1: Schematic drawings of the operative procedure using collagen sponge. A silicone tube stent was inserted and fixed by sutures. A collagen sponge scaffold was then applied to wrap across over the gap. Finally, the scaffold was wrapped with omentum (redrawn with permission from Hori et al. 2002).

In their study collagen scaffold worked as a kind of extracellular matrix for tissue regeneration. According to them, if the conditions on the scaffold are able to support tissue regeneration, then the required host cells migrate onto the scaffold and the tissue regenerates at its own site. The length of the graft used was 5cm long. We cannot however say with confidence whether similar migration of the adjacent cells would occur to regenerate tissue if much longer segments of the small intestine are resected and replaced with acellular sponge scaffolds. Another drawback in their study was that proper thick muscle layer essential for functional peristalsis was not observed. Also, mucosal function for nutrient absorption was not evaluated and stenosis of the regenerated intestine was observed in some cases (Hori et al. 2001).

3.2 Synthetic scaffold

In the field of tissue engineering of small intestine so far, the most commonly used scaffold has been the biodegradable polymer made of polyglycolic acid.

Vacanti and colleagues have pioneered the arena of small intestinal tissue engineering by using a highly porous, synthetic, biodegradable polymer tubes fabricated from nonwoven sheets of polyglycolic acid (PGA) fibres marketed from Smith and Nephew, Heslington, York, U.K. Mooney et al in their study on biomaterials have emphasised the role of poly(L-lactic acid) (PLLA) and a 50/50 copolymer poly(D,L-lactic-co-glycolic acid) (PLGA) in stabilizing PGA meshes to form three dimensional structures like tubes when sprayed over PGA meshes. They showed that PGA meshes when sprayed with PLLA or PLGA were capable of withstanding large compressive forces *in vitro* (50-200 mN) and maintained their structure *in vivo* when implanted into the omentum in rats (Mooney et al. 1996b).

3.2.1 Scaffold fabrication

Highly porous, synthetic, biodegradable polymer tubes were fabricated from nonwoven sheets of PGA fibres as described by Mooney et al. Vacanti and colleagues in most of their experiments used a 15 × 10 mm rectangle of PGA mesh with a fibre diameter of 5 µm, mesh thickness of 2 mm, bulk density of 60 mg/cm³, porosity of 95% and a mean pore size of 250 µm. This piece of mesh was wrapped around a Teflon cylinder to form a tube and the overlapping ends were manually interlocked to form a seam. The Teflon cylinder was then rotated at 20 rpm using a stirrer. A solution of poly-L-lactic acid (PLLA) dissolved in 5% w/v chloroform was placed in an atomizer and

sprayed over the polymer tube for 10 seconds. After spraying was completed, the solvent was allowed to evaporate and the polymer tubes were lyophilized for 48 hr to remove residual solvent. The polymer tubes were cold gas-sterilized with ethylene oxide and then coated with 600 µg/polymer collagen type I overnight. The collagen-coated polymer tubes were subsequently washed three times with HBSS before seeding (Kim et al. 1999b).

Poly(D,L-lactide-co-glycolide) (PLGA), a biodegradable synthetic polymer, is widely used in a variety of tissue-engineered applications, including drug-delivery systems. In a study the polymer has also been impregnated with SIS to develop (SIS/PLGA) hybrid. Fabrication parameters, including ratios of SIS, PLGA and salt, were optimized to produce the desired macroporous foam. The scaffolds had a relatively homogeneous pore structure, good interconnected pores from the surface to core region and showed an average pore size in the range 69-105 micron and over 90% porosity. The SIS/PLGA scaffolds degraded with a rate depending on the contents of the SIS. After the fabrication of the SIS/PLGA hybrid scaffolds the wettability of the scaffold was greatly enhanced, resulting in uniform cell seeding and distribution. So, it was observed that cell attachment to the SIS/PLGA scaffolds increased gradually with increasing SIS contents (Lee et al. 2004).

3.2.2 Nanocomposites

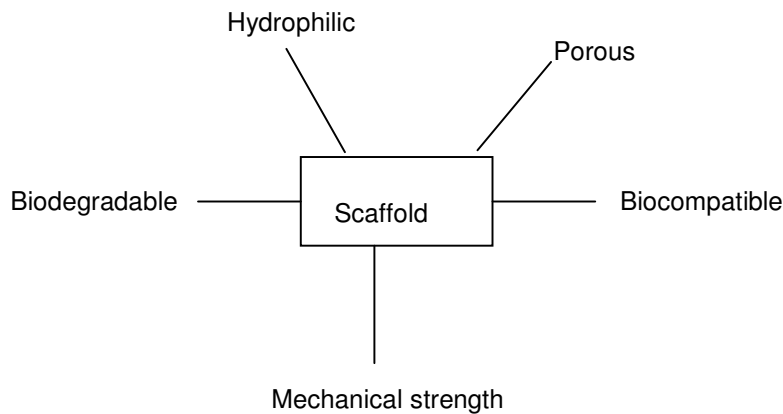
Nanocomposites are new generation of polymer used for development of tissue and organ engineering. So far only PLGA or PGA alone has been predominantly experimented for small intestinal tissue engineering. Although mainly due to lack of constant cell source supply, investigations into small intestinal tissue engineering have ceased moving. As a fresh perspective we intend to use our house made relatively new nanocomposite. Our laboratory has developed a biodegradable nanocomposite by incorporating the biostable POSS nanocages into a poly(caprolactone/carbonate)urethane urea. Nanocomposites can be defined as multiphase solid materials where one of the phases has a dimension of less than 100 nanometres (nm) (Ajayan et al. 2003; Kannan et al. 2005). Our nanocomposite is made of polyhedral oligomeric silsesquixane (POSS) and polycaprolactone (PCL). POSS molecules are 6 nm in size. Studies on biodegradation of this polymer have been done separately (Raghunath et al. 2008). The nanocages provide a “shielding effect” on the soft phase of the polymer. Polycaprolactone is degradable aliphatic polyester which has been extensively reported to demonstrate biocompatibility in vivo. Its degradation by hydrolysis and enzymes is well documented. PCL has been used in several copolymers and polymer blends as the foundation to a tailor-made polymer with specific properties. In vivo host response of POSS-PCL has not been studied but POSS-PCU, the nonbiodegradable counterpart lacking polycaprolactone, made by the same group, was implanted in sheep for 36 months and showed only minimal inflammation as compared to silicone implants

(Kannan et al. 2007). It is proposed that caprolactone will provide controlled degradation whilst the POSS nanocages will contribute to the mechanical strength required for a tissue engineering scaffold for soft tissue such as small intestine.

Scaffolds need to be pliable for soft tissue engineering especially when tubular structures are required like in vascular or intestinal tissue engineering. Both PGA and PLA are crystalline polymers and PGA has higher crystallinity than PLA. We fabricated pure PGA and PLA macroporous scaffolds using simple salt leaching techniques but the scaffolds damaged macroscopically when attempts were made to roll the sheets into tubular structures. Studies have shown that blending PGA, PLA or their copolymers with substances like PEG have resulted into the desired pliability (Wake et al. 1996).

Another disadvantage to fabricate PGA into scaffolds is its peculiar solubility in only very highly fluorinated organic solvents like hexafluoroisopropanol, whereas other biodegradable polymers like PLLA and PCL are soluble in most of the common organic solvents like chloroform, methylene chloride, DMAC, etc.

3.3 Scaffold Properties



3.3.1 Biodegradable vs Nonbiodegradable

Biodegradation mainly occurs through chemical hydrolysis although other mechanisms like oxidation or per-oxidation may be responsible for degradation as well. Combining chemical groups such as esters, anhydrides and amides add to hydrolytic instability of the polymers and hence aid biodegradation. Homogenous bulk erosion involves diffusion of water into the polymer bulk. If degradation is faster than the diffusing water, diffusing water gets absorbed quickly by hydrolysis inhibiting water reaching the bulk of the polymer, and the degradation occurs only on the surface of the polymer, known as heterogenous surface erosion. Usually biodegradation of polymer scaffolds is a combination of both bulk and surface erosion (Voytik-Harbin et al. 1997). Degradation depends on chemical and physical properties such as molecular weight, crystallinity, porosity, hydrophilicity, and surface to volume ratio.

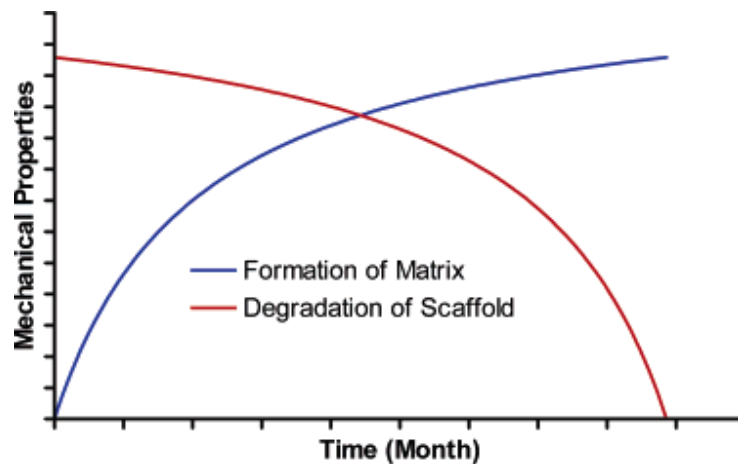


Figure 3.2: Optimal relationship between matrix formation and scaffold degradation

Biodegradable polymers have now been universally accepted as material of choice for scaffolds to be used in the purpose of tissue engineering. The rationale behind this is their disappearance from the implanted site as new engineered tissue (matrix) begins to form, thus reducing chances of extrusion and foreign body reaction. It is also believed that the newly generating tissue needs room to grow and expand and this can be inhibited by the presence of remaining scaffold material. The material should degrade into non-toxic products allowing neo-tissue to survive.

Non-biodegradable material like metals and ceramics are still widely used for surgical implants, particularly in orthopaedic applications like hip prosthesis, despite their limited processability (Yang et al. 2001). Ceramic implants for osteogenesis are based mainly on hydroxyapatite for its inorganicity. The usual fabrication technique for ceramic implants is sintering of ceramic

powders at high temperatures (Karageorgiou and Kaplan 2005). Other ceramics include bioglass having different compositions of SiO_2 , CaO , Na_2O , and P_2O_5 . Biodegradable bioceramics such as α -tricalcium phosphate, β -tricalcium phosphate have received significant attention due to their biodegradation and easy processability. Particularly, in bone tissue engineering, composites of biopolymer with bioactive ceramic or glass are believed to provide – (a) better cell seeding and growth environment due to good osteoconductivity properties provided by the bioactive phase, (b) buffering effect to the acidic degradation by-products of polyesters, and (c) better mechanical properties owing to stiffer particulates in form of ceramics (Boccaccini and Blaker 2005). In bone tissue engineering, where mechanical strength of the implants is crucial, metals have been the materials of choice as the bulk phase of the implants, while titanium particle coatings create a porous surface.

In soft tissue engineering, biomaterials used for fabricating scaffolds have mostly been biodegradable. Biodegradable polymers can be natural like collagen, SIS (small intestinal submucosa) or fibrin, or they can be synthetic such as polyglycolic acid (PGA), poly L-lactic acid (PLLA), copolymer poly D,L-lactic-co-glycolic acid (PLGA) or polycaprolactone (PCL). Synthetic polymers in general are much favoured over natural ones as they can be modified in terms of physical and chemical properties in order to obtain tailor made scaffolds, and they are more reliable source of raw material.

In this study, we use our laboratory made biodegradable nanocomposite of polyhedral oligomeric poly (carbonate-urea)-silsesquioxane and polycaprolactone (POSS-PCL) wherein we have incorporated the biostable POSS nanocages into a poly(caprolactone/carbonate)urethane urea. It is a polyurethane with a soft segment composed of polycaprolactone (80%) and polycarbonate (20%) and a urea hard segment. The polymer is ~22% by wt hard segment. This formula is the first of a series of biodegradable nanocomposites being developed by our department for use in tissue engineering for a variety of tissue types. Eighty percentage of polycaprolactone diol (mwt) was considered an appropriate initial formula for use as a tissue engineering scaffold for small intestine. Such a scaffold would be required to maintain its structural integrity for at least 4–6 months. It is proposed that caprolactone will provide controlled degradation whilst the POSS nanocages will contribute to the mechanical strength required for a tissue engineering scaffold for soft tissue such as small intestine.

This composite has been tested for degradation in a separate study (Raghunath et al. 2008). The nanocomposite (POSS-PCL) was exposed to a selection of degradative solutions for up to 8 weeks. The samples were analyzed by infra-red spectroscopy, scanning electron microscopy, X-ray microanalysis, contact angle analysis, and stress-strain mechanical analysis. Degradation of hard and soft segments of the nanocomposite was evident by infra-red spectroscopy in all conditioned samples. POSS nanocage

degradation was evident in some oxidative/peroxidative systems accompanied by gross changes in surface topography and significant changes in mechanical properties. The hydrophobic polymer became more hydrophilic in all conditions. This biodegradable nanocomposite demonstrated steady degradation with protection of mechanical properties when exposed to hydrolytic enzymes and plasma protein fractions and exhibited more dramatic degradation by oxidation. However it has not been clear from this study that how long will this composite take to degrade. It is assumed that it may take approximately 6 months for 50% degradation, based on other studies on degradation of PCL without POSS.

3.3.2 Hydrophobic versus Hydrophilic and Surface Modification

Usually, scaffolds fabricated have a hydrophobic surface unless hydrophillised by adding agents like polyvinyl alcohol (PVA), polyethylene glycol (PEG), polyethylene oxide, etc. When polyuethanes are added with agents like polyethylene oxide, they become highly hydrophilic materials. With increasing polyethylene oxide content, the composite can act as hydrogels, absorbing a lot of water. A balance between the hydrophilicity and hydrophobicity of polymers is sometimes needed to enhance biocompatibility. Our POSS-PCL composite when was subjected to degradative solutions, the hydrophobic polymer became more hydrophilic (Raghunath et al. 2008).

Most of the biodegradable synthetic polymers (like PGA and PLA) are hydrophobic and may require modifications on their surface for better cell attachment. This can be achieved by surface coating, chemical coating, plasma treatment, or modifying the fabrication of scaffold itself (Wang et al. 2005c). A rough than a smooth fibre surface is favourable for cell attachment. Nanopatterning of biomaterial surfaces has been used as surface modification strategy to enhance protein activities, cellular functions and tissue responses. Coating the surface with extracellular matrix (ECM) proteins such as fibronectin, vitronectin, and collagen, provides an adhesive interface between the polymer scaffold surface and cells that resemble the native cellular milieu. It is one of the simplest surface modification methods. The cell-binding domain of fibronectin, vitronectin and collagen contains the tripeptide RGD (Arg-Gly-Asp) (Wang et al. 2005c). Stem cells from adipose tissue are found to attach better to scaffolds coated with peptide sequences derived from ECM laminin (Santiago et al. 2006). Surface modification is described in section 3.5.

3.3.3 Biocompatibility

Apart from biodegradable, the scaffold material has to be biocompatible as well, i.e., it has to allow cell growth and proliferation, and when implanted in vivo, should not lead to unwanted tissue response. Biocompatibility of a polymer can be assessed by in vitro tests before the material can be tested

in animal models. Toxic material is released in culture medium when cells are grown onto the polymer scaffold due to incorporation of toxic organic solvents. Cytotoxicity depends on manufacturing process of a polymer. Repeated washing of the culture medium is recommended in order to avoid cell death. The surface modification techniques described above also help promote the biocompatibility by enhancing cell-cell and cell-polymer interactions. We report cell culture results to test the biocompatibility of our polymer composite POSS-PCL in the chapter 7.

3.3.4 Porosity

Pores in the scaffolds play a vital role in the tissue generation. Interconnected pores are required for infiltration of the cells into scaffold, and to facilitate the exchange of nutrients and cellular waste products (Hou et al. 2003). Pore size requirements differ in different applications, for example, the minimum pore size required to regenerate mineralized bone is generally considered to be $\sim 100\ \mu\text{m}$ (Hulbert et al. 1970; Karageorgiou & Kaplan 2005); and for soft tissue engineering like small intestine, pore size widely used has been in the range of $250\ \mu\text{m}$ (Kaihara et al. 1999; Kim et al. 1999c). Whereas on one hand pore size $>50\ \mu\text{m}$ facilitate better nutrient and cell transport, on the other hand micropores in sizes around $<20\ \mu\text{m}$ are responsible for a greater surface area for protein adsorption, better ionic solubility in the microenvironment and cell attachment. In literature it has

also been shown that a combination of macro- and micro-pores have resulted in better drug delivery, strength and stiffness particularly in bone tissue engineering, as compared to non-microporous scaffolds (Hing et al. 2005; Woodard et al. 2007). The pore interconnectivity is also important in removing cellular waste products as well as facilitating neo-vascularisation within the scaffold to supply the new generating tissue. Pore interconnectivity is known to influence fluid permeation, cell migration, and tissue ingrowth. Optimizing pore size and interconnectivity poses a great challenge in tissue engineering and there is little information in the literature about the 'ideal' pore size and interconnectivity for various tissue engineering applications. In one of the studies, NaCl particles have been fused by subjecting them to 95% humidity prior to processing them in order to obtain better pore-interconnectivity (Murphy et al. 2002).

3.3.5 Mechanical Strength

Another factor in scaffold manufacturing is mechanical strength so that the scaffolds should be able to bear the stress load after implantation. Increased porosity and pore size in a scaffold should ideally result in increased tissue growth however it does compromise the mechanical strength of the scaffold. Although increased porosity and pore size facilitate tissue genesis, they result in reduction of mechanical properties of the scaffold due to change in its structural integrity. In a study on scaffold design (Hollister 2005), it is

shown that increasing the amount of material increases elastic properties while decreasing permeability for a particular scaffold design; however, for a given porosity, different scaffold microstructures will lead to different effective stiffness and permeability. The same study also shows that permeability decreases as expected with volume fraction and that for a given volume fraction the cylindrical pore design is more permeable.

Scaffolds need to be pliable for soft tissue engineering especially when tubular structures are required like in vascular or intestinal tissue engineering. Both PGA and PLA are crystalline polymers and PGA has higher crystallinity than PLA. We fabricated pure PGA and PLA macroporous scaffolds using simple salt leaching techniques but the scaffolds damaged macroscopically when attempts were made to roll the sheets into tubular structures. Studies have shown that blending PGA, PLA or their copolymers with substances like PEG have resulted into the desired pliability (Wake, Gupta, & Mikos 1996).

3.4 Fabrication Methods

3.4.1 Particulate Leaching

The solvent casting/ particulate leaching method is a simple and inexpensive way to fabricate scaffolds. In this technique, water soluble salt particles are mixed into a biopolymer solution. The mixture is then cast into the desired

shape mould and the solvent is removed by evaporation, or vacuum drying and lyophilisation (Liao et al. 2002).

Table 3.1: Main Scaffold Fabrication Techniques

| Technique | Main Advantages | Pitfalls |
|--|--|---|
| Particulate leaching/Solvent casting | Simple, inexpensive, Controlled pore size and porosity. | Irregularity of pores, repeatability less precise, residual particulate matter, toxic organic solvents, time consuming, limited scaffold thickness, limited to 2D structures, inability to incorporate protein based growth factors while processing. |
| Compression Molding | Better control of scaffold thickness and surface uniformity. | Thermal degradation of the polymer can occur. |
| Freeze drying | Avoids an extra step of washing/leaching, pore size can be increased by increasing polymer Mw and volume fraction of dispersed phase. | Pore morphology highly dependent on parameters like emulsion viscosity, polymer wt% and polymer Mw. Small pore size. |
| Phase separation/ Emulsification | Allows incorporation of bioactive agents. Does not require an extra leaching step | Inability to form large pores. Need of organic solvent. |
| Gas foaming | Avoidance of residual organic solvents/ or high temperatures. | Usually closed pore structure |
| Fibre Bonding | High porosity with interconnected pores, easy process | Presence of organic solvents could be toxic. May need several hours of vacuum drying before usable. Cells likely to be damaged if seeded during processing of scaffold. |
| Electrospraying & Electrospinning | Can produce ultrafine fibres in range of nanometers. | Limited thickness of scaffolds, less porosity. |
| Rapid Prototyping/ Solid freeform fabrication. 3 D printing or Direct Writing | Highly reproducible architecture. Precise control over pore-morphology and mechanical properties. Solvent-free and Porogen-free systems. Can include bioactive components like cells, growth factors and drugs during fabrication. | Expensive, Sophisticated equipment required, Relatively less porosity obtained as compared to the conventional techniques (~80%) |
| Extrusion/ Injection moulding | Straightforward technique for solid implants | Difficult to fabricate pliable scaffolds needing high porosity |

The water soluble salt particles are then leached out with water to leave a porous structure. Sodium chloride is the most commonly used salt, however other salts such as ammonium bicarbonate has also been used, which worked as an efficient gas foaming agent as well as a particulate porogen salt (Nam et al. 2000). Other salts include sodium citrate and sodium tartrate. In reported studies (Mikos et al. 1994), when 70-90 wt% salt was used, the membranes were homogeneous with interconnected pores. The membrane properties were independent of the salt type and were only related to the salt weight fraction and particle size. The porosity increased with the salt weight fraction, and the median pore diameter increased as the salt particle size increased. The advantages and disadvantages of this technique are well described in studies (Liao et al. 2002). As the amount and size of the salt particles can be adjusted, this technique offers an adequate control of the pore size and porosity of the scaffold. However, the distribution of the soluble salt is not uniform within the polymer solution, because of the difference between the density of the liquid polymer solution and that of the solid salt. Another problem often encountered is the complete wrapping of the salt particles by the polymer solution thus hindering the easy leaching of the salt particles when washed with water. Moreover, a skin like smooth, only minimally porous layer is formed on the cast surface of the scaffold, when the solvent of the polymer is removed. This layer can inhibit removal of salt and organic solvent. To overcome the above limitations, the authors

(Liao et al. 2002) mixed the salt particles in the solid state polymer and placed into a mould, introducing the solvent under negative pressure to flow through the voids of the mixture. Particulate leaching technique has also been seen to be modified in various reported studies. For example, waxy hydrocarbons (Shastri et al. 2000) or gelatin/ paraffin microspheres (Chen and Ma 2004; Draghi et al. 2005) have been used as porogens. After compacting the particulate hydrocarbon porogen with a viscous polymer solution in a Teflon mold, the mixture is subjected to extraction in hydrocarbon solvent, like pentane or hexane, that is a nonsolvent for the polymer but miscible with the polymer solvent. Sugar (Hou, Grijpma, & Feijen 2003; McGlohorn et al. 2004) and paraffin microspheres (Draghi et al. 2005) are other types of porogens used in some studies.

3.4.2 Electrospinning

Electrospun fibres have a greater specific surface area and a high porosity, hence has a better suitability for their application in fabrication of scaffolds. Electrospinning is capable of producing nano-scale fibres. Nano-scale fibres mimic the fibrous architecture of type 1 collagen, a component of extracellular matrix, and hence nanotechnology has gained widespread recognition in the field of biomaterials aiming for tissue engineering. Nano-scale fibres are believed to result in a higher cell adhesion due to the high surface-to-volume ratio provided by them.

3.4.3 Compression Molding

This is a technique where solid salt and polymer particles are mixed and then subjected to a compression in a mold at a high temperature (just above the melting or glass transition point of the polymer) and high pressure. The resultant composite is then removed from the mold after cooling to room temperature. Usually the composite is molded into cylindrical form, and then the cylinder is cut into discs of desired thickness before leaching in water. This technique is more likely to have a precise control of scaffold thickness and surface uniformity, as compared to the conventional solvent casting/particulate leaching technique (Liao et al. 2002). However, there can be a thermal degradation of the polymer when subjected to high temperatures, and can be concerning (Mikos and Temenoff 2002).

3.4.4 Gas Foaming

Most of the techniques utilized to fabricate porous scaffolds typically use organic solvents. The residual organic solvent in the scaffold can be harmful to the seeded cells or growth factors. To overcome the above hazards, Mooney et al (Mooney et al. 1996a) developed an alternative technique called gas foaming which employs high pressure carbon dioxide saturating the solid polymer discs at room temperature for around 72 hours. The

solubility of the gas in the polymer is then rapidly decreased by reducing the gas pressure to atmospheric levels. This creates a thermodynamic instability for the CO₂ dissolved in the polymer discs and results in the nucleation and growth of gas cells within the polymer matrix (Agrawal and Ray 2001). This technique has an advantage of obtaining porosity without using organic solvents. In a liquid polymer solution, gas bubbles can also be introduced by blowing an inert gas or using chemical blowing agents which liberate gas bubbles when heated. Gas foaming has been combined with particulate leaching when ammonium bicarbonate was used as salt. Literature shows that the mechanical properties were higher in scaffolds formed using gas foaming combined with solvent casting/particulate leaching when compared to those formed by standard solvent casting/particulate leaching process (Nam, Yoon, & Park 2000).

3.4.5 Fibre meshes with fibre bonding

As one of the earliest techniques to form constructs in tissue engineering, woven or knitted polymeric fibres have been widely accepted as useful scaffolds due to their property of large surface area for cell attachment and rapid diffusion of nutrients for cell survival and growth. Their structural instability *in vivo* was addressed by fibre bonding techniques (Mikos et al. 1993) where the authors removed PLLA from PGA-PLLA copolymer by selective dissolution leaving PGA fibres physically joined at their cross points.

This fabrication technique results in foams with porosities as high as 81% and pore diameters of up to 500 microns (Mikos et al. 1993).

3.4.6 Freeze Drying

Emulsion freeze drying (Whang et al. 1995) is a technique where an emulsion is created by homogenization of a polymer solvent solution and water, rapidly cooling the emulsion to lock in liquid-state structure, and removing the solvent and water by freeze drying. Although large pore sizes of more than 200 μm were seen in the resultant samples, the median pore size ranged from 15 to 35 μm . Scaffolds had good pore interconnectivity and porosity greater than 90%. However the precise control of processing parameters is crucial to obtain the desired pore morphology, such as, volume fraction of the dispersed phase (water), polymer weight%, and polymer molecular weight. The use of organic solvents still remains a hindering factor to incorporate protein based growth factors during processing. Freeze drying combined with particulate leaching, as shown in a study using sugar template (Hou, Grijpma, & Feijen 2003) may result in an architecture consisting of relatively large interconnected pores due to the leached template, and smaller pores resulting from freeze drying process.

3.4.7 Phase separation

Phase separation involves dissolving a polymer in a suitable solvent, placing it in a mould, and then cooling the mould rapidly until the solvent is frozen. The solvent is removed by freeze-drying, leaving behind the polymer as a foam with pore sizes of 1-20 μm in diameter (Akki et al. 1999).

3.4.8 Solid Free-Form fabrication (SFF)/ Rapid Prototyping (RP)

Complex scaffold architecture designs may be created either using image-based design approaches, or using approaches based on computer-aided design (Hollister 2005; Leong et al. 2003). The image based approach heavily employs computed tomography (CT) or magnetic resonance imaging (MRI), which design the scaffold exterior. However, designs can not be built readily using conventional techniques. Hence, scaffold architectures must be built using layer-by-layer manufacturing process known as Solid Freeform Fabrication (SFF) or Direct Writing or Rapid Prototyping. This technique usually incorporates the use of computer controlled four-axis machine with a multiple-dispenser head, or in other words a Rapid Prototyping Robot Dispensing (RPBOD) system, as called in one of the papers (Geng et al. 2005). Concentrated HA inks with tailored viscoelastic properties were developed to enable the construction of complex 3-D architectures comprised of self-supporting cylindrical rods in a layer-by-layer patterning sequence (Michna et al. 2005). Viscoelasticity of the polymeric ink is the most significant parameter in such 3D printing in order to allow the

construction of complex 3-D architectures comprised of self-supporting cylindrical rods in a layer-by-layer patterning sequence.

SFF techniques can be based on laser, such as, Stereo- Lithography Apparatus (SLA) and Selective Laser Sintering (SLS), or can be based on print technology, such as, 3D printing (Hutmacher et al. 2004). Other forms of SFF include assembly technology-based systems such as Shape Deposition Manufacturing (SDM), or extrusion technology-based systems such as Fused Deposition Modelling (FDM), 3D plotting, Multiphase Jet Solidification (MJS) and Precise Extrusion Manufacturing (PEM). SLA uses UV laser that polymerises the liquid polymer material, which is then repeated in order to build up the design model, layer by layer (Hutmacher, Sittinger, & Risbud 2004). SLS uses a CO₂ laser beam to sinter thin layers of powdered polymeric materials, forming solid 3D objects. 3D printing (Giordano et al. 1996) uses an inkjet print head to deposit the binder solution to the selected regions of the layer of powder (polymer) bed. After the 2D layer is printed, a fresh layer of powder is laid down. Such steps are repeated a selected number of times to produce successive layers of selected regions of bonded powder material so as to form the desired component. The unbonded powder material is then removed. In some cases the component may be further processed as, for example, by heating it to further strengthen the bonding thereof. SDM involves the fabrication of a layered scaffold in a customized geometry by processing the clinical imaging data and translating

it to the desired scaffold layer by a computer-numerically-controlled cutting machine. FDM employs the concept of melt extrusion of heated biomaterial through a small nozzle in order to obtain a layer of scaffold containing parallel material roads (Leong, Cheah, & Chua 2003). Changing the laydown pattern while adjusting the space between material roads, can provide the desired pore morphology with good interconnectivity (honeycomb pattern). The 2D structure thus obtained can be deposited onto the consecutive layers by changing the direction to obtain a 3D design.

3.5 Surface modification of scaffolds

Most of the biodegradable synthetic polymers (like PGA and PLA) are hydrophobic and may require modifications on their surface for better cell attachment. This can be achieved by surface coating, chemical coating, plasma treatment, or modifying the fabrication of scaffold itself (Wang, Cui, & Bei 2005c). Incorporation of a signal peptide into the biomaterial (scaffold) has attempted to mimic the extracellular matrix, modulate cell adhesion, and induce cell migration (Shieh & Vacanti 2005). A rough than a smooth fibre surface is favourable for cell attachment. Nanopatterning of biomaterial surfaces has been used as surface modification strategy to enhance protein activities, cellular functions and tissue responses. Coating the surface with extracellular matrix (ECM) proteins such as fibronectin, vitronectin, and collagen, provides an adhesive interface between the polymer scaffold

surface and cells that resemble the native cellular milieu. It is one of the simplest surface modification methods. The cell-binding domain of fibronectin, vitronectin and collagen contains the tripeptide RGD (Arg-Gly-Asp) (Wang, Cui, & Bei 2005c). Stem cells from adipose tissue are found to attach better to scaffolds coated with peptide sequences derived from ECM laminin (Santiago et al. 2006).

Examples of other coating methods include: chitosan nanoscaffolds modified with a sugar unit (Phongying et al. 2006), electrostatic coating of hyaluronic acid and chitosan onto polymeric scaffolds making them protein resistant (Croll et al. 2006; Mao et al. 2003), and coating of IGF 1 (insulin like growth factor) to collagen scaffolds showing increased osteoblast proliferation (Schleicher et al. 2005).

In one of studies investigating tissue engineering of oesophagus, a biodegradable and flexible poly(L-lactide-co-caprolactone) (PLLC) copolymer was surface modified using aminolysis by 1,6-hexanediamine to introduce free amino groups. Using these amino groups as bridges, fibronectin and collagen were subsequently bonded with glutaraldehyde as a coupling agent. Protein-bonded surface presented to be more hydrophilic and homogeneous. In vitro long-term (12d) culture of porcine esophageal cells proved that fibronectin- and collagen-modified PLLC surface could more effectively support the growth of smooth muscle cells and epithelial cells (Schleicher et al. 2005; Zhu et al. 2006).

Self assembling peptide hydrogel scaffolds have been shown in many studies to effectively promote cell-material and cell-cell reactions enabling significant improvements in generating bone (Bokhari et al. 2005), cartilage (Kisiday et al. 2002), cardiovascular (Narmoneva et al. 2005) and neural tissues (Ellis-Behnke et al. 2006). These are basically amphiphilic peptides that have alternating repeating units of positively-charged lysine or arginine and negatively-charged aspartate and glutamate residues. These peptides contain 50% charged residues and are characterized by their periodic repeats of alternating ionic hydrophilic and hydrophobic amino acids; thus, the interaction between the distinct polar and non-polar surfaces facilitates self-assembly of the material into a nanofiber hydrogel scaffold which can coat surfaces or encapsulate cells as a 3-D weak gel (Holmes et al. 2000;Kisiday et al. 2002;Zhang 2002).

In the field of small intestinal tissue engineering, most studies have used synthetic polymers, commonly PGA (Gardner-Thorpe et al. 2003;Grikscheit et al. 2004;Kim et al. 1999a;Kim et al. 1999b;Ramsanahie et al. 2003;Tavakkolizadeh et al. 2003), and some have used SIS (Chen & Badylak 2001;Demirbilek et al. 2003;Wang, Watanabe, & Toki 2003) or collagen sponge (Hori et al. 2001). In majority of studies using PGA, the polymer was coated with 0.1-1 % collagen type I. As shown in one of the studies, a significant improvement was seen in cell engraftment, and larger cysts were formed when collagen was coated (92.9% v 63.6%) (Choi et al.

1998). SIS due to its richness in collagen has obviously an advantage over polymers to be used as a scaffold as far as cell attachment is concerned. All studies investigating small intestinal tissue engineering have used in vivo implantation of cell-polymer constructs. How intestinal epithelial units can be expanded ex vivo prior to their implantation is not clear and not published so far. All studies incorporating the use of intestinal epithelial units as the cell source have used only PGA polymers with or without PLLA. It is also not clear whether use of other synthetic polymers or natural polymers in a similar setup would have resulted in different results. Regulation of epithelial cell proliferation, migration and differentiation under physiological conditions is poorly understood. A better understanding of how the intestinal epithelial cells interact with their underlying basement membrane is required. A likely mechanism of this interaction as suggested by Beaulieu J F is through integrins, a specific subset of cell surface binding proteins (Beaulieu 1992). The epithelial basement membrane (BM) of the human intestine contains all major components specific to most BMs such as type IV collagens, laminins, and proteoglycans. However, a direct cause-to-effect relationships between particular integrins and specific cell functions, and the signalling molecules specifically involved need to be ascertained (Beaulieu 1992).

3.6 Discussion

An ideal scaffold should be highly porous, and biocompatible with a

controlled degradation rate; should have an appropriate surface for cell adhesion, proliferation, and differentiation; and should maintain mechanical properties.

Although macroporous scaffolds are generally accepted as ideal for soft tissue engineering, the size of the pore can depend on the size of the cell seeded. Interconnected pores larger than the cell size are generally required for infiltration of the cells into scaffold. Whereas on one hand pore sizes of greater than 50 μm facilitate better nutrient and cell transport, on the other hand micropores in sizes less than 20 μm are responsible for a greater surface area for protein adsorption, better ionic solubility in the microenvironment and cell attachment. In literature it has also been shown that a combination of macro- and micro-pores have resulted in better drug delivery, strength and stiffness particularly in bone tissue engineering, as compared to non-microporous scaffolds (Hing et al. 2005;Woodard et al. 2007). Pore size requirements differ in different applications, for example, the minimum pore size required to regenerate mineralized bone is generally considered to be around 100 μm (Hulbert et al. 1970;Karageorgiou & Kaplan 2005); and for soft tissue engineering like small intestine the pore size most widely used has been in the range of 250 μm (Kaihara et al. 1999;Kim et al. 1999c), mainly because of the large size of intestinal epithelial organoid units used as the cell source.

Our laboratory has already demonstrated the advantages and the successful applications of silica nanocomposite based polyurethanes in producing vascular tissue engineered grafts, such as improved cell adhesion characteristics using a silicon pendant nanocage (Kannan et al. 2006b). PCL in our experience has been less expensive, and easily dissolvable in commonly available organic solvents unlike PGA which is very hard in consistency and requires highly fluorinated solvents such as hexafluoroisopropanol. Our nanocomposite maintains mechanical stability due to nanocages while simultaneously allowing controlled degradation.

In this chapter, we analysed different methods available to fabricate scaffolds, and also attempted to address pitfalls associated with them. Although Solid Freeform Fabrication (SFF) techniques offer the most reliable methods to design and fabricate complex 2D and 3D scaffolds with more or less precise reproducibility and control over pore morphology, they are not free from shortfalls. Due to shrinkage after processing, Stereo Lithography Apparatus (SLA) has a compromised resolution, and due to scattering of laser beam, there can be deformation of the smaller scaffolds (Hutmacher, Sittinger, & Risbud 2004). Selective Laser Sintering (SLS) also has a potential problem of material shrinkage when sheet like structure is desired, and porosity may not be obtained as desired. 3D printing is vastly explored and in fact is one of the most promising methods to produce accurate design of scaffolds; however the resolution of the 3D printer is limited by the nozzle

size and the inkjet print head movement. Polymers may need special processing techniques to make them in powder form prior to 3D printing, and the particle size of the powder governs the layer thickness (Giordano et al. 1996;Hutmacher et al. 2004). Fusion Deposition Modeling (FDM) is one of the most investigated SFF methods, and has been quite successful in producing scaffolds (Hutmacher et al. 2001;Zein et al. 2002) using biopolymers as well as ceramics, but the technique is not without limitations. High processing temperatures and hence limited material range, inconsistent pore opening in different directions, and requirement of support structures for irregular shapes are some of the limitations (Leong, Cheah, & Chua 2003). The combination of toxic organic solvents and extreme temperatures, for example, in fiber bonding technique, presents difficulties if cells or bioactive molecules, such as growth factors, are to be included in the scaffold during processing. Another issue can be the choice of solvent, as suggested by a study (Sander et al. 2004), which suggests that solvent choice can create small but significant differences in scaffold properties, and that the rate of evaporation is more important in affecting scaffold microstructure. For example, specimens fabricated in methylene chloride were the stiffest, followed by acetone and then chloroform.

Particulate leaching/ solvent casting is a simple and inexpensive method to fabricate 2D scaffold sheets of desired thickness. Different porosities and pore sizes can be obtained. The sheets can be rolled in a tubular structure if

needed to simulate structures like vessels or intestine. One of the significant disadvantages of solvent casting/ particulate leaching, and other techniques including phase separation, fiber bonding and gas foaming, is the need of organic solvent which can be cytotoxic, and hence there is a need to remove the solvent which can take long processing time. The newly developed techniques of rapid prototyping/ solid freeform fabrication can certainly be the answer to the above problems as they are usually porogen free and solvent free. They can be used to result in highly reproducible architecture, there is a precise control over pore-morphology and mechanical properties, and the technique can include bioactive components like cells, growth factors and drugs during fabrication. However, these techniques are expensive, sophisticated equipment is required, and relatively less porosity is obtained as compared to the conventional techniques. Methods commonly employed in characterization of scaffolds include SEM and mercury intrusion porosimetry (MIP). SEM is a simple and relatively inexpensive tool to show surface topography of a 3D scaffold in form of pore size, pore density, pore structure, and pore interconnectivity to an extent. However, only 2D analysis and destruction of the scaffold sample are the limitations associated with it. Despite these limitations, SEM remains the most widely accepted characterization method of choice. MIP offers a better idea of the porosity of the scaffold sample as a whole. Relatively newer tools such as micro-CT has been quite successful to demonstrate pore morphology, mainly pore-interconnectivity, but quantification of pore-interconnectivity has not been

simple, as it requires use of complicated computer software to analyse data.

Following our review of literature, we experimented our laboratory made nanocomposite POSS-PCL for its fabrication characteristics using two main techniques: solvent casting/particulate leaching and electrohydrodynamic atomisation. These experiments are described in chapters 5 and 6 respectively.

Chapter 4: Materials and Methods

4.1 Introduction

Experiments were carried out exploring biodegradable nanocomposite developed in our laboratory to form scaffolds for small intestinal tissue engineering as described in the following three chapters. First experimental chapter includes synthesis of nanocomposite, its characterisation, and fabricating porous scaffolds using solvent casting/particulate leaching technique. These porous scaffolds were then characterised for their mechanical strength, porosity, and chemical structure. In the second experimental chapter, electrohydrodynamic atomisation technique was employed to attempt fabricating porous scaffolds. In the third experimental chapter, these scaffolds were tested in vitro for intestinal epithelial cell growth.

Our laboratory has developed a biodegradable nanocomposite by incorporating the biostable polyhedral oligomeric silsesquixane (POSS) nanocages into a poly(caprolactone/carbonate)urethane urea. They are approximately 6 nm in size. The molecular structure of nanosized silicon-oxygen cages (POSS) is shown in **figure 4.1**.

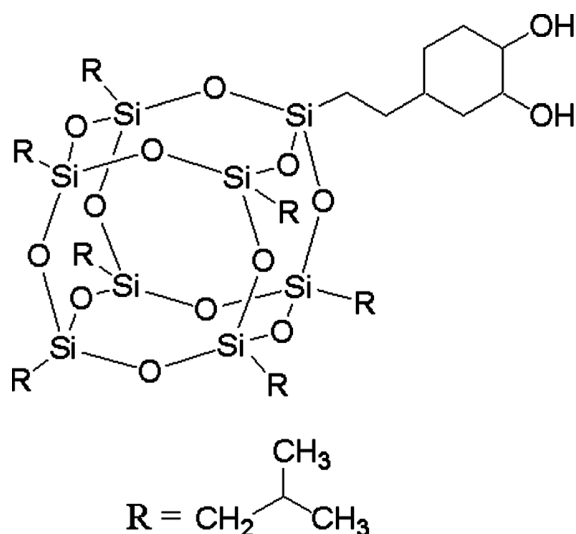


Figure 4.1: Molecular structure of trans-cyclohexane diol isobutyl-POSS.

Our nanocomposite is polyurethane which has a soft segment composed of polycaprolactone (80%) and polycarbonate (20%), and hard segment composed of urea. The polymer is approximately 22% by wt hard segment. Eighty percentage of polycaprolactone diol (mwt) was considered an appropriate initial formula for use as a tissue engineering scaffold for small intestine or cartilage. Such a scaffold would be required to maintain its structural integrity for at least 4–6 months (Raghunath et al. 2008). PCL is relatively slow to degrade as compared to PGA or PLLA, which is an added advantage in tissue engineering of soft structure like small intestine where a slow degradation is required over a period of few months rather than weeks. It is proposed that caprolactone will provide controlled degradation whilst the POSS nanocages will contribute to the mechanical strength required for a tissue engineering scaffold for soft tissue such as small intestine.

4.2 Synthesis of POSS-PCL nanocomposite

Dry polyol blend (80% by wt polycaprolactone diol and 20% by wt polycarbonate diol) and trans-cyclohexanediolisobutyl-polyhedral oligomeric silsesquioxane (POSS) were placed in a 250ml reaction flask equipped with mechanical stirrer and gas inlet. The mixture was heated to 130°C to dissolve the POSS cage into the polyol and then cooled. Subsequently, flake MDI was added to the polyol blend and then reacted, under nitrogen, at 70°C - 80°C to form a pre-polymer. Dry DMAC was added slowly to the pre-polymer to form a solution, which was cooled to 40°C. Chain extension of the pre-polymer was carried out by the drop wise addition of a mixture of ethylenediamine and diethylamine in 80g of dry DMAC. After completion of the chain extension 1-butanol in DMAC was added to the polymer solution to form a 2% polyhedral oligomeric silsesquioxane – polycaprolactone (POSS-PCL) solution. The resultant polymer solution was 20 wt % in DMAC. All chemicals and reagents were purchased from Aldrich Ltd., Gillingham, UK.

4.3 Characterisation of polymer solutions

20 wt% polymer in DMAC were used in all experiments. The surface tension, viscosity and electrical conductivity, properties which affect electrohydrodynamic behaviour, were measured. Surface tension was measured using a Kruss Tensiometer K9 (Du Novy's ring method). Viscosity

was estimated using a Visco-Easy rotational viscometer. Electrical conductivity was assessed using a HACH SensION[™] 156 probe. All measurements were performed at the ambient temperature and all instruments were calibrated before use.

4.4 Preparation of scaffolds using particulate leaching/solvent casting

We intended to develop scaffolds with two pore sizes: 150-250 microns (macroporus) and <150 microns (microporous). Dried NaCl was sieved in the desired pore size range using stainless steel sieves (Fisher Scientific, U.K). 10 wt. % POSS-PCL in DMAC was used in all experiments. Two different salt concentrations - 40 and 80 weight percentages in polymer were used for both macroporous and microporous salt sizes. Both salt sizes were mixed in one of the samples to obtain a mixed pore sized sample. Control sample was prepared without any salt in it. Salt was mixed in the polymer solution using a hand held homogeniser (Ultra-Turrax T25 from IKA labortechnik, Staufen, Germany) and then poured over stainless steel plates to spread. The mixture was left in the oven at 50° C for 20 hours. The sheets of polymer were peeled off the plates and kept in de-ionised water for 48 hours with a regular change of water at 4 hourly intervals. After 48 hours the polymer sheets were air dried and specimen from the samples were studied for their physical and chemical properties.

4.5 Extrusion – Coagulation combined with Solvent Casting/

Particulate Leaching

Extrusion-coagulation or extrusion-phase inversion is a process where exchange between solvent and non-solvent takes place resulting in formation of pores. In this process a casting solution consisting of polymer and solvent is immersed into a nonsolvent coagulation bath (Young and Chen 1995). Interchange of solvent and nonsolvent due to diffusion causes the casting solution to go through a phase transition by which the membrane is formed. Pore size and its distribution, can be controlled for each specific application depending on the choice of the polymer, solvent, non-solvent and preparation parameters. Liquid-liquid phase separation in miscible polymer solution can be caused by variation in temperature and/or composition of the mixture. When a homogeneous solution becomes thermodynamically unstable, the solution can decrease its free energy from mixing by dividing into two liquid phases of different composition, i.e., a nucleus of the polymer-poor phase that forms the nascent pore and a polymer-rich phase that surrounds the pore. Hence, a nascent pore comprises the polymer-poor phase surrounded by the polymer-rich phase.

We used the salt mixed nanocomposite as the polymer having DMAC as solvent; and de-ionised water as the non-solvent. We used 80 wt % NaCl in

the size range of 150-250 microns in sample 1, and NaHCO_3 salt particles in the range of <50 microns in sample 2. Sample 3 was extruded without any salt in it serving as a non-porous control. A mechanical arm was positioned such that it held a 5 mm diameter stainless steel cylindrical mandrel within the exit aperture of a stainless steel polymer chamber. This latter structure comprised a circular 5 mm entry aperture superiorly; a luer-lock syringe compatible polymer introduction channel laterally; a 6 mm circular exit aperture inferiorly; and a PTFE sliding cover for the exit aperture (Sarkar et al. 2009a). The mandrel cross-section was aligned perfectly concentric with respect to the exit aperture. With the mandrel's base level with the exit aperture, the PTFE sliding cover was closed before 3.5 ml of nanocomposite that was injected slowly into the polymer chamber. For this step it was imperative that the syringe contained no air bubbles. A vertical column of coagulant solution was placed directly below the sliding cover leaving a 5 mm gap between the two. The cover was opened and the mandrel driven vertically into the coagulant at 10 mm/s immediately afterwards. The column was undisturbed for 20 min then placed in a separate chamber having de-ionised water for 48 hours. Thereafter, the mandrel was removed from the coagulant, dried and the scaffold tube removed from the mandrel. Scanning electron microscopy was used to visualise the details of the wall cross-section and pores.

4.6 Characterisation of Scaffolds

We used scanning electron microscopy as our main tool to aid characterisation of the porous scaffolds, particularly to look into the pore morphology like pore size, pore-pore interconnectivity, and pore shape. To measure porosity in percentage, we used the formulae given below, where density of the polymer was first calculated and then of the scaffold. Further pore morphology and interconnectivity was studied using micro CT as described in section 4.6.3.

4.6.1 Porosity of Scaffolds

The porosity of the scaffolds was calculated by using simple formulae:

$$P = 1 - \frac{d}{d_p}$$

Where P is the porosity of the scaffold sample, d is the density of the scaffolds, and d_p is the density of the nonporous polymer. Density of the scaffold d was calculated from:

$$d = \frac{m}{v}$$

Where, m is the mass and v is the volume of the scaffold. The volume, v was calculated using thickness and diameter of the scaffolds obtained when

casted over circular steel plates.

4.6.2 Scanning Electron Microscopy (SEM)

SEM provides a high resolution, highly detailed views of a surface of scaffold, however it is limited to the 2D measurements. Moreover, although the pore-interconnectivity can be seen in the 2D views, its quantification is not easy to perform unless the number and size of pores inside the pores, is measured (Murphy et al. 2002). Pore interconnectivity has been better quantified using micro-Computed Tomography (micro CT) (Moore et al. 2004). The samples were attached to aluminium stubs with double sided sticky tabs and then coated with gold using an SC500 (EMScope) sputter coater before being examined and photographed using a Philips 501 scanning electron microscope at 15KV.

4.6.3 Micro-CT

Scanning Electron Microscopy and Mercury Intrusion Porosimetry have a disadvantage of sample destruction. Micro-CT has an advantage of non-destructiveness and 3D image analysis including structural measurements (Filmon et al. 2002; Moore et al. 2004). X-ray microtomography is a non-destructive technique to provide internal and microstructural details of an object. There is no need for extensive sample preparation, and three-

dimensional information can be obtained at high spatial resolution. Polymer scaffolds with high void fractions are analysed for the volume of their void space remaining accessible to outside air at increasing minimum connection sizes. The accessible volume is the pore volume that is accessible, from the outside, to an object of selected diameter. The scaffold microstructure can then be assessed quantitatively with the use of a computer programme of image display and analysis. The accessible void fraction can be calculated as the number of air voxels maintaining connections with the outside air as a percentage of the total air voxels. Micro-CT data can be reconstructed to obtain 3D structure of cross sectional images taken at a mere 8 μm distance throughout the thickness of the scaffold.

In this study, although the pore morphology was mainly studied by SEM and the porosity was calculated by using formula mentioned above, however for one sample (sample 1), porosity and pore size of the scaffolds were also investigated by X-ray microtomography, in order to validate the results. The porous scaffold sample was examined using a SkyScan-1072 high resolution desktop X-ray microtomography system (Skyscan, Belgium). The X-ray radiographs were collected at 20kv/120 μA with 0.5mm Al filter, a 8 μm pixel size, 0.23° angle step (0° to 180° rotation) and 3 frame averages per acquired radiograph. A cone-beam accusation was selected and cone-beam volumetric reconstruction (Feldkamp algorithm) was employed for image reconstruction. During the image reconstruction process, the beam

hardening correction parameter was set to 20 ~ 30%, depending upon the individual sample. Each original reconstructed image contained 1024x1024 pixels. The porosity and pore size were calculated and analysed using CTAn software as the mean value of 100 sections studied.

4.6.4 Mechanical Properties

Mechanical tests were performed in uniaxial tension on a ZWICK BDO-FB.5TS tester (Ulm, Germany) unit at room temperature. Specimens in the form of flat dumbbells with a 40-mm-long working part were loaded at a constant tension rate of 100 mm/min. Thickness of samples was measured using a digital electronic outside micrometer (UKAS Calibration, Corby, U.K) at three places of the dumbbell and averaged. Stress-strain relationships were obtained for the samples and graphs were plotted.

4.6.5. Fourier transform infrared spectroscopy (FTIR)

Infrared spectra of a porous and nonporous scaffold were recorded on a Perkin-Elmer 1750 FTIR spectrometer equipped with a triglycine sulphate detector. Spectral data were acquired from a 10 μ l volume gas tight CaF_2 cell (path length 6 μ m) and the temperature of recorded spectra was 25°C. A sample shuttle was employed to permit the sample to be signal-averaged with the background. For each sample, 200 scans were signal averaged at a

resolution of 4 cm^{-1} .

4.7 Electrohydrodynamic print-patterning for development of scaffolds

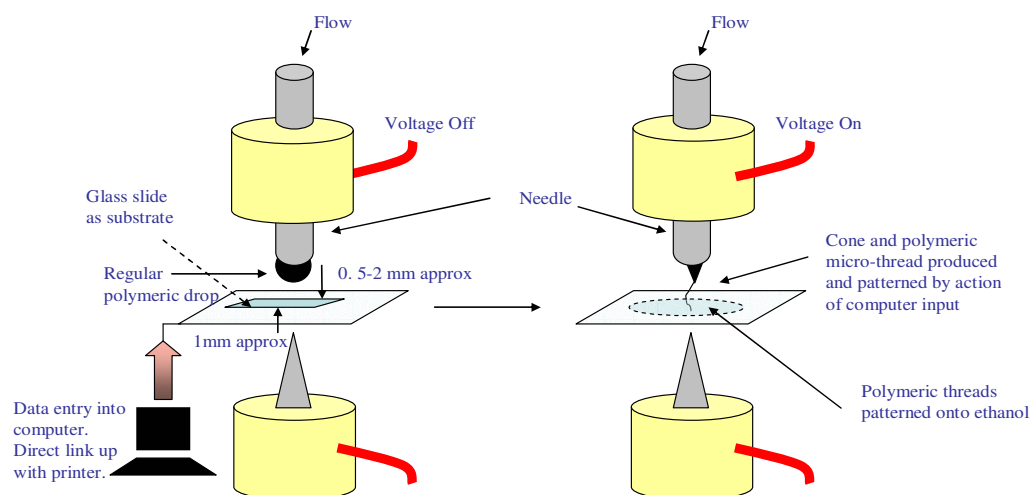


Figure 4.2: Schematic illustration of the electrohydrodynamic process

Electrohydrodynamic jetting is a process where a liquid medium forms a jet and breaks into droplets as it is released at a controlled flow rate through a needle while being exposed to an electric field caused by the existence of a potential difference between the needle and a ground electrode (Rayleigh 1878; Taylor 1964; Zeleny 1917) (figure 4.2). This method was first adapted for the processing of advanced materials in 1997 (Teng et al. 1997).

POSS-PCL solution was printed onto standard microscope glass slides (75mm x 25 mm) using a needle of internal diameter 750 μ m and an applied voltage in the range of 8.0 to 10.0 kV, which was further optimised depending on the type of polymer used and the presence or absence of ethanol on the glass slide as a substrate. The distance between the needle exit and the glass slide was also carefully adjusted from ~500 μ m to ~2mm depending upon the above mentioned two variables. The flat-bed printing speed was kept constant at 10m/s. Using Motion Planner software, the computer was programmed to generate a 10x10 mm square sheet in the X-Y plane, with the distance between the grid lines (scaffold window size) set at 250 μ m. Assuming that all the droplets of polymer may not deposit over their predecessors, and also as the diameter of the material forming the structure would occupy some of the pore space, we increased the window size from 250 to 500 μ m, in order to eventually achieve ~250 μ m. The schematic representation of electrohydrodynamic printing is shown in **figure 4.3**

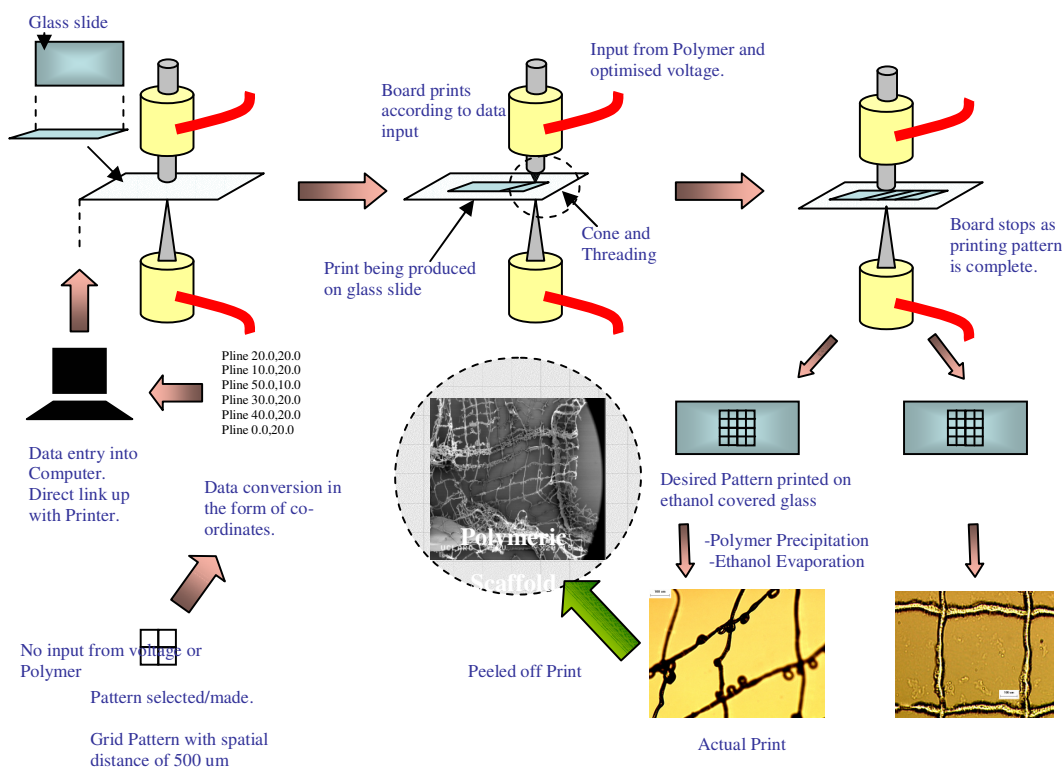


Figure 4.3: Schematic representation of electrohydrodynamic printing.

The program was set up so that the pattern was repeated in the Z direction up to 20 and then 50 times, with an intention of obtaining $\sim 500\mu\text{m}$ to 1 mm thick scaffold, assuming the printing generates material strands of diameter 15-50 μm . The polymer solution wetted and spread on the glass slides even at a very low infusion rate of $1\mu\text{litre/hour}$, and hence only a drop of polymer was mechanically pushed through the needle onto the glass slide. However, when over-printing in the Z-direction was explored, the sample dried after about 5-6 repetitions as enough polymer did not emerge through the needle tip. In any case, the resultant sample could not be peeled off the glass slide

as it was not sufficiently thick. In another set of experiments, the same printing technique was used to collect polymers on a glass slide having a layer of ethanol. The latter samples could be peeled off the glass slides. Firstly, printed scaffolds were studied under low magnification (5x) with a Nikon Eclipse optical microscope. Subsequently, samples were also investigated using a JEOL JSM-6301F scanning electron microscopy operating at an acceleration voltage of 5-10 kV. Samples were sputter coated with gold prior to electron microscopy. The equipment used consisted of a stainless steel needle with an internal orifice diameter of 750 μm . It was held in epoxy resin and a point-like electrode was held directly below the axis of the needle. The needle was connected to a high voltage power supply (Glassman Europe Ltd., Tadley, UK), which was capable of applying up to 30 kV. The inlet of the needle was connected to a Harvard PHD 4400 programmable syringe pump (HARVARD Apparatus Ltd., Edenbridge, UK) using a silicone rubber tube, allowing the flow rate of liquid to the needle exit set to $\geq 1\mu\text{l}/\text{hour}$. This equipment was coupled together with servomotor drive in the x and y directions and stepper-motor drive in the z direction. The three-axis system was controlled using a programmable motion controller, which communicates directly with a personal computer. A perspex table was mounted firmly on the y-axis cradle. The top of the table accommodates a frame for the substrate. The frame was fitted to the base of the table using four polyethylene terephthalate stilts. Three pieces of software were used for generating the final geometry. Initially TurboCad was used and subsequently

CompuCAM translates the computer aided design file into the Motion Planner software. Eventually, this software is downloaded to the three-axis controller using x, y, and z coordinates.

4.8 Cell Work

The following flow chart (**figure 4.4**) summarises the sequence of in vitro experiments to grow rats' intestinal epithelial cells (IEC-6) on polymer scaffolds.

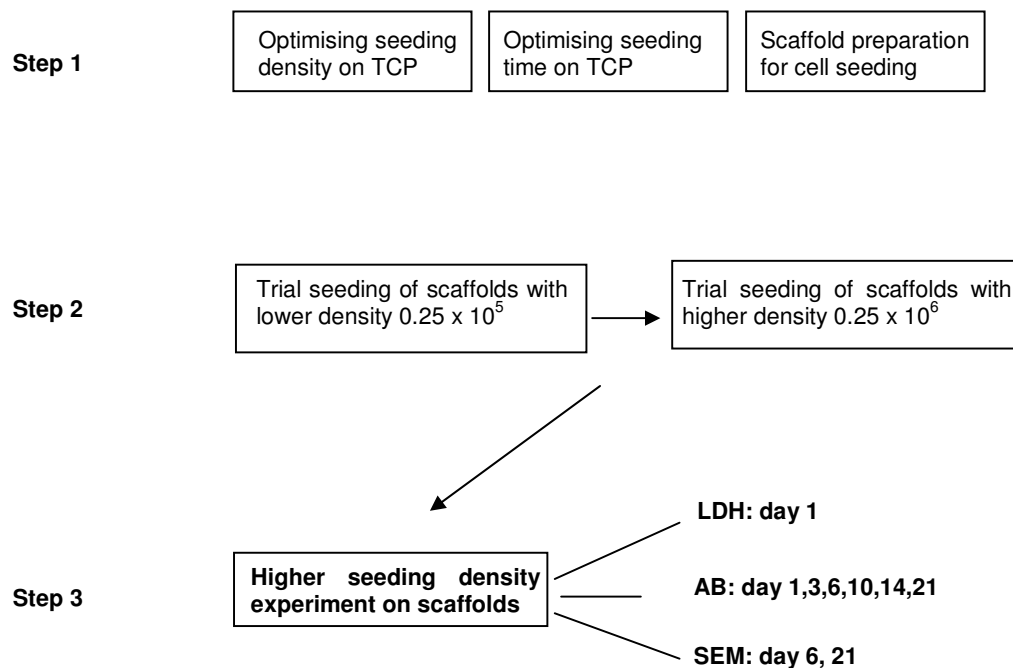


Figure 4.4: An overview of cell culture experiments. TCP = Tissue Culture Plastic; LDH = Lactate Dehydrogenase; AB = Alamar Blue; SEM = Scanning Electron Microscopy

4.8.1 Optimising seeding density for IEC-6 cells on tissue culture plastic without scaffolds

As a preliminary step an optimum cell density was obtained by culturing rat's intestinal epithelial cells (IEC 6 cell line, ECACC, Salisbury, U.K.) on tissue culture plastic without using scaffolds. Cells were counted and diluted to obtain 2, 1, 0.5, 0.125, 0.0625, 0.03125 x 10⁵ cells per ml of culture medium {DMEM supplemented with 0.1 IU/ml Insulin and 5% Foetal Bovine Serum plus penicillin at 100U/ml and streptomycin at 10µg/ml (all Invitrogen, Paisley, U.K.)}. Six wells of a 24 well plate (BD Falcon, Oxford, U.K.) were seeded for each concentration above and one left as blank. They were seeded overnight. The next day (Day 1), medium was removed, washed with PBS and 1 ml 10% Alamar Blue (AB) was added. AB was left for four hours and then removed. Duplicate samples of 100µl were read on fluorescent plate reader. AB assay was repeated on Day 4, Day 7, and Day 14.

4.8.2 Optimising seeding time for IEC-6 cells on tissue culture plastic without scaffolds

Two cell concentrations 1 x 10⁶ cells /ml and 0.25 x 10⁶ cells /ml, were seeded (n=6 each) on tissue culture plastic without scaffolds in 24 well plates. Alamar Blue assays were performed at time points 2, 3, 4, 6 and 24

hours (n=6 each) on Day 1 and Day 3 with a blank row. At each time point non-adherent cells were removed, washed with 1 ml PBS and 1 ml fresh medium was added.

4.8.3 Scaffold preparation for cell seeding

Scaffold sheets were cast by solvent casting and salt leaching in order to obtain desired porosity, as described earlier, and thoroughly washed in distilled water. Circular discs of 15mm diameter from each sample were then cut using a metal die. Discs were then autoclaved to sterilise them.

4.8.4 Trial seeding of scaffold samples with lower density of 0.25×10^5 cells

Scaffold samples and controls were seeded overnight with 0.25×10^5 cells in 24 well plates. On Day 1 (next day), 500 μ l AB was added for 4 hours to each well after washing with PBS. Single 100 μ l samples were read on fluorescent plate reader. AB assay was repeated on Day 3 and Day 7.

4.8.5 Trial seeding of scaffold samples with higher density of 0.25×10^6 cells

Two samples each of scaffolds were cut and used for cell culture in 24 well plates. 0.25×10^6 cells per ml concentration was used for trial seeding of the grafts. 1 ml was added to each well with controls. Cells were allowed to seed

overnight on the scaffolds. Alamar blue assays were done on samples above and the samples were read in duplicates (day 2). Alamar Blue assays were repeated on Day 8.

4.8.6 Higher cell density seeding of scaffolds washed with stringent washing regime

In this set of experiments, a more stringent regime of washing the scaffold samples was used before seeding them with cells. Scaffolds were rinsed in deionised water for 72 hours on a shaker with changes of water every 4 hours. A higher cell density of 0.25×10^6 was used to seed scaffold samples (n=6 each) plus blanks and positive controls. All experiments were carried out in 24 well plates. Samples were left overnight to seed. Plastic inserts were used to avoid floating of the scaffold sample in the medium. Tissue culture plastic wells with no scaffold in were seeded with an identical amount of cells as a positive control. Wells with scaffold but no cells were employed as a negative control. Cells were allowed to attach for 24 hours after which the medium containing unattached cells was removed for lactate dehydrogenase (LDH) analysis to assess initial cell damage. The seeded scaffold discs were then transferred to a fresh 24 well plate (to avoid the possibility of measuring cells seeded onto the initial well bottom during the seeding process) and cell metabolism assessed using an Alamar blueTM assay. AB was added for 4 hours and single 100 µl samples were read on

the fluorescent plate reader. 1 ml fresh medium was replaced in each well. On Day 3 and Day 6, same was repeated except no samples were collected for LDH. On Day 6, one set of samples (6th sample from each scaffold) was saved for SEM (scanning electron microscopy). On Day 9 LDH assay was repeated and samples of scaffold were dismembrated and weighed. Alamar Blue assays were repeated on Day 10, 14, and 21. One set of scaffold samples was collected for SEM analysis.

4.8.7 Assessment of Initial Cell Damage by LDH analysis

LDH was measured using a CytoTox 96[®] Non-Radioactive Cytotoxicity assay kit (Promega, Southampton, U.K.). LDH is a stable cytosolic enzyme released upon cell lysis into the cell culture medium. The amount of LDH released is measured using a 30-minute coupled enzymatic assay based on the conversion of a tetrazolium salt INT (2-p-iodophenyl-3-p-nitrophenyl-5 – phenyl tetrazolium chloride) into a red formazin product, with the amount of colour formed being proportional to the number of lysed cells. 50µl cell culture medium from each sample was transferred to a 96 well plate (Helena Biosciences, Sunderland, U.K.). 50µl Substrate Mix (1 vial substrate plus 12mls assay buffer) was added to each well and the plate covered in foil to prevent light access. Samples were then incubated at room temperature for 30 minutes after which the reaction was stopped by the addition of 50µl stop solution (1M acetic acid). Absorbance was then read at 450nm using a

Multiscan MS UV visible spectrophotometer (Labsystems, Ashford, U.K.).

4.8.8 Assessment of Cell Growth and Metabolism by Alamar blueTM assay

Alamar blueTM (Serotec, Kidlington, U.K.) is a commercially available assay which aims to measure quantitatively cell proliferation, cytotoxicity and viability. This is achieved by incorporating resazurin and resarfurin as colorimetric oxidation reduction indicators. These indicators respond to chemical reduction resulting from cell metabolism by changing colour. This colour change may be measured by monitoring fluorescence (excitation at 530nm, emission at 620nm). The advantages of this assay are that it is soluble in media, stable in solution, minimally toxic to cells and produces changes that are easily monitored.

Alamar blue was added to cell culture medium at a concentration of 10% (v/v). At each time point polymer samples were washed with 1 ml PBS and transferred to a fresh 24 well plate to prevent the possibility of measuring cells growing on the bottom of the plate. 0.5 ml of the Alamar blue/cell culture medium mixture was then added to each sample and the positive control wells. 0.5 ml of the mixture was placed into each of the negative control samples. After 4 hours a 100µl sample of the mixture was removed and the absorbance at fluorescence (excitation at 530nm, emission at 620nm) measured in a 96-well plate (Helena Biosciences, Sunderland, U.K.)

using a Fluorscan Ascent FL spectrophotometer (Thermo Labsystems, Ashford, U.K).

4.8.9 Statistical analysis

Statistical analysis of the results was performed using GraphPad Prism version 5 software. The groups were analysed for statistical significance by one way ANOVA tests. $P < 0.05$ was considered statistically significant. Tukey's multiple comparison test was used to compare individual set of readings.

Chapter 5

Development and Characterisation of highly porous scaffolds by Solvent Casting and Particulate-Leaching

In this chapter we report the successful use of solvent casting and particulate leaching technique in fabrication of scaffolds from POSS-PCL in desired porosity considered suitable for tissue engineering of small intestine. These scaffolds were cast in linear sheets. The scaffolds were then characterised for their pore morphology, pore interconnectivity and mechanical strength.

5.1 Experimental details

Scaffolds were made porous by using sodium chloride particles in two size ranges: 150-250 microns (macroporus) and <150 microns (microporous). Dried NaCl was sieved in the desired pore size range using stainless steel sieves. 10 wt. % POSS-PCL in DMAC was used in all experiments. Two different salt concentrations - 40 and 80 weight percentages in polymer were used for both macroporous and microporous salt sizes (**table 5.1**). Both salt sizes were mixed in one of the samples to obtain a mixed pore sized sample. Control sample was prepared without any salt in it. As shown in **figure 5.1**, circular discs of 1.5 cm diameter were cut using a metal die and these specimens from the samples were studied for their physical and chemical properties.

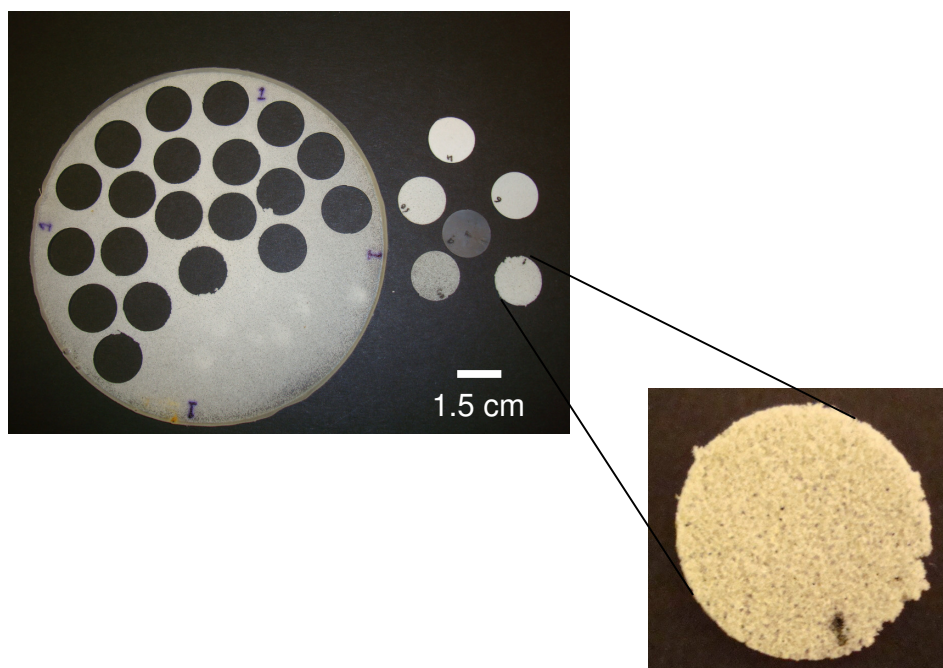


Figure 5.1: Porous scaffold developed using solvent casting/ particulate leaching. Circular discs of 1.5 cm diameter were cut using a metal die for cell culture purposes.

Table 5.1 Scaffold samples with different salt concentrations and size

| Sample# | Concentration of NaCl in polymer (wt %) | NaCl particle size (μm) |
|-------------|---|--------------------------------------|
| 1 | 80 | 150-250 |
| 2 | 40 | 150-250 |
| 3 | 80 | <100 |
| 4 | 40 | <100 |
| 5 (control) | 0 (No salt) | - |
| 6 | 80 | <100 + 150-250 |

5.2 Characterisation of the scaffolds

We used scanning electron microscopy as our main tool to aid characterisation of the porous scaffolds, particularly to look into the pore morphology like pore size, pore-pore interconnectivity, and pore shape. To measure porosity in percentage, we used the formulae described in materials and methods. Scaffolds were further characterised for pore morphology and pore interconnectivity using Micro CT, and for their mechanical properties using stress-strain graphs. FTIR was used to provide further evidence of POSS surface enrichment, and to assess any deviation in the basic structure of the nanocomposite after solvent casting/ particulate leaching was used.

5.3 Results

5.3.1 Properties of polymer

Table 5.2 shows the physical properties of nanocomposite POSS-PCL used in this study. The methods used to measure these properties have been described in section 4.3. Viscosity of POSS-PCL nanocomposite is significantly high making the nanocomposite a viscous solution to fabricate into scaffolds.

Table 5.2 Physical properties of the POSS-PCL polymer and organic solvent. Values are mean \pm SD (n=3).

| Sample | Surface Tension (mNm ⁻¹) | Electrical Conductivity (10 ⁻⁴ Sm ⁻¹) | Viscosity (mPa s) |
|----------|---|---|-----------------------|
| DMAC | 36 \pm 0.4 | 0.2 \pm 0.01 | 2.2 \pm 0.12 |
| POSS-PCL | 48 \pm 0.3 | 1.7 \pm 0.10 | 9720 \pm 120 |

We also tested the viscosity of non-biodegradable counterpart of our nanocomposite (POSS-PCU), which was 2494 \pm 106. The nanocomposites have DMAC within and possible interactions of soft segment with DMAC give the biodegradable nanocomposite a much higher viscosity. In order to facilitate homogenous mixing of salt in solvent casting/particulate leaching process, the nanocomposite was diluted with DMAC to make 10 wt % solution.

5.3.2 Porosity of scaffolds

The table below (**table 5.3**) shows varying porosity obtained when salt was used in different concentrations and different particle sizes. The porosity obtained was calculated using simple formulae described in materials and methods, section 4.5.1. Composite mixture of salt and POSS-PCL was weighed before casting and dried porous sheets after peeling off the stainless plates were also weighed before being submerged in de-ionised water for particulate leaching.

Table 5.3: Porosity of POSS-PCL scaffolds using different salt concentrations and salt sizes. Sample 5 (control) is the sample with no salt. Porosity values are mean \pm SD (n=3)

| Sample | Concentration of NaCl (wt%) in polymer | NaCl particle size (μm) | Porosity obtained (%) |
|-------------|---|---|--------------------------|
| 1 | 80 | 150-250 | 83.9 \pm 0.5 |
| 2 | 40 | 150-250 | 59.5 \pm 0.9 |
| 3 | 80 | <100 | 74.6 \pm 0.4 |
| 4 | 40 | <100 | 61.9 \pm 0.3 |
| 5 (control) | - | - | 5.4 \pm 6.0 |

** Porosity, $P = 1 - \frac{d}{d_p}$ and $d = \frac{m}{v}$

To estimate the density and porosity of scaffolds after particulate leaching, the diameter and height of each scaffold were measured to calculate the volume of each scaffold. The results show that the porosities obtained (%) are in the desired range and close to the weight percentage of salt used as a porogen.

5.3.3 Scanning Electron Microscopy (SEM)

Porous morphology of scaffolds was examined by SEM taken from the surface of linear 2D sheets, as well as from their cross section as shown below. Pore interconnectivity was seen in SEM micrographs and confirmed by micro CT pictures which are described in section 5.3.5.

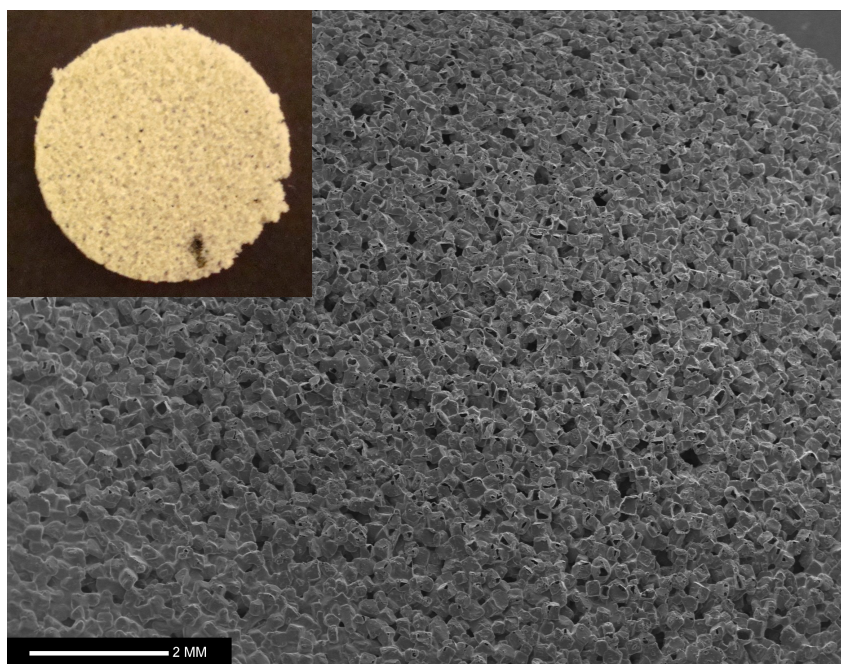


Figure 5.2: SEM of scaffold sample 1 (80% porous). Magnification x10. Scale bar is 2 mm. Inset is the photograph of 1.5 cm diameter disc cut from scaffold sample 1.

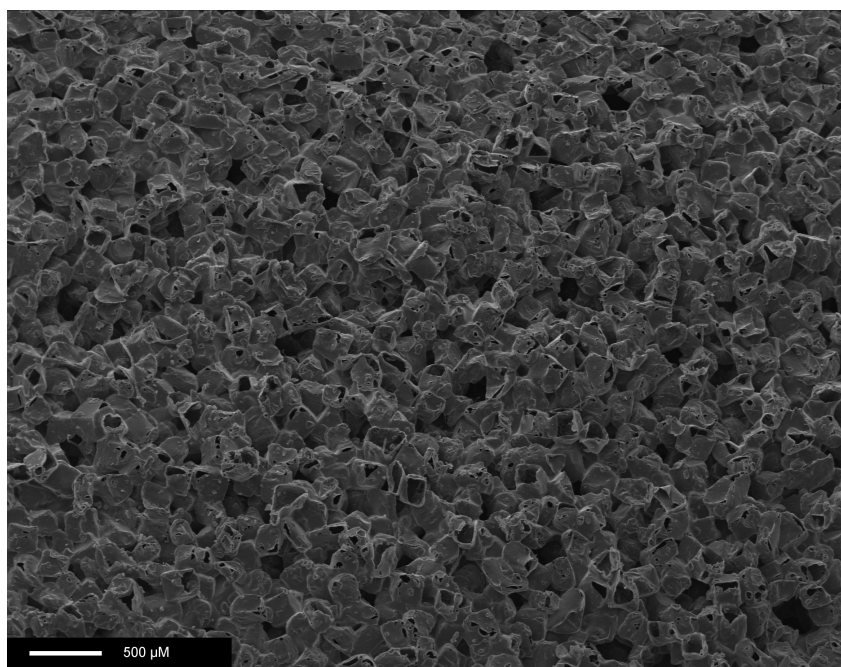


Figure 5.3: Surface SEM of scaffold sample 1 (80 % porosity). Magnification x20. Scale bar is 500 μm.

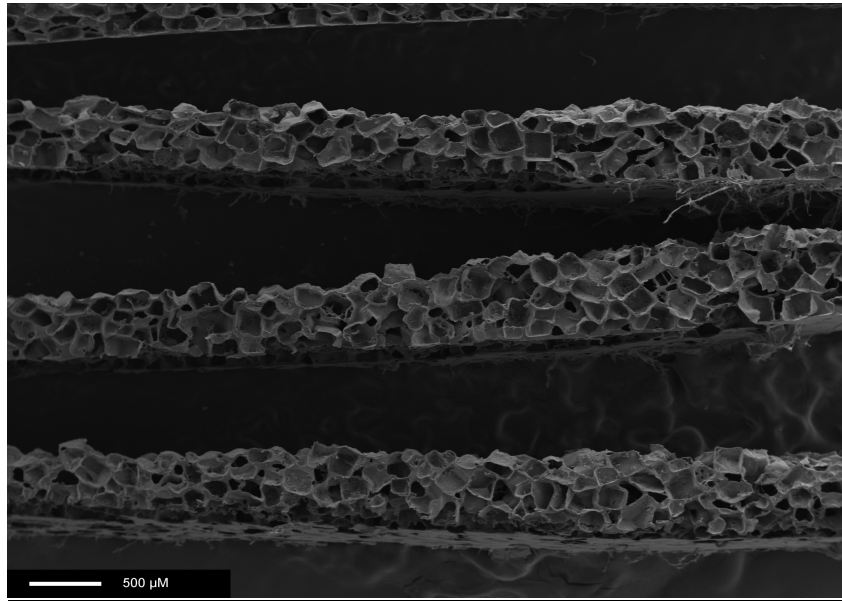


Figure 5.4: Cross sectional SEM of scaffold sample 1 (80 % porosity). Magnification x20. Scale bar is 500 μm.

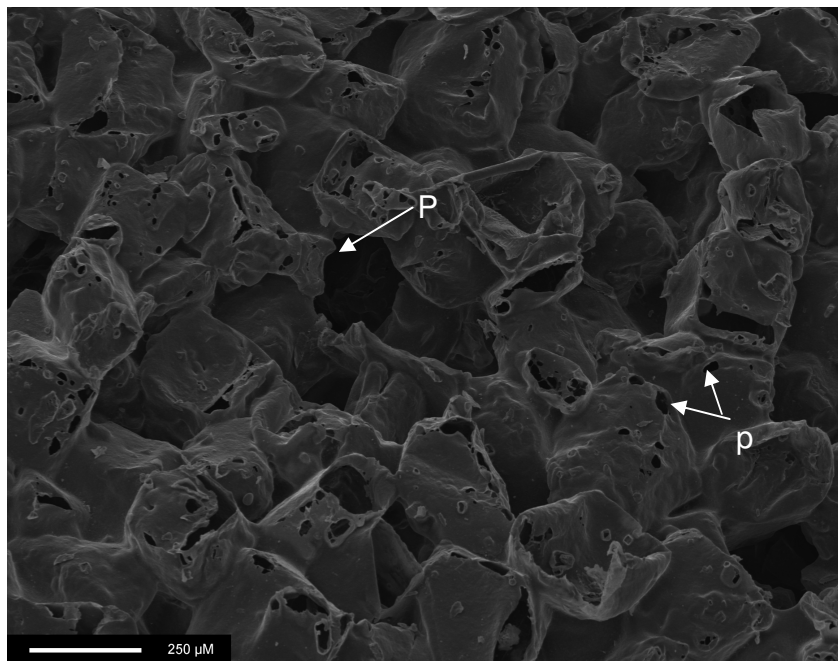


Figure 5.5: SEM of scaffold sample 1 (80 % porosity). Magnification x80. Surface micrograph. Scale bar is 250 μm. Pore within a pore can be seen (P). Small pores (p) are likely due to undesired small salt particles after sieving.

Figure 5.2 and figure 5.3 show a surface SEM picture where a homogenous distribution of pores can be seen. Pores are in the size range of the salt particles used, i.e. 150 – 250 microns and pore interconnectivity can be seen as well. **Figure 5.4** is a cross sectional micrograph of the same scaffold sample 1 with 80 % salt concentration to achieve porosity in the range of 80%. **Figure 5.5** is the magnified surface micrograph of the same scaffold where pore within a pore can be seen. The small pores seen are likely to be due to undesired small salt particles and some air bubbles trapped while mixing salt in the polymer using a homogenizer. Pore interconnectivity was further characterized using micro CT as described in section 5.3.5.

Samples 2 and 4 showed porosity in the range of 40 % as desired (**figure 5.6**); however sample 2 has a larger pore size than sample 4, as expected.

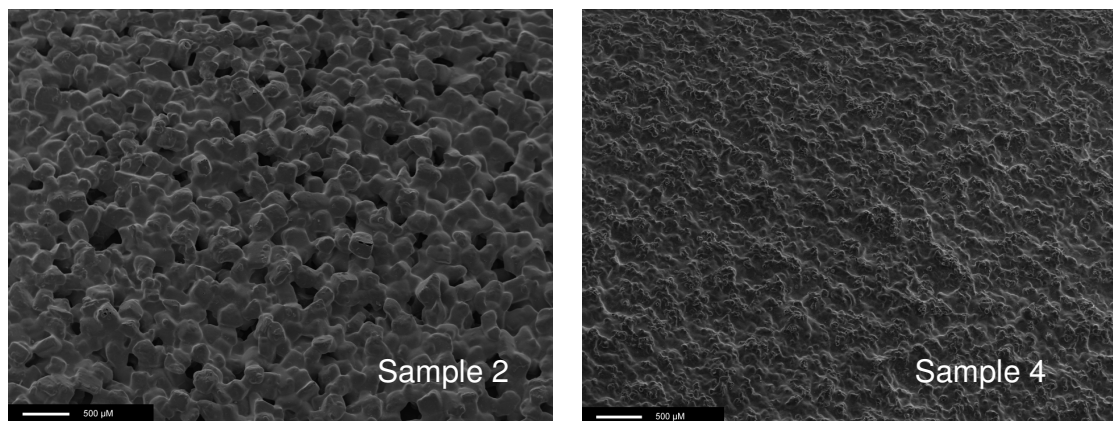


Figure 5.6: Scaffold samples 2 and 4 in the range of 40 % porosities but sample 2 has a larger pore size (150 – 250 µm) as apposed to sample 4 which has smaller pore size (<100 µm). Scale bar is 500µm. Magnification is x 20 in both micrographs.

Sample 3 was intended to have a small pore size (< 100 microns), which can be seen in **figure 5.7**. This sample of scaffold was mixed with 80 % salt of < 100 micron salt particles. As can be seen in the micrographs, pore sizes are in the desired range. The porosity was confirmed to be in the range of 74.6% as shown in **table 5.3**.

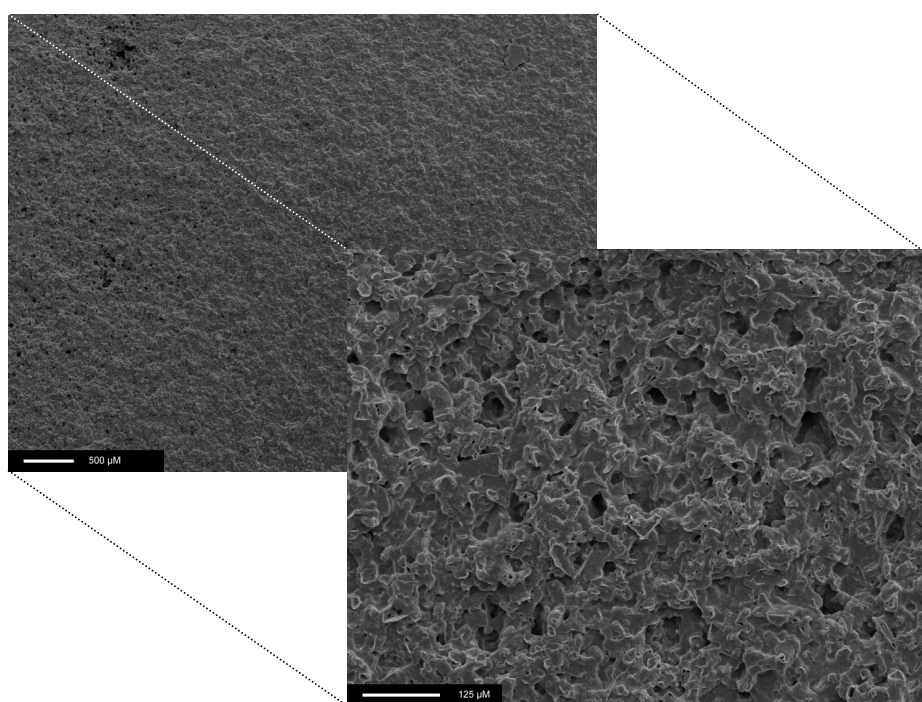


Fig 5.7: SEM of sample 3 (80 % salt concentration with salt particle size < 100 microns). Magnification x 20 and x 160. Scale bar is 125 microns as shown. Pore size can be seen < 100 microns as desired.

The non-porous sheet of scaffold (sample 5) where no salt was used served as a control. As we know, coagulation of a polymer into a non-solvent results in pore formation, however, no pores can be seen in SEM micrograph of sample 5, **figure 5.8**, suggesting all the solvent (DMAC) evaporated as expected, resulting in no coagulation process when the dried sheet was

leached in de-ionised water.

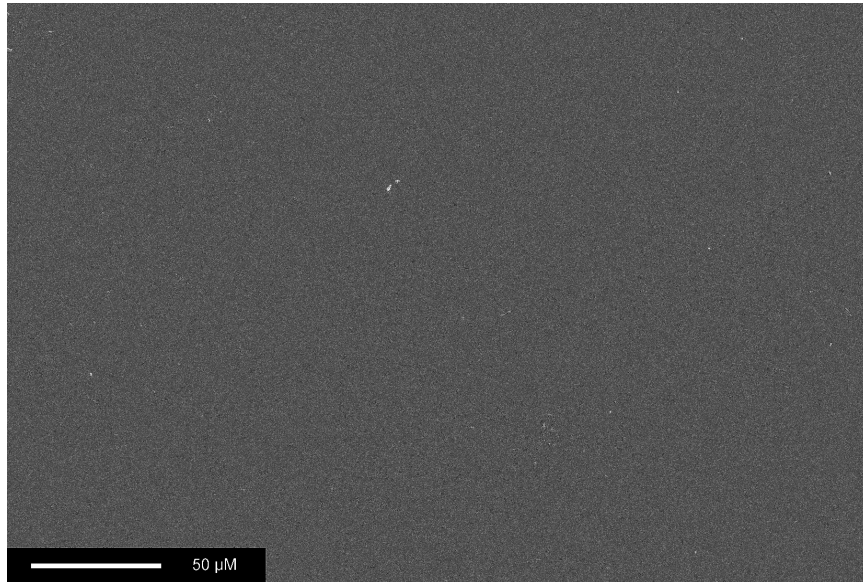


Figure 5.8: Surface SEM micrograph of scaffold (sample 5). No salt was used for casting. No pores can be seen. Magnification x 80.

5.3.4 Extrusion-coagulation combined with salt leaching

Porous scaffolds in form of 5 mm tubes were developed by the method of extrusion –coagulation as described in section 4.5. This method is also called liquid-liquid phase inversion. In this method the tubes of scaffolds obtained were kept in deionised water for 48 hours not only for coagulation of the liquid polymer, but also to facilitate controlled porosity by leaching the salt particles with known size range and quantity. SEM pictures (**figure 5.9**) of the samples showed mixed pore sizes, due to a combined effect of particulate leaching resulting in large pores (150-250 microns); and small pore (<50 microns) formation due to phase inversion.

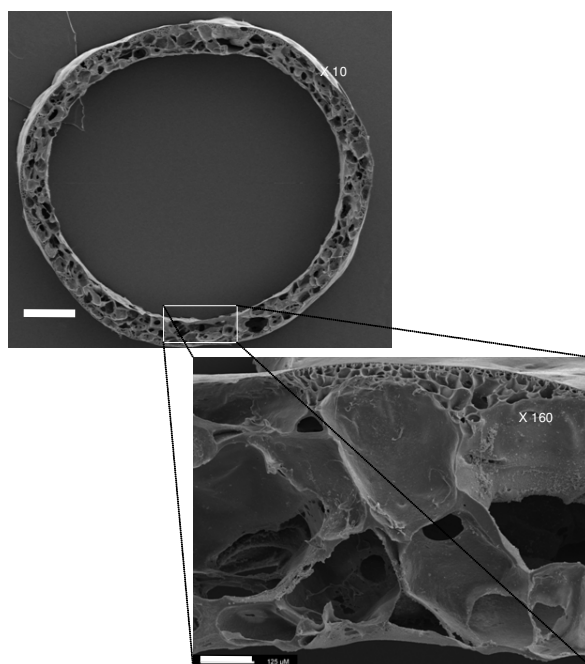


Figure 5.9: SEM of tubular scaffold (sample 1) developed using combined extrusion-coagulation and particulate (NaCl 150-250 μm) leaching. Mixed pore size is observed. Scale bar is 125 μm .

Sample 2 was obtained by using NaHCO_3 in place of NaCl . NaHCO_3 is much finer salt as compared to NaCl and the salt particles are in the range of < 50 μm . SEM (**figure 5.10**) of the tubular scaffold graft obtained using combined phase-inversion and particulate (NaHCO_3) leaching reveals pores in the range of <50 μm and porosity in the range of 80%.

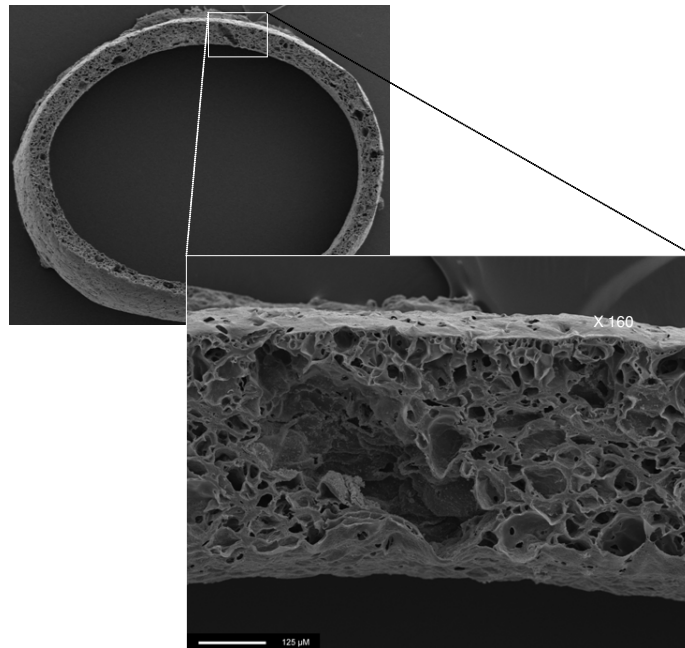


Figure 5.10: SEM of tubular scaffold (sample 2) developed using combined extrusion-coagulation and particulate ($\text{NaHCO}_3 < 50 \mu\text{m}$) leaching. NaHCO_3 leads to formation of small pore size as opposed to NaCl . Scale bar is $125 \mu\text{m}$.

5.3.5 Micro CT

The results of Micro CT (**Figure 5.11**) confirmed the porosity calculated by using simple formulae. As a mean value from 100 sections of the sample 1 was found to be $80\% \pm 2\%$, and the pore size varied from $140\text{-}250 \mu\text{m}$, as expected from the polymer-salt ratios. Good pore interconnectivity was seen in the sample studied.

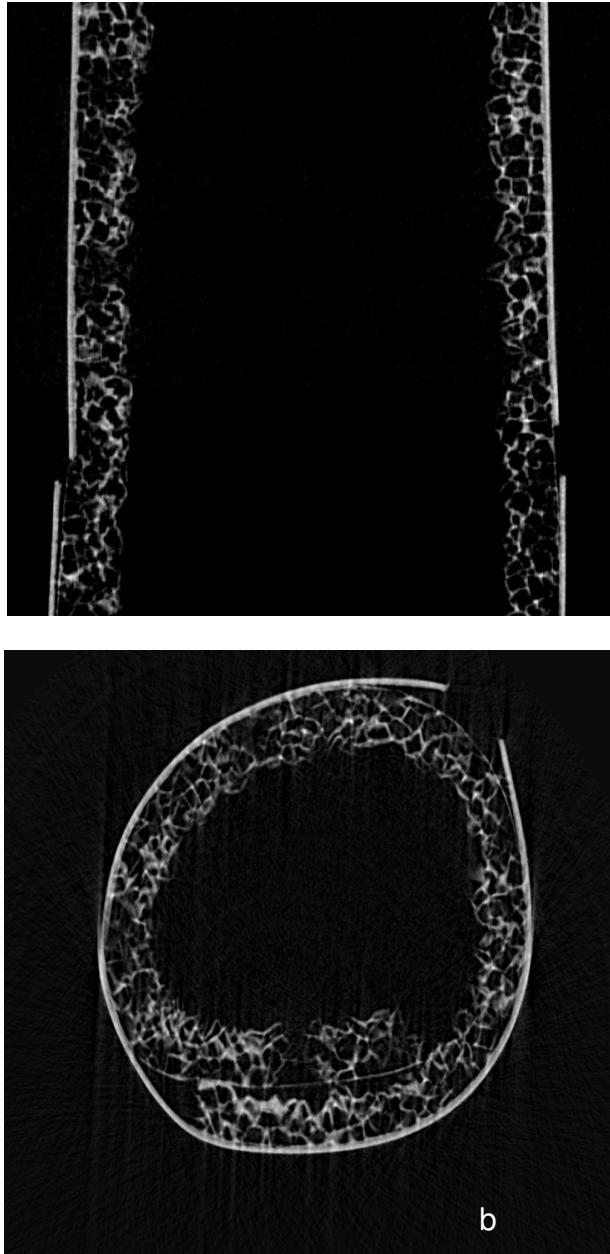


Figure 5.11: Micro-CT images of the cast scaffold of sample 1 rolled as a tubular graft (a) sagittal section (b) cross section. Pore interconnectivity can be seen in both sections. The outer thick white line is an artefact from the tape used to secure the sample while processing for micro-CT. Pores are seen black whereas polymer and very little salt left is seen white.

5.3.6 Stress-Strain values

Stress–strain patterns of scaffold samples are shown in **figure 5.12**. Porous scaffolds (samples 1, 2, 3, 4 and 6) are significantly less stiff as compared with the non-porous scaffold (sample 5); $P<0.05$. As expected, the porous scaffolds were less strong than the non-porous scaffold; however, among the porous scaffolds with different porosities and pore sizes, there was no significant difference observed. Pore size has no significant influence on stress strain patterns. **Table 5.4** shows stress-strain measurements of POSS-PCL macroporous and microporous scaffolds.

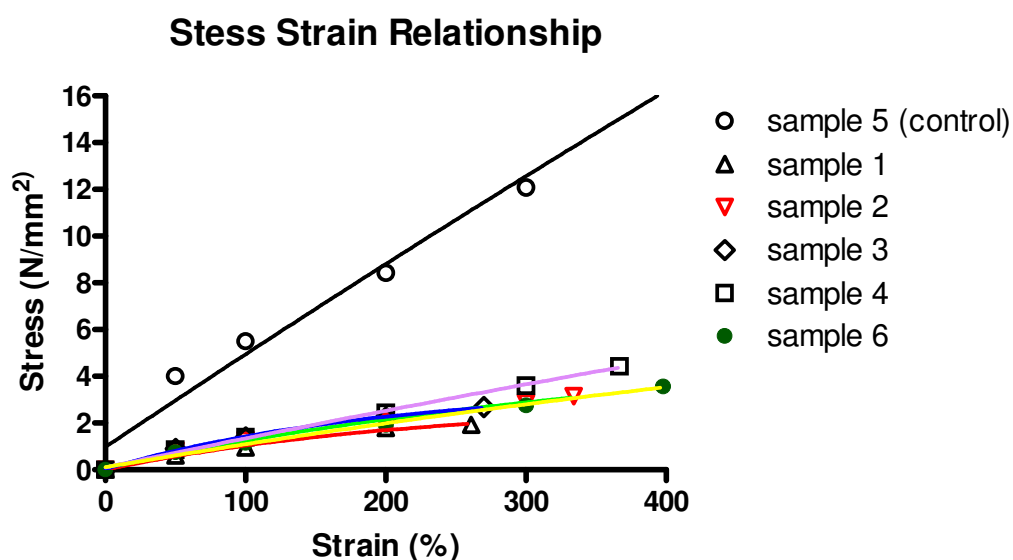


Figure 5.12: Graph represents stress-strain of POSS-PCL scaffolds samples 1-6. Sample 5 is the non-porous (control). The data are mean values (n=3) prepared with salt concentrations of 40 and 80 wt %.

Table 5.4: Stress-Strain values of scaffolds

| Sample # | a0 mm | B0 mm | L0 mm | S0 mm ² | σFmax N/mm ² | σR N/mm ² | εR % | σ50 N/mm ² | σ100 N/mm ² | σ200 N/mm ² | σ300 N/mm ² | σ500 N/mm ² |
|----------|----------|----------|----------|-----------------------|----------------------------|-------------------------|-------|--------------------------|---------------------------|---------------------------|---------------------------|---------------------------|
| 1 | 0.64 | 4 | 22.50 | 2.58 | 1.93 | 1.84 | 261.1 | 0.62 | 0.95 | 1.79 | 3.04 | - |
| 2 | 0.41 | 4 | 21.42 | 1.54 | 3.15 | 3.08 | 334.7 | 0.82 | 1.27 | 2.06 | 2.86 | - |
| 3 | 0.46 | 4 | 21.11 | 1.86 | 2.69 | 2.53 | 270.9 | 0.90 | 1.39 | 2.23 | - | - |
| 4 | 0.28 | 4 | 20.99 | 1.12 | 4.43 | 4.41 | 367.4 | 0.86 | 1.39 | 2.45 | 3.61 | - |
| 5 | 0.16 | 4 | 20.20 | 0.64 | 46.21 | 41.92 | 942.5 | 4.01 | 5.50 | 8.44 | 12.09 | 20.12 |
| 6 | 0.54 | 4 | 21.25 | 2.19 | 3.57 | 3.52 | 398.3 | 0.75 | 1.15 | 1.91 | 2.76 | - |

Keys: a0-thickness, b0-width, L0-length experimented, S0-cross sectional area, σFmax-maximum stress, σR- shear stress at break, εR – percent elongation, σ50 – shear stress at 50% elongation.

5.3.7 Fourier transform infrared spectroscopy (FTIR)

FTIR was performed as a characterization tool for scaffolds prepared by solvent casting/particulate leaching technique. The aim was to confirm the preservation of the basic structure of scaffold despite attaining porosity by adding salt particles. We studied FTIR for a porous (sample 1) and a nonporous (sample 5) and plotted the graph as shown in **figure 5.13**.

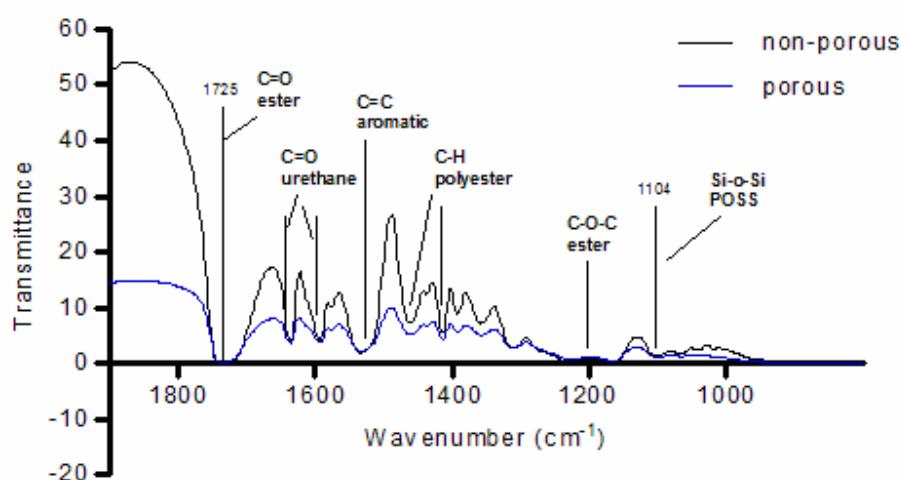


Figure 5.13: FTIR of porous sample (sample1) and non-porous sample (control – sample 5), essentially showing preservation of basic structure of scaffold after particulate leaching.

The results showed that the basic structure of scaffold remained preserved after particulate leaching. The carbonyl segment of ester/carbonate (--CO--O--), the urethane carbonyl groups (--NHCOO--) and the C--O--C bonds of the CO--O--C segments have characteristic peaks at wavelengths 1725,

1640, and 1240–1250 cm^{-1} respectively and constitutes the soft segment. The urethane amides of the hard segment have characteristic peaks at 1525 and 1223 cm^{-1} . The Si-O bonds of the POSS nanocages revealed characteristic peaks at a wavelength of 1100 cm^{-1} . PCL exhibits characteristic C-O and C-C bond stretching at a wavelength of 1157 cm^{-1} and carbonyl stretching at 1728 cm^{-1} .

5.4 Discussion

Although macroporous scaffolds are generally accepted as ideal for soft tissue engineering, the size of the pore can depend on the size of the cell seeded. Interconnected pores larger than the cell size are generally required for infiltration of the cells into scaffold. Whereas on one hand pore sizes of greater than 50 μm facilitate better nutrient and cell transport, on the other hand micropores in sizes less than 20 μm are responsible for a greater surface area for protein adsorption, better ionic solubility in the microenvironment and cell attachment (Woodard et al. 2007). In literature it has also been shown that a combination of macro- and micro-pores have resulted in better drug delivery, strength and stiffness particularly in bone tissue engineering, as compared to non-microporous scaffolds (Hing et al. 2005). Pore size requirements differ in different applications, for example, the minimum pore size required to regenerate mineralized bone is generally considered to be around 100 μm (Hulbert et al. 1970; Karageorgiou & Kaplan

2005); and for soft tissue engineering like small intestine the pore size most widely used has been in the range of 250 μm (Kaihara et al. 1999; Kim et al. 1999c), mainly because of the large size of intestinal epithelial organoid units used as the cell source.

Our laboratory has already demonstrated the advantages and the successful applications of silica nanocomposite based polyurethanes in producing vascular tissue engineered grafts, such as improved cell adhesion characteristics using a silicon pendant nanocage (Kannan et al. 2006b). In this study we developed and characterised similar, although biodegradable, nanocomposite POSS-PCL scaffolds for intended use in small intestinal tissue engineering. Another aim of this study was to suggest suitability of alternative biodegradable polymers like POSS-PCL for soft tissue engineering, as opposed to the widely accepted sole use of PGA/PLLA copolymers in small intestinal tissue engineering. PCL in our experience has been less expensive, and easily dissolvable in commonly available organic solvents unlike PGA which is very hard in consistency and requires highly fluorinated solvents such as hexafluoroisopropanol. Our nanocomposite maintains mechanical stability due to nanocages while simultaneously allowing controlled degradation. In this study, we used mainly two pore sizes – 150-250 μm and < 100 μm . Apart from the pore size, we also used two different porosities, one in the range of 80% and the other in the range of 40%. Solvent casting and salt leaching resulted in the production of scaffolds

with pore size and porosity in the desired range. The pores were interconnected as can be seen on SEM and micro CT. Solvent casting unlike extrusion-coagulation (phase inversion) offers an added advantage of controlled pore size and porosity. Our scaffold samples when tested for stress strain relationships show that the strength of scaffold reduces with increasing porosity.

We employed simple and inexpensive method of particulate leaching/solvent casting to fabricate 2D scaffolds of desired thickness. We developed sheets of scaffolds in different porosities and different pore sizes. Our aim was to test our house made biodegradable nanocomposite (POSS-PCL) for its fabrication properties, and then to subject the scaffold to physical and chemical tests in order to characterise its suitability as a scaffold to grow intestinal cells first in vitro, and then in vivo. With the technique of solvent casting/particulate leaching described above, we obtained 2-3 mm thick two dimensional porous sheets of polymer which could be rolled in a tubular structure if needed in future. The surface of the sheets towards the stainless plates on which they were cast was smooth and relatively non porous as compared to the porous surface exposed to air. This is a well known finding by other researchers who have used the similar method of solvent casting and particulate leaching (Wake et al. 1996; Liao et al. 2002). It is believed that the solvent as well as the salt (particulate) particles evaporate and disperse towards a gas interface due to buoyancy, resulting in a porous

exposed surface and a relatively smooth inner surface in contact with the metal plate on which the composite is cast. This difference in surface morphology can be overcome by making thicker sheets and then essentially bisecting the base (smooth skin) to give porosity at both surfaces. This can be achieved by using compression moulding technique where the salt-polymer composite can be compression moulded in cylindrical form, and then the cylinder is cut into discs of desired thickness before leaching. However, high temperatures can degrade the polymer in this process (Thomson et al. 1998). One of the significant disadvantages of solvent casting/ particulate leaching, and other techniques including phase separation, fiber bonding and gas foaming, is the need of organic solvent which can be cytotoxic, and hence there is a need to remove the solvent which can take long processing time. The newly developed techniques of rapid prototyping/ solid freeform fabrication can certainly be the answer to the above problems as they are usually porogen free and solvent free (Hutmacher et al. 2004; Hollister 2005). They can be used to result in highly reproducible architecture, there is a precise control over pore-morphology and mechanical properties, and the technique can include bioactive components like cells, growth factors and drugs during fabrication. However, these techniques are expensive, sophisticated equipment is required, and relatively less porosity is obtained as compared to the conventional techniques. Moreover, for our intention to develop scaffolds for tissue engineering of small intestine, highly sophisticated structure was not

required. We aimed to develop a highly porous and macroporous scaffold of our nanocomposite which has a large surface area and thickness of approximately 2 mm in order to allow cells to grow and survive, in vitro. The simple linear sheets of scaffolds can be rolled out in tubular structures in future for vivo studies, if necessary, to simulate a tubular small intestine. The main objective for engineering small intestinal remains to increase the absorptive surface of gut, which can be achieved by forming scaffold in any shape, whether tubular like an intestine, or, spherical like a cyst. With solvent casting and salt leaching, a highly porous scaffold was obtained with desired thickness in the range of 2-3mm, and porosity in the range of 80%. Methods commonly employed in characterization of scaffolds include SEM and mercury intrusion porosimetry (MIP) (Liao et al. 2002; Mikos et al. 1994; Nam et al. 2000; Murphy et al. 2002). SEM is a simple and relatively inexpensive tool to show surface topography of a 3D scaffold in form of pore size, pore density, pore structure, and pore interconnectivity to an extent. However, only 2D analysis and destruction of the scaffold sample are the limitations associated with it. Despite these limitations, SEM remains the most widely accepted characterization method of choice. Relatively newer tool, such as, micro-CT has been quite successful to demonstrate pore morphology, mainly pore-interconnectivity, but quantification of pore-interconnectivity has not been simple, as it requires use of complicated computer software to analyse data.

The scaffold samples in different pore sizes and porosity were analysed with scanning electron microscopy for pore morphology, and the scaffolds were also tested for their mechanical strength by a tensometer. Pore morphology was further confirmed by micro CT which clearly demonstrated the pore interconnectivity, and testified our porosity calculated from simple formulae. The porosity achieved was in accordance to the amount of salt used. FTIR was performed to identify the amount of residual salt in the scaffold samples and also to know the deviation from the original structure of the polymer after the processing was done in form of solvent casting/ particulate leaching. FTIR of porous (sample1) and non-porous sample (control-sample 5) showed preservation of basic structure of scaffolds after particulate leaching. We have used samples of scaffolds with two different porosities of 80% and 40%, and two pore sizes of $<100\text{ }\mu\text{m}$ and $150\text{-}250\mu\text{m}$, for our in vitro experiments to test cell growth and cell proliferation. The in vitro experiments are described in chapter 7.

Chapter 6

Electrohydrodynamic atomisation – novel use for print patterning of biopolymer scaffolds

6.1 Introduction

Electrohydrodynamic jetting is a process where a liquid medium forms a jet and breaks into droplets as it is released at a controlled flow rate through a needle while being exposed to an electric field caused by the existence of a potential difference between the needle and a ground electrode (Rayleigh 1878; Taylor 1964; Zeleny 1917) and this method was first adapted for the processing of advanced materials in 1997 (Teng et al. 1997). Electrohydrodynamic jetting occurs in many modes (Cloupeau and Prunetfoch 1990; Jaworek and Krupa 1999), e.g., microdripping, spindle, cone-jet, multi-jet, and the mode is mainly determined by the properties of the liquid, the flow rate, and applied voltage. The cone-jet mode is where the formation of a cone takes place at the exit of the needle; a jet emerges from its apex, breaking down into droplets further away from the apex (Hartman et al. 1999). The stable cone-jet mode is most desirable, as it can generate a near monodispersion of droplets (Edirisinghe and Jayasinghe 2004; GananCalvo et al. 1997; Hartman et al. 2000). Both microsuspensions and nanosuspensions have been subjected to this process successfully in our earlier studies and print patterned in 2D (Jayasinghe et al. 2002; Wang et al. 2005a) and, more recently, with high resolution patterning device in 3D (Wang et al. 2005b). Electrospinning is another related process and is accompanied by a cone of liquid at the exit of the needle where a jet evolves and elongates into one or more filaments, which solidify on or soon after

deposition (Doshi and Reneker 1995;Shin et al. 2001). This process is an attractive way of preparing fibres and fibre-mats from advanced materials (Sigmund et al. 2006;Zhang and Edirisinghe 2006). Recently it was shown that electrically forced microthreading is a related but distinctly different phenomenon, which could be exploited in materials processing (Zhang et al. 2006b). We achieved this with biopolymers in this experimental work and to the best of our knowledge; this was the first time electrohydrodynamic printing was used to prepare scaffolds for tissue engineering. One advantage of electrohydrodynamic printing over ink-jet printing is that much larger sized nozzles used (750 μm in this work) prevent needle-blockages allowing easier processing of the viscous polymer solutions to finer dimensions. Our direct writing electrohydrodynamic print-patterning procedure described in this chapter is attractive as with little modification, the structure of scaffold prepared can be tailored to the needs of many applications.

6.2 Experimental Details

Experimental details are described in section 4.7. POSS-PCL solution was subjected to the process of electrohydrodynamic atomisation and when aided with computer software, as described in section 4.7, resulted in printing fibres in a pre-designed pattern. This was printed onto standard microscope glass slides.

6.3 Results

Details of the structural features of the polymers are described in section 4.1 (Kannan et al. 2006a). The polymer contains hard and soft segments and show three regions, POSS segments, which are surrounded by urethane and these two constitute the hard segment, and carbonate soft segments, which also incorporate POSS. In the biodegradable polymer the soft segments are predominantly composed of polycaprolactone, which contains ester groups.

Table 6.1: Properties of the nanocomposite polymer, DMAC and ethanol

| Sample | Surface Tension/mNm ⁻¹ | Electrical Conductivity/ 10 ⁻⁴ Sm ⁻¹ | Viscosity/mP a.s |
|----------|-----------------------------------|--|------------------|
| Ethanol | 23 | 1.5 | 1.3 |
| DMAC | 36 | 0.2 | 2.2 |
| POSS-PCL | 48 | 1.7 | 9720 |

Due to soft segment differences and also the possibly different interactions with DMAC gives the biodegradable polymer a much higher viscosity and a lower electrical conductivity (**table 6.1**). However, the latter quantity is comparable with ethanol and much higher than the electrical conductivity of silicone oils we investigated recently and therefore classical electrohydrodynamic jetting is anticipated (Zhang et al. 2006a). However, the influence of higher viscosity seems to favour stable electrically forced

microthreading (Zhang, Jayasinghe, & Edirisinghe 2006b) rather than simple jetting and droplet generation (**figure 6.1**).

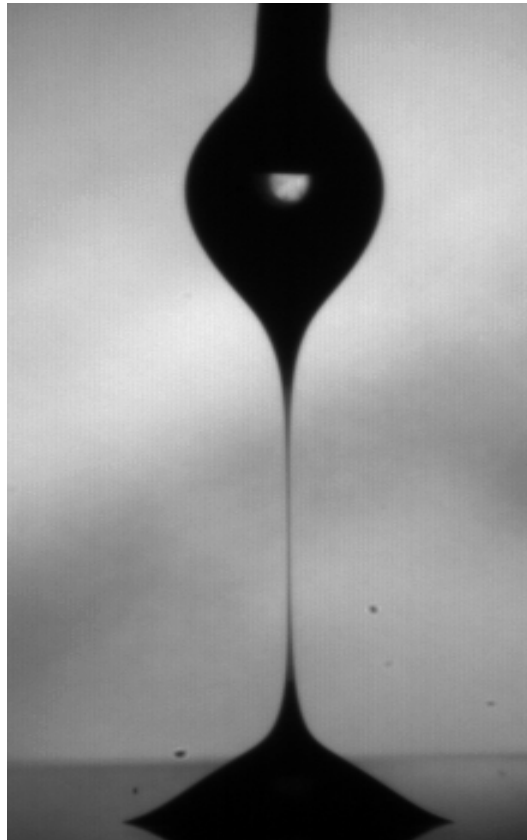


Figure 6.1: Stable electrically forced microthreading of the biopolymer

6.3.1 Scaffold characteristics

Initial print-patterning results showed discontinuities in the scaffolds prepared from the polymer (**figure 6.2**). This problem was overcome with the careful adjustment of the distance between the needle tip and the glass slide to approximately 500 μm (**figure 6.3**); however, the printed structures could not be peeled-off from the glass substrate. When polymer was printed onto

ethanol kept on the glass slide, instant precipitation of the polymer deposits occurred. Printing on to ethanol was much smoother with stable jetting. A few discontinuities are seen in the scaffolds prepared and these are caused by unstable jetting probably caused by variations of flow rate, the importance of flow rate is discussed below. Microscopy of the scaffolds prepared showed that a wavy and coil-like pattern prevailed when polymer was deposited on to ethanol (**figure 6.4**). Moreover, single layer prints with or without ethanol on the glass slides were fragile and did not sustain their structure when peeled off the substrate. When overprinting was performed five times in the presence of ethanol, the resultant scaffold could be peeled-off the glass slide and sustained its structure (**figure 6.5**).

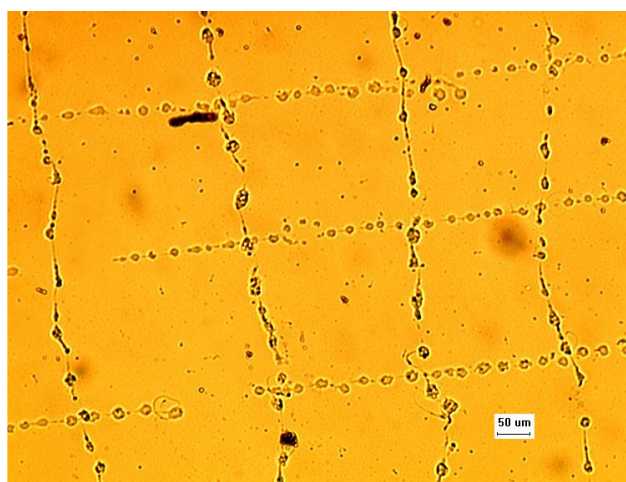


Figure 6.2: Optical micrographs showing discontinuous printing

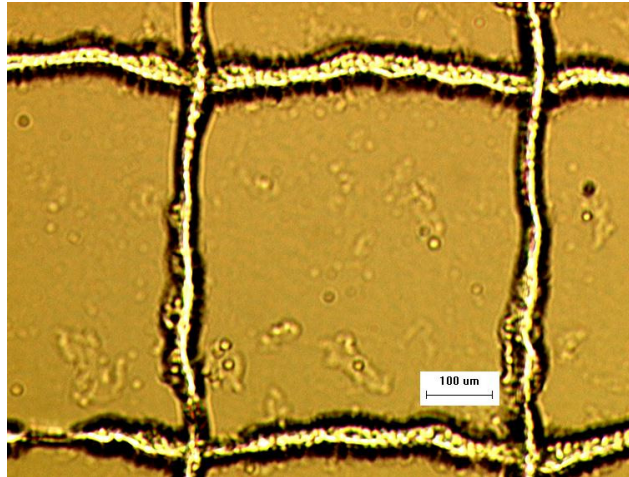


Figure 6.3: Optical micrographs showing continuous printing

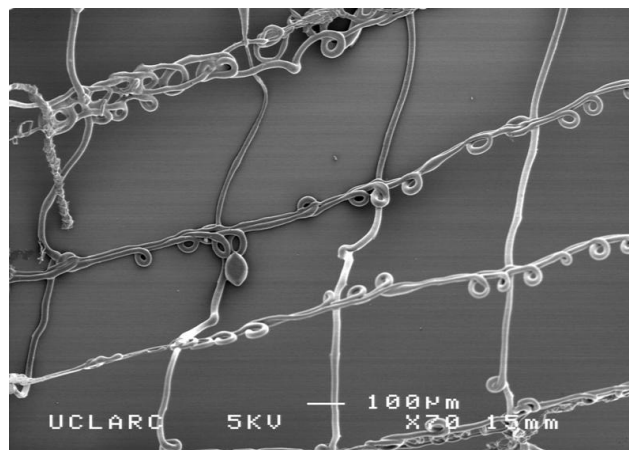


Figure 6.4: Scanning electron micrograph of a single layer of scaffold printed from polymer, showing coiling.

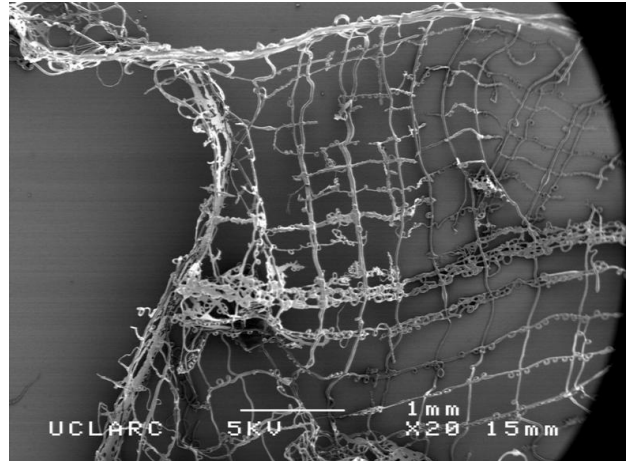


Figure 6.5: Scanning electron micrograph of a scaffold printed from polymer and subsequently peeled off the glass substrate.

6.4 Discussion

This work was carried out in relation to our research on tissue engineering small intestines and in most reports of other workers (Choi & Vacanti 1997; Duxbury et al. 2004; Kaihara et al. 1999; Kim et al. 1999a; Kim et al. 1999c; Vacanti et al. 1988) where the scaffold used has been made of tubes fabricated from non-woven sheets of polyglycolic acid fibres with or without poly (L-lactic acid) with a fibre diameter of 5-15 μm , mesh thickness of 1-2 mm with a porosity of 95% due to a mesh window size of 250 μm . The use of a macroporous scaffold (pore diameter >100 μm) in tissue engineering of soft structures like the small intestine is justified to facilitate important functions of better cell attachment, mass transport and waste disposal. Therefore, in this experimental work, our aim was to prepare 10x10 mm square sheets with a pore size in the range of 250 μm using the

nanocomposite POSS-PCL.

In this study we printed two grid patterns – a smaller grid (window size 250 μ m) and a larger grid (window size 500 μ m). As seen in scanning electron micrographs, the samples are macroporous with a reduction of window size by \sim 30-100 μ m than the designed levels corresponding to the size of the polymer strand forming the window. One of the factors affecting smaller than expected window size could be the possible shrinkage of the scaffold due to drying after printing.

The coiled appearance of the polymers printed on ethanol may be attributed to the instant precipitation of the polymer solution in ethanol. Selecting a liquid medium where precipitation of the polymer is more controlled may be important. Polymer deposits printed directly on the glass slide without ethanol are seen to be straight or wavy but not coiled. Desired uniform polymeric threads were obtained at an applied voltage of 9.5 kV when POSS-PCL was printed onto glass slides without ethanol. The distance between the exit of the needle and the glass slide was \sim 500 μ m. However when ethanol was used as a layer of substrate over glass slide, this distance had to be increased to \sim 1.5mm in order to avoid spreading of the polymer threads away from the main printed line. Also, with ethanol present, the optimum voltage for smooth continuous was found to be slightly higher, in the range of 9.5-10.0 kV. This change could be attributed to an increased

electric force required for the polymeric threads to precipitate through ethanol onto the glass slide, and for a higher voltage required to atomise the more viscous biodegradable polymer.

One of the limitations of our experiments was the inability to obtain 0.5-1 mm thick scaffolds because over-printing could not be carried out more than five times in the z direction. This was directly related to the flow rate of the polymer from the needle. The best scaffolds were obtained when a drop of polymer was manually pushed to the tip of the needle and atomised. This quantity was sufficient to over-print five times, after which the polymer at the tip of the needle solidified due to evaporation of solvent. More than the optimal amount of polymer solution required for atomisation was delivered even at a minimum infusion rate of 1 μ l/hour of the pump used, making “blobs” of polymer deposit on the scaffolds. This limitation may be overcome by refining the flow rate using better and finer adjustable infusion in future.

Due to the ability to pre-design the scaffold structure, window size can be tailored to the desired levels by altering the distance between the grid lines while writing the programme on the computer. This technique can also be exploited to design various shapes of the scaffolds as the medium subjected to electrohydrodynamic jetting can also be printed in the form of curvilinear and circular pattern in addition to straight lines.

6.5 Conclusions

This was a successful attempt to print polymer solution into a pre-designed structure of a scaffold for tissue engineering using electrohydrodynamic technology. Prints on ethanol resulted in almost instantaneous precipitation of the polymer facilitating peeling off the scaffold from the substrate. Scanning electron microscopy of the peeled scaffolds revealed a macroporous structure with polymer strands of diameter 15-50 μm . The polymer strand diameter was found to be dependent on the distance between the needle exit and the substrate, the voltage applied and the viscosity of the polymer solution. Further studies are required to study the exact relationship of the former with the latter three variables. Further work is also required to attempt making thicker scaffolds, may be by controlling the flow rate more accurately. The window morphology and the physical properties of the scaffold need to be tested in further studies. An ideal polymer ink with optimal characteristics for printing by electrohydrodynamic flow remains a viable option.

Chapter 7

In vitro small intestinal epithelial cell growth on a nanocomposite polycaprolactone scaffold

7.1 Introduction

In chapter 5 we developed and characterised porous scaffolds aimed at tissue engineering of small intestine using solvent casting/ particulate leaching; and in chapter 6 we employed electrohydrodynamic printing to develop scaffolds in desired pore size. The scaffolds developed were characterised for their physical properties and pore morphology. In this chapter we further characterised them for their cell compatibility by culturing rats' intestinal epithelial cells *in vitro*, before they can be tested *in vivo* in experimental animal models. We chose scaffolds developed using solvent casting/ particulate leaching for the studies. The reason was firstly an inability to obtain sufficiently thick scaffolds from the later technique, and secondly a requirement for large number of scaffolds to be tested which was achieved by the easy processability of solvent casting/ particulate leaching technique. Our aim was to test the cell viability and cell proliferation when grown on scaffolds as substrates of different porosities and different pore sizes. We also aimed at optimising the number of cells required to be seeded before a confluent cell growth could be achieved.

7.2 Experimental Details

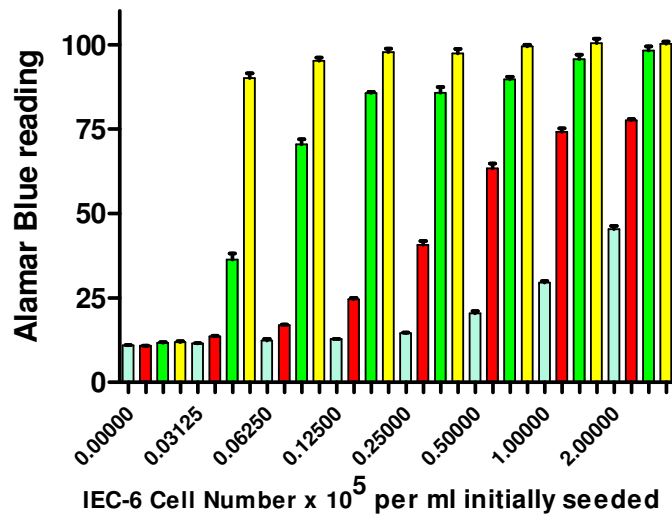
In vitro studies were conducted using circular discs of POSS-PCL scaffolds on which rats' intestinal epithelial cells were attempted to grow. The aim was

to test the scaffolds for cytocompatibility and cell proliferation. Firstly, cell culture was done on tissue culture plastic without scaffolds in order to get optimisation of cell density and cell seeding time. Cells were allowed to seed for 24 hours. Trial experiments of cell culture on POSS-PCL scaffolds with 0.25×10^5 cells per ml was followed by increase in cell density to 0.25×10^6 cells per ml. A more stringent washing of scaffolds prior to cell culture was done in the final experiments with higher cell density seeding. Cell adhesion was studied by Alamar Blue assays. Initial cell damage was studied by lactate dehydrogenase assay. Samples of seeded scaffolds were also analysed by scanning electron microscopy at day 7 and day 21.

7.3 Results

7.3.1 Optimising seeding density for IEC-6 cells on tissue culture plastic without scaffolds

Rats' intestinal epithelial cells (IEC-6) were grown on tissue culture plastic (n=3) in order to obtain an optimal seeding cell density. Cells were diluted to obtain concentrations ranging from 0.03125 to 2×10^5 cells per ml. Our aim was to seed the scaffold samples with minimum possible cell density, as higher cell densities are likely to inhibit cell growth after a certain time due to overcrowding and subsequent cell death, and can spuriously show high readings on Alamar blue assays.



Optimal Seeding Density for IEC-6 Cells

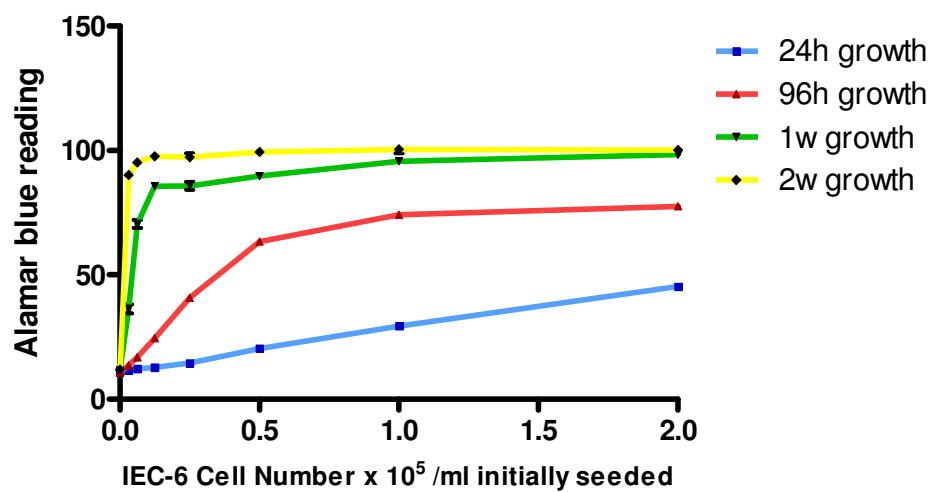


Figure 7.1: Optimal cell density (column graph above and bar graph below). Alamar blue assay for growth on tissue culture plastic over a period of 2 weeks at different cell densities. Results are mean \pm SEM (n=3).

In **figure 7.1** it can be seen that cell densities of 0.5×10^5 cells per ml and

higher attain confluence after 1 week, whereas 0.25×10^5 cells per ml and lower still significantly continue to grow till the 2 week period ($p < 0.05$). There was a significant difference ($p < 0.05$) between cell growth from 96 hours to 1 week at a density of 0.25×10^5 cells per ml; as compared to growth at cell density of 0.5×10^5 cells per ml. The minimum cell density which resulted in significant cell proliferation over next two weeks was 0.25×10^5 cells per ml. Cell density below this concentration was not sufficient to proliferate.

7.3.2 Optimising seeding time for IEC-6 cells on tissue culture plastic without scaffolds

Prior to carrying out the cell seeding experiments on scaffold some preliminary work was done to examine cell adhesion and proliferation on tissue culture plastic. The cell adhesion study examined adhesion after 2, 3, 4, 6 and 24 hours seeding time at two seeding densities (0.25 and 1×10^6 cells per well) as shown in **figure 7.2**.

Optimal Seeding Time for IEC-6 Cells

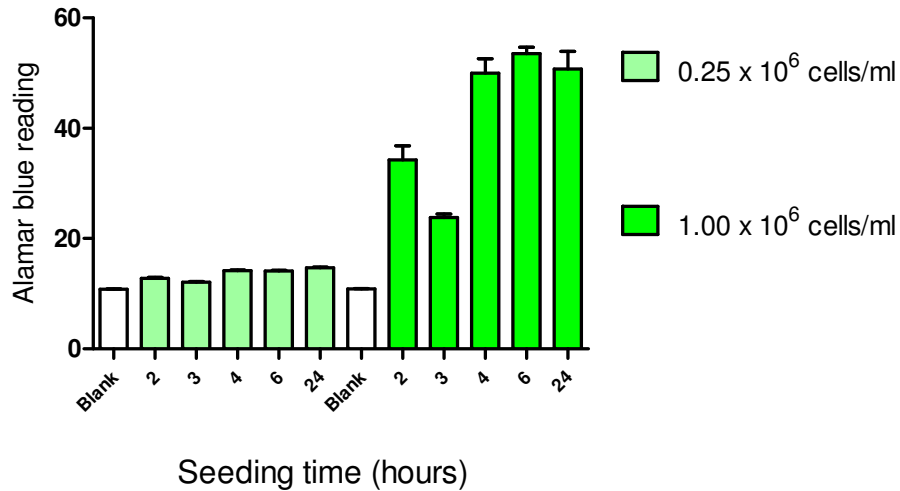


Figure 7.2: Optimal seeding time for cell adhesion. Alamar blue assay for adhesion on tissue culture plastic at different time points for optimising cell seeding time. Results are mean \pm SEM (n=3).

These studies indicated that all the cells were adherent after 4 hours seeding. Based on this a 24 hour seeding period was used in the scaffold experiments on the assumption that the maximum number of cells would have attached by this time point. For both cell densities, there was no significant difference after 4 hours ($p>0.05$).

7.3.3 Trial seeding of scaffold samples with lower density of 0.25×10^5 cells

Polymer scaffolds (P1-6) were seeded in 24 well plates with 0.25×10^5 for a period of one week. Alamar Blue assays were performed on day 1, 3, and 7 (**figure 7.3**). No significant difference in cell growth was observed over one

week period ($p>0.05$).

Graft segments seeded at 0.25×10^5 cells/ml

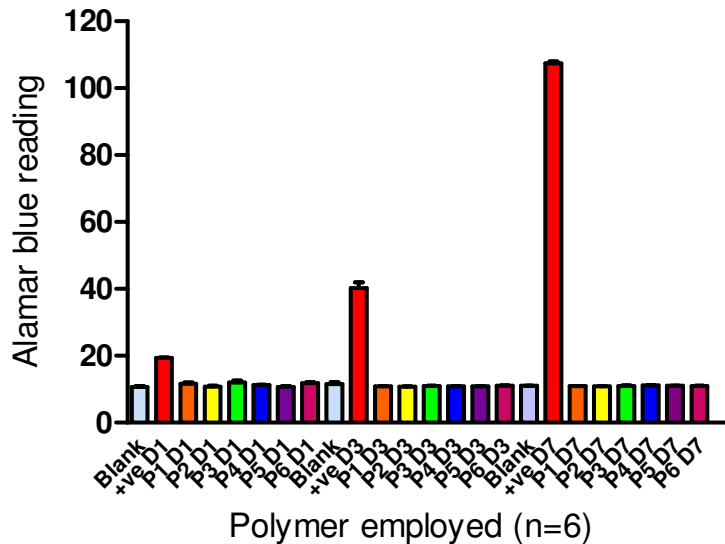


Figure 7.3: Trial seeding of the grafts with 0.25×10^5 cells per ml. Results are mean \pm SEM ($n=6$). P1-6 are polymer scaffold samples; D1, D3 and D7 are days after cell seeding.

In the graph for trial seeding (**figure 7.3**), the red bars represent tissue culture plastic (TCP) on which significant cell growth occurs over one week period ($p<0.01$). TCP with cells but no scaffold served as a positive control. Growth on TCP indicates optimal growing conditions and technique. It is possible that the cell seeding density as suggested by trial growth on TCP is suboptimal when grown on the scaffold surface rather than TCP alone.

7.3.4 Trial seeding of scaffold samples with higher density of 0.25×10^6 cells

After unsuccessful attempt at growing cells onto the scaffold with a cell density of 0.25×10^5 cells per ml, a higher cell density of 0.25×10^6 cells per ml was used in the study to examine cell growth over a period of 8 days. As can be seen in **figure 7.4**, cell growth occurred when Alamar Blue assays were done on day 2. However Alamar Blue assays when repeated at day 8, there was a significant drop ($p>0.05$) in the graph bars suggesting either cell death due to cytotoxic agents while growing, or cell death due to over crowding. It was believed that the residual salt used as particulate while developing cast sheets of porous scaffold could be cytotoxic. The other possible cytotoxic agent could be residual DMAC. The washing regime was initially to just rinse the scaffolds in de-ionised water. This was then made more stringent by rinsing the scaffolds for 72 hours on a shaker with changes of water every 4 hours.

Graft segments seeded at 0.25×10^6 cells/ml

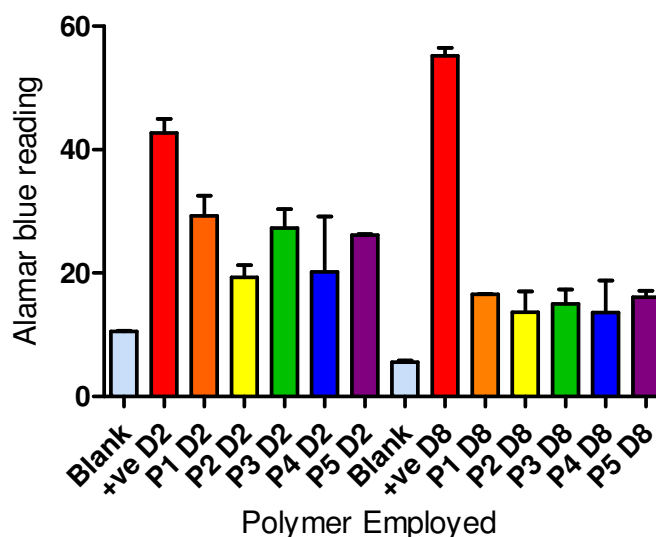


Figure 7.4: Trial seeding of scaffolds with 0.25×10^6 cells per ml. Alamar Blue assays

were performed on day 2 and day 8 of cell seeding. Results are mean \pm SEM (n=3)

7.3.5 Higher cell density seeding of scaffolds washed with stringent washing regime

After trial seeding of cells onto scaffolds, a higher cell density of 0.25×10^6 cells per ml, rather than 0.25×10^5 cells per ml, was deemed optimal; and the washing regime of scaffolds was made more stringent with regular change of de-ionised water. The results obtained from the investigation of cell growth and metabolism of IEC cells seeded on the various polymer samples demonstrate that cell growth occurred over the course of the 21 day study (**figure 7.5**). When seeded on tissue culture plastic cells reached confluence by day 10 (TCP control). All polymer samples showed a reduction in cell metabolism compared to the positive control, $p < 0.01$ (as anticipated, tissue culture plastic being optimal for cell growth). However cell growth occurred on each polymer sample over the whole 21 day period suggesting a slower growth rate compared to tissue culture plastic. There was no significant difference in growth ($p > 0.05$) for different porosities and pore sizes over the time period investigated.

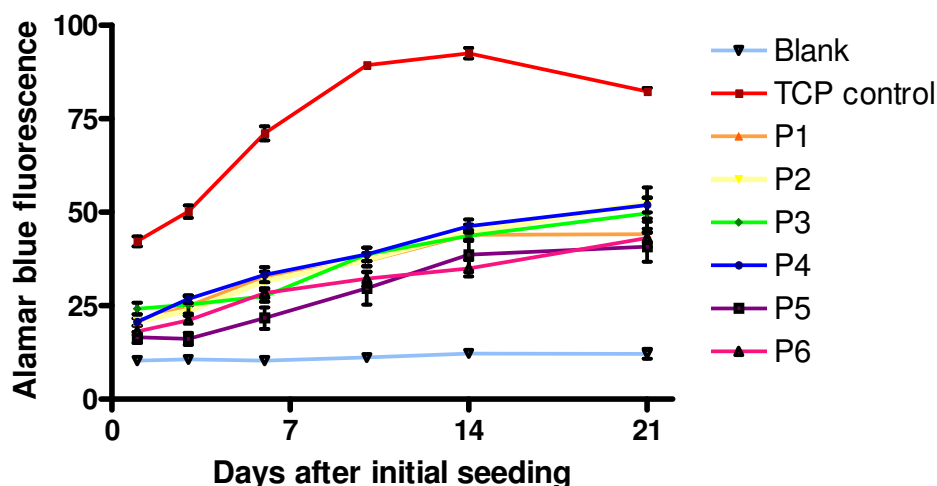


Figure 7.5: Alamar blue cell viability assay test on IEC seeded on POSS-PCL samples over 21 days. Data are mean \pm SEM (n=6). P1-P6 are discs of polymer samples 1-6. TCP is tissue culture plate control.

No further data was collected after 21 days growth as we believed that this was a reasonable period to demonstrate successful cell growth on the scaffolds and wished to collect samples for SEM analysis at this point. The cells grew at a reasonably steady rate over this time period and the SEM pictures demonstrate that they were approaching confluence at this point.

7.3.6 Assessment of Initial Cell Damage by LDH analysis

LDH release was examined to look at potential cell damage in the initial seeding period (**figure 7.6**). The differences in LDH levels are actually quite small compared to the levels from the tissue culture plastic seeded cells indicating that little initial cell damage has occurred. It is not possible to

calculate the number of cells represented by the LDH levels.

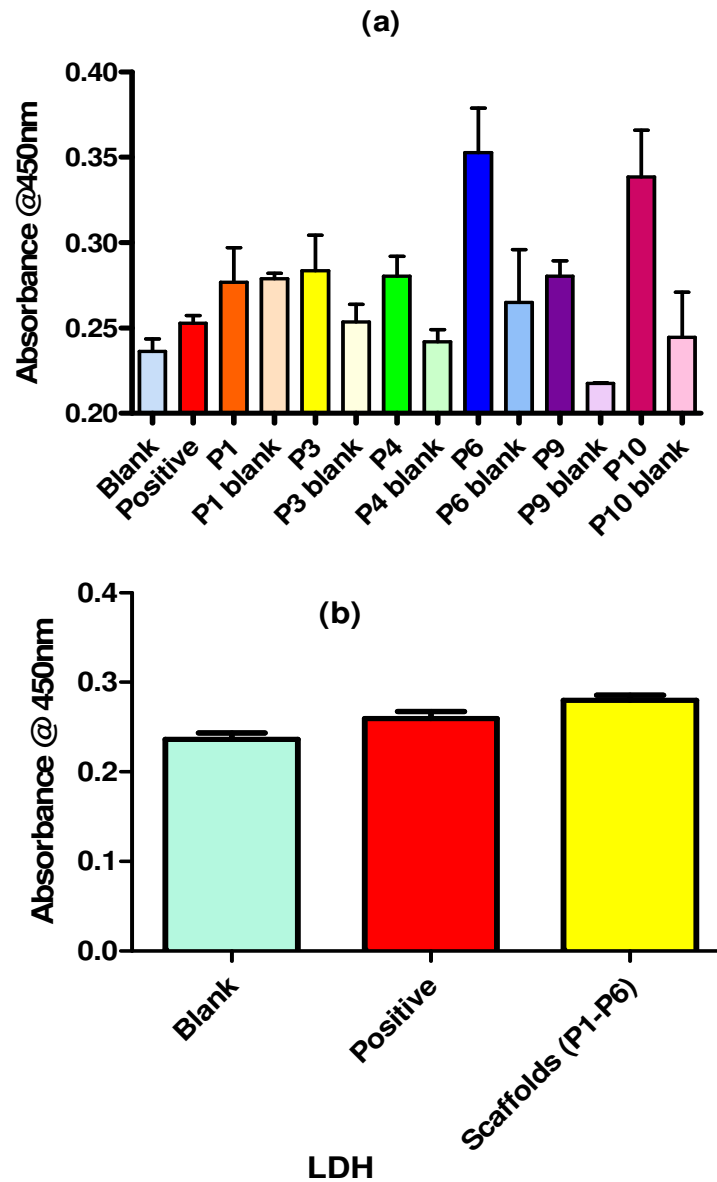


Figure 7.6: LDH assay test on IEC seeded on POSS-PCL samples for 24 hours. Absorbance was measured in arbitrary units at 450 nm wavelength. Data are mean \pm SEM (n=3). P1 to P6 are the seeded discs of polymer samples 1-6. 'Positive' indicates sample with equal number of cells seeded on the tissue culture plate without the polymer discs, serving as a positive control. (a) individual readings (b) combined scaffolds' readings.

When statistical analysis was carried out on the levels for the scaffold samples there was in fact no significant difference ($p > 0.05$) between the cell damage from positive and scaffold samples.

7.3.7 Assessment of Cell Seeding by Scanning Electron Microscopy

The results obtained from SEM examination of seeded polymer samples at Day 21 show cells present on all polymers examined and confirm the findings of the cell metabolism study (**figure 7.7**).

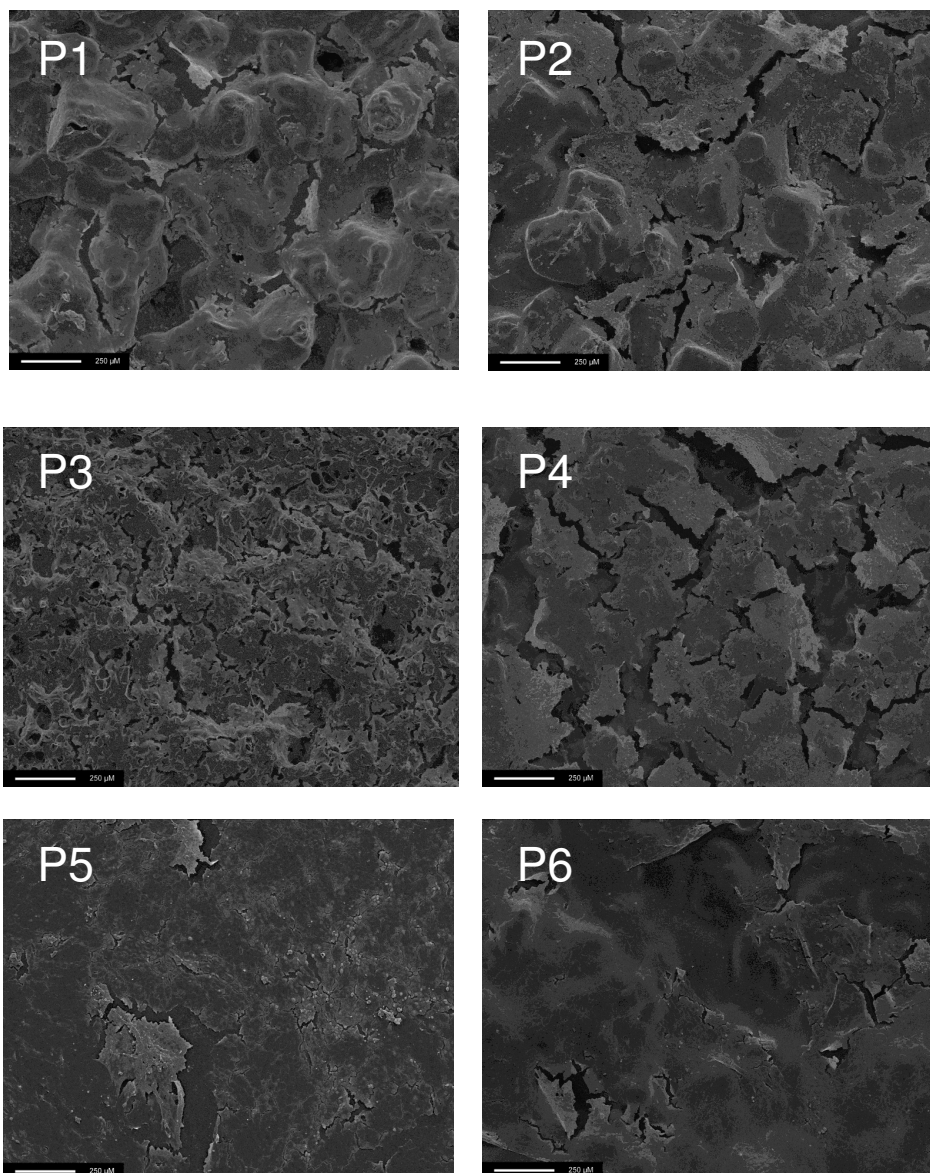


Figure 7.7: SEM of scaffolds (P1-P6) after 21 days of cell (IEC 6) seeding. Scale bar is 250μm. Results show cells approaching confluence at day 21.

Cells are seen in figure 7.7 to approach confluence at day 21. P1 – P6 are scaffolds with different pore sizes and porosities. P5 is the non porous scaffold. A confluent cell layer is formed in all the scaffolds on their surface

and cell in-growth in porous scaffolds is suggested as seen in figure 7.8. Figure 7.5 shows the alamar blue results for the different scaffolds over a 21 day period. It demonstrates that cell growth did occur as there is a significant increase in alamar blue levels over the period examined. Cell in-growth is suggested by growth of cell layer within pores as seen in the **figure 7.8**.

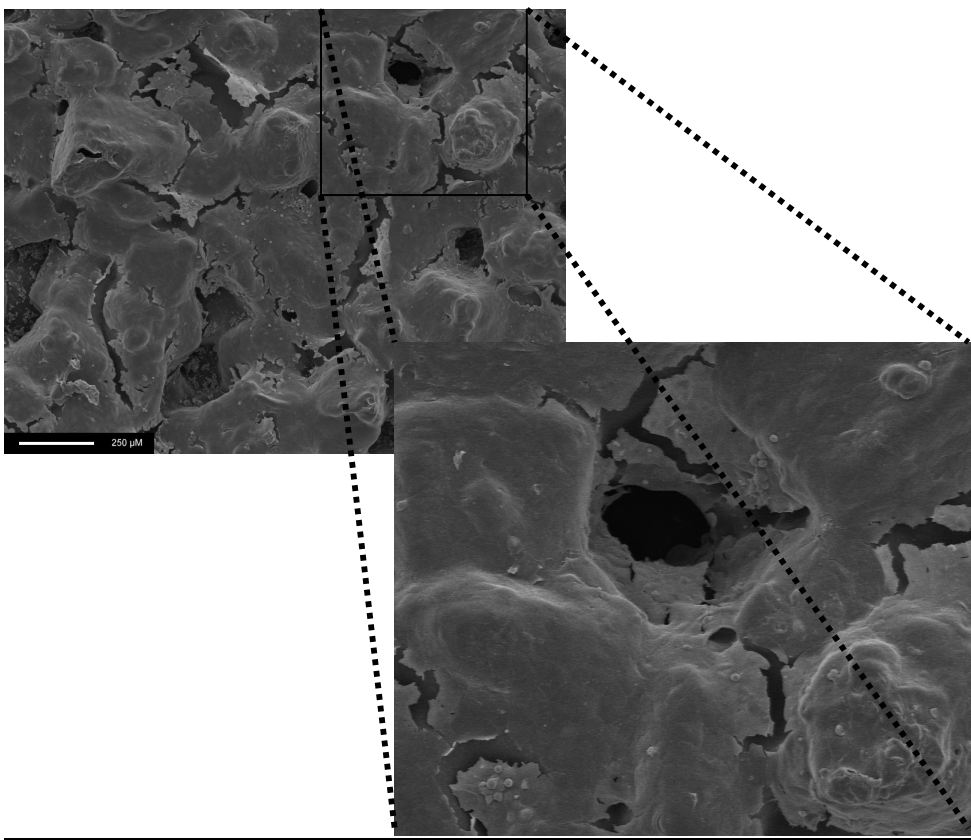


Figure 7.8: Cell layers are seen to encroach in pores from the surface suggesting cell in-growth.

7.4 Discussion

Multipotent stem cells in intestinal layers are believed to regulate intestinal epithelial cell lineages; and can regenerate whole intestinal crypts (Brittan & Wright 2002). However their location and fate is not much identified due to lack of distinct cell markers. Attempts have been made to grow cells on polymeric scaffolds but with little success. They include seeding autologous mesenchymal cells onto collagen scaffold (Alison et al. 2000;Hori et al. 2002); epidermal growth factor induction to grow pluripotent stem cells from peripheral blood to differentiate into epithelial cells (Zhao, Glesne, & Huberman 2003) has not been much successful.

Intestinal epithelial organoid units isolated from neonatal rats (Choi & Vacanti 1997) have been seeded onto PLGA copolymers with some success. Unit-polymer constructs when implanted in rats' omentum have grown cysts with characteristics of intestinal tissue regeneration.

However an ideal cell source for intestinal tissue engineering has not been identified yet. Perhaps stem cells which can be signalled to grow towards intestinal lineage may prove to be the solution to this complex problem.

In this study, we used rat's intestinal epithelial cell (IEC-6) to test our nanocomposite POSS-PCL for supporting cell growth and proliferation. IEC-6 cells have an epithelioid morphology, grow as monolayers of closely opposed polygonal cells, and has a population doubling time of 19-22 hours

(Quaroni et al. 1979). These cells have features of undifferentiated small intestinal crypt cells. We tested cell viability and proliferation onto our scaffolds so that these scaffolds can be used in future *in vivo*.

Our laboratory has already demonstrated the advantages and the successful applications of silica nanocomposite based polyurethanes in producing vascular tissue engineered grafts, such as improved cell adhesion characteristics using a silicon pendant nanocage (Kannan et al. 2005). In this study we assessed whether similar, although biodegradable, nanocomposite POSS-PCL was safe and compatible with *in vitro* cell cultures when intestinal epithelial cells were employed. Another aim of this study was to suggest suitability of alternative biodegradable polymers like POSS-PCL for soft tissue engineering, as opposed to the widely accepted sole use of PGA/PLLA copolymers in small intestinal tissue engineering. PCL in our experience has been less expensive, and easily dissolvable in commonly available organic solvents unlike PGA which is very hard in consistency and requires highly fluorinated solvents such as hexafluoroisopropanol. Poly (ϵ -caprolactone), $-\text{[(CH}_2\text{)}_5\text{COO]}_n-$, is a synthetic biodegradable polyester which has been widely used in controlled-release drug formulations. It has the advantage of leading to neutral degradation products which is in contrast to the acidic degradation products of other commonly used biodegradable polymers such as poly(lactide-co-glycolide) (PLGA) and polylactic acid (PLA). Another feature of PCL is its

slower degradation rate that may be advantageous in applications that require prolonged release times. Our nanocomposite maintains mechanical stability due to nanocages while simultaneously allowing controlled degradation. In this study, we used mainly two pore sizes – 150-250 μm and $< 100 \mu\text{m}$. Apart from the pore size, we also used two different porosities, one in the range of 80% and the other in the range of 40%. Solvent casting and salt leaching resulted in the production of scaffolds with pore size and porosity in the desired range. The pores were interconnected as can be seen on SEM and micro CT. In this study, we assessed the suitability of cell growth on this polymer. All the samples supported cell viability and proliferation and a confluent layer of cell growth was seen on SEM in all samples of seeded cells. We used two dimensional scaffolds in this study. In a three dimensional scaffold, a larger porosity is more likely to positively affect the overall cell growth especially within the deeper layers of the scaffold.

In this study, the approximate cell size was much smaller than the organoid unit employed in the previously mentioned rat studies. The results of cell growth were not better in scaffolds of pore size in the range of 150-250 μm than those in the range of $<100\mu\text{m}$. Rather the later group showed slightly better proliferation than the former. It is assumed that if much larger pore size is used as compared to the cell size, a number of cells may fail to attach when seeded. In the scaffold of mixed porosity, results of cell growth were not significantly different from the ones with either microporous or

macroporous structure alone. IEC proliferation was followed for 21 days on scaffolds made of high and low porosity; and, large and small pore size. All samples examined were able to support both initial cell seeding and prolonged cell growth over the course of the 21 days investigated. Studies of LDH levels demonstrated that there was little initial cell damage. There was no significant difference in cell seeding or growth between any of the samples investigated. These findings were confirmed by the SEM studies which demonstrated cells present on all samples at Day 21. The potential of the POSS-PCL scaffold to support cell seeding and growth was therefore confirmed.

Chapter 8: Discussion

Short bowel syndrome (SBS) is a condition of nutritional malabsorption related to the surgical removal or disease of a large portion of the small intestine. It is generally believed that a loss of more than 70% small intestine causes SBS, which is characterised by diarrhoea, steatorrhoea, severe weight loss, malnutrition, and eventually failure to thrive resulting in a high incidence of mortality both in children and adults. The mainstay of treatment of SBS remains to improve the nutritional status of the patients by enteral (EN) or parenteral (PN) feeding. Home parenteral nutrition (HPN) has been used as a life-saving treatment for patients with intestinal failure. Other methods to treat SBS include surgical procedures like sequential intestinal loop lengthening. For patients dependent on PN, intestinal transplantation is the last hope in the present medical field. However, high mortality rates of about 50% as well as shortage of donor organs limits intestinal transplantation to progress rapidly. An off-the-shelf artificial intestine would definitely prove to be a novel therapy for patients with SBS. Attempts have been made to engineer small intestine, as a definitive solution to the complex problem of SBS, since 1998. In our published review (Gupta et al. 2006); we have highlighted the major advances done so far in this field. Vacanti *et al* have employed rat's intestinal epithelial organoid units as the cell source to be seeded onto porous synthetic biodegradable polymer scaffolds made of Polyglycolic acid (PGA) or copolymer poly(lactic-co-glycolic acid) (PLGA) and achieved considerable success in regenerating neointestinal tissue. Their laboratory was the first to report in 1997,

developing tissue engineered small intestine, in form of cysts having intestinal neomucosa, by the transplantation of organoid units on a polymer scaffold into the omentum of the Lewis rat (Choi & Vacanti 1997). These intestinal epithelial organoid units were isolated from neonatal rats as per the method first developed by Evans et al in 1992 (Evans et al. 1992). Intestinal epithelial organoid units are multicellular units derived from neonatal rat intestine, containing a mesenchymal core surrounded by a polarized intestinal epithelium (Takezawa 2003), and contain all of the cells of a full-thickness intestinal section (Evans et al. 1992; Weiser 1973). These studies used highly porous, synthetic, biodegradable polymer tubes as scaffolds, fabricated from nonwoven sheets of polyglycolic acid (PGA) fibres [with or without coating of poly(L-lactic acid) (PLLA)], with a fibre diameter of 5 μm , mesh thickness of 2 mm, bulk density of 60 mg/cm^3 , porosity of 95% and a mean pore size of 250 μm .

Apart from the above experimental model in rats where organoid units-polymer constructs have been implanted in rat's omentum for neo-intestinal tissue generation, other research groups have used different methods in different animal models aiming towards the same goal. Some have done experiments in dogs when they used 'acellular' collagen sponge scaffold grafting with a silicon tube stent sutured in place of 5 cm intestinal defect (Hori et al. 2002), and some have used porcine small intestinal submucosa (SIS) as a natural scaffold replacing jejunal defects in rabbits (Demirbilek et

al. 2003). Such experiments were done based on the principle of cell migration from adjacent healthy intestinal epithelium, however were limited in their success by lack of muscle layer, contraction of graft, and by unlikelihood of similar cell migration if much longer defects in intestine had to be replaced with a scaffold tube.

So far in most of the studies investigating small intestinal tissue engineering, the main polymer used to fabricate scaffolds has been polyglycolic acid (PGA) or poly(L-lactic acid) (PLLA), or copolymer poly(lactic-co-glycolic acid) (PLGA). The main reason behind their predominant use appears to be firstly, that vast of the studies conducted in this topic has been done by only one group of scientists from University of Massachusetts (Gardner-Thorpe et al. 2003; Grikscheit et al. 2004; Kaihara et al. 1999; Kim et al. 1999c; Vacanti et al. 1988), and secondly, that they are easily commercially available as porous non-woven sheets from the market. Investigating tissue engineering of small intestine still remains in its infancy and is a continually evolving subject. However, other polymers like polycaprolactone have not been investigated, in vitro or in vivo. PGA or PLLA are biodegradable, thermoplastic aliphatic polyesters. PLLA has a crystallinity of around 37%, a glass transition temperature between 50-80 °C and a melting temperature between 173-178 °C. PGA has a glass transition temperature between 35-40 °C and its melting point is reported to be in the range of 225-230 °C. PGA has a crystallinity of around 45-55%, thus rendering insoluble in water. In our

experience, PGA is a very stiff polymer and insoluble in commonly available organic solvents due to its high molecular weight. It is only soluble in selective highly fluorinated solvents like hexafluoroisopropanol.

For some years now, concept of nanocomposites have evolved where one of the phases has one, two, or three dimensions of less than 100 nanometers or structures having nano-scale repeat distances between the different phases that make up the material (Ajayan et al. 2003; Kannan et al. 2005). The main advantage of nanocomposites over conventional polymers is the high surface to volume ratio of nanoparticulates resulting in better physical properties and higher performance than the original matrix.

Our laboratory has developed a biodegradable nanocomposite by incorporating the biostable polyhedral oligomeric silsesquixane (POSS) nanocages into a poly(caprolactone/carbonate)urethane urea. Our nanocomposite is a polyurethane which has a soft segment composed of polycaprolactone (80%) and polycarbonate (20%), and hard segment composed of urea. The polymer is approximately 22% by wt hard segment. Eighty percentage of polycaprolactone diol (mwt) was considered an appropriate initial formula for use as a tissue engineering scaffold for small intestine or cartilage. Such a scaffold would be required to maintain its structural integrity for at least 4–6 months (Raghunath et al. 2008). PCL is relatively slow to degrade as compared to PGA or PLLA, which is an added

advantage in tissue engineering of soft structure like small intestine where a slow degradation is required over a period of few months rather than weeks. It is proposed that caprolactone will provide controlled degradation whilst the POSS nanocages will contribute to the mechanical strength required for a tissue engineering scaffold for soft tissue such as small intestine.

Dental composites containing polyhedral oligomeric silsesquioxanes (POSS) were found to possess improved flexural strength and Young's modulus (Fong et al. 2005). POSS can be incorporated into the hard segment of polyurethane as a pendant side chain. Studies using an octahedral dimeric silsesquioxane in polycarbonate polyurethanes have shown excellent biocompatibility such as cell viability in vitro and the absence of inflammation or capsule formation in vivo (Kannan et al. 2005; Kannan et al. 2006a). Therefore, it is proposed that a biodegradable form of this generation of polyurethane might be an ideal choice as a tissue engineering scaffold for soft tissue. Polycaprolactone is degradable aliphatic polyester which has been extensively reported to demonstrate biocompatibility in vivo. Its degradation by hydrolysis and enzymes is well documented. PCL has been used in several copolymers and polymer blends as the foundation to a tailor-made polymer with specific properties (Raghunath et al. 2008).

In vivo host response of POSS-PCL has not been studied but POSS-PCU (poly(carbonate)urethane urea), the nonbiodegradable counterpart lacking

polycaprolactone, made by the same group, was implanted in sheep for 36 months and showed only minimal inflammation as compared to silicone implants (Kannan et al. 2007).

This composite has been tested for degradation in a separate study (Raghunath et al. 2008) where the nanocomposite (POSS-PCL) was exposed to a selection of accelerated degradative solutions for up to 8 weeks. Degradation of hard and soft segments of the nanocomposite was evident by infra-red spectroscopy in all conditioned samples. POSS nanocage degradation was evident in some oxidative/peroxidative systems accompanied by gross changes in surface topography and significant changes in mechanical properties. The hydrophobic polymer became more hydrophilic in all conditions. This biodegradable nanocomposite demonstrated steady degradation with protection of mechanical properties when exposed to hydrolytic enzymes and plasma protein fractions and exhibited more dramatic degradation by oxidation.

POSS-PCU, the non-degradable counterpart made and patented by our laboratory showed considerable success in vascular tissue engineering when scaffolds for microvascular grafts (Sarkar et al. 2009b), heart valves (Kidane et al. 2009) and aortic stent (Bakhshi et al. 2009) were attempted. Our aim in this work was to investigate characteristics of POSS-PCL, the biodegradable nanocomposite in view of fabricating porous scaffolds for use in small intestinal tissue engineering. We aimed at studying the polymer's

processibility into porous scaffolds, its physical properties, mechanical strength, degradation, biocompatibility and cytocompatibility.

In our first experimental chapter, we used solvent casting/particulate leaching technique to fabricate 2 mm thick sheets of porous scaffolds from POSS-PCL. Scaffolds were obtained in two pore size ranges of 150-250 microns (macroporous) and <150 microns (microporous), and two porosities of 80 and 40 percents. This was achieved by using different salt sizes and salt concentrations in each sample. Both salt sizes were mixed in one of the samples to obtain a mixed pore sized sample. Control sample was prepared without any salt in it. The porosities obtained by calculations as per the formula were in accordance to the percentage of the salt particles used. For example, in sample 1, we used 80% salt by weight, and the mean porosity obtained was 83.9 ± 0.5 .

Scanning electron microscopy showed spherical pores and pore-pore interconnectivity. The pore size was in the expected range as per the size of salt particle. Further pore morphology and interconnectivity was studied using micro CT.

Micro-CT has an advantage of non-destructiveness and 3D image analysis including structural measurement. There is no need for extensive sample preparation, and three-dimensional information can be obtained at high

spatial resolution. The results of Micro CT confirmed the porosity calculated by using simple formulae. A mean value from 100 sections of the sample 1 was found to be $80\% \pm 2\%$, and the pore size varied from 140-250 μm , as expected from the polymer-salt ratios. Good pore interconnectivity was seen in the sample studied.

Mechanical tests were performed in uniaxial tension on a tensometer. Stress-strain relationships were obtained for the samples and graphs were plotted. The porous scaffolds were found to be much less stiff as compared to the nonporous sample. In other words, increasing porosity resulted in decreasing strength of the scaffold. Pore size had no significant influence on stress strain patterns.

Infrared spectra of a porous and nonporous scaffold were recorded on a FTIR spectrometer and the results showed that the basic structure of scaffold remained preserved after particulate leaching.

POSS-PCL was successfully able to be fabricated in highly porous sheets of scaffolds with pore sizes in the desired range, using a simple and inexpensive technique of solvent casting/ particulate leaching. Increasing porosity was found to reduce the strength of scaffolds. Pore-pore interconnectivity was achieved as seen on SEM and micro CT. The basic structure of the scaffold as in the control sample was preserved after solvent

casting/ particulate leaching as seen in FTIR.

In the second experimental chapter, we subjected POSS-PCL to electrospraying, electrospinning, and electroprinting. Electrohydrodynamic jetting is a process where a liquid medium forms a jet and breaks into droplets as it is released at a controlled flow rate through a needle while being exposed to an electric field caused by the existence of a potential difference between the needle and a ground electrode. We achieved this with biopolymers in this experimental work and to the best of our knowledge; this was the first time electrohydrodynamic printing was used to prepare scaffolds for tissue engineering, and was published (Gupta et al. 2007). One advantage of electrohydrodynamic printing over ink-jet printing is that much larger sized nozzles used (750 μm in this work) prevent needle-blockages allowing easier processing of the viscous polymer solutions to finer dimensions.

Initial print-patterning results showed discontinuities in the scaffolds prepared from both polymers. This problem was overcome with the careful adjustment of the distance between the needle tip and the glass slide; however, the printed structures could not be peeled-off from the glass substrate. When polymer was printed onto ethanol kept on the glass slide, instant precipitation of the polymer deposits occurred. Printing on to ethanol was much smoother with stable jetting. A few discontinuities were seen in

the scaffolds prepared and these were caused by unstable jetting probably caused by variations of flow rate. Microscopy of the scaffolds prepared showed that a wavy and coil-like pattern prevailed when polymer was deposited on to ethanol. Moreover, single layer prints with or without ethanol on the glass slides were fragile and did not sustain their structure when peeled off the substrate. When overprinting was performed five times in the presence of ethanol, the resultant scaffold could be peeled-off the glass slide and sustained its structure.

In this study we printed two grid patterns – a smaller grid (window size 250 μ m) and a larger grid (window size 500 μ m). As seen in scanning electron micrographs, the samples were macroporous with a reduction of window size by \sim 30-100 μ m than the designed levels corresponding to the size of the polymer strand forming the window. Another factor affecting smaller than expected window size could be the shrinkage of the scaffold due to drying after printing.

The coiled appearance of the polymers printed on ethanol may be attributed to the instant precipitation of the polymer solution in ethanol. Selecting a liquid medium where precipitation of the polymer is more controlled can be important. Polymer deposits printed directly on the glass slide without ethanol were seen to be straight or wavy but not coiled. When ethanol was used as a layer of substrate over glass slide, this distance had to be

increased to ~1.5mm in order to avoid spreading of the polymer threads away from the main printed line. Also, with ethanol present, the optimum voltage for smooth continuous was found to be slightly higher, in the range of 9.1-10.0. This change could be attributed to an increased electric force required for the polymeric threads to precipitate through ethanol onto the glass slide, and for a higher voltage required to atomise the more viscous biodegradable polymer.

In summary, this was an attempt to print polymer solutions into a pre-designed structure of a scaffold for tissue engineering using electrohydrodynamic technology. Prints on ethanol resulted in almost instantaneous precipitation of the polymer facilitating peeling off the scaffold from the substrate. Scanning electron microscopy of the peeled scaffolds revealed a macroporous structure with polymer strands of diameter 15-50 μm . The polymer strand diameter was found to be dependent on the distance between the needle exit and the substrate, the voltage applied and the viscosity of the polymer solution.

One of the limitations of our experiments was the inability to obtain 0.5-1 mm thick scaffolds because over-printing could not be carried out more than five times in the z direction. Hence these scaffolds could not be tested for in vitro cell compatibility tests. This was directly related to the flow rate of the polymer from the needle. The best scaffolds were obtained when a drop of

polymer was manually pushed to the tip of the needle and atomised. This quantity was sufficient to over-print five times, after which the polymer at the tip of the needle solidified due to evaporation of solvent. More than the optimal amount of polymer solution required for atomisation was delivered even at a minimum infusion rate of 1 $\mu\text{l}/\text{hour}$ of the pump used, making “blobs” of polymer deposit on the scaffolds. This limitation may be overcome by refining the flow rate using better and finer adjustable infusion in future.

In experimental chapter 7, in vitro tests were conducted to assess cyto-compatibility of POSS-PCL scaffolds when rats’ intestinal epithelial cells were cultured onto them. Our aim was to test the cell viability and cell proliferation when grown on scaffolds as substrates of different porosities and different pore sizes. We also aimed at optimising the number of cells required to be seeded before a confluent cell growth could be achieved. Discs of polymer samples were seeded with rat small intestine epithelial cells at a concentration of 2.5×10^6 cells per well in 1 ml cell culture medium. Cells were allowed to attach for 24 hours after which the medium containing unattached cells was removed for lactate dehydrogenase (LDH) analysis to assess initial cell damage. The seeded polymer discs were then transferred to a fresh 24 well plate (to avoid the possibility of measuring cells seeded onto the initial well bottom during the seeding process) and cell metabolism assessed using an Alamar BlueTM assay. Cell metabolism was then further measured at days 3, 6, 10, 14 and 21 post initial seeding. Samples of seeded polymer were also taken for analysis by scanning electron

microscopy at Day 21 as above.

LDH release was examined to look at potential cell damage in the initial seeding period. The differences in LDH levels were actually quite small compared to the levels from the tissue culture plastic seeded cells indicating that little initial cell damage has occurred. When statistical analysis was carried out on the levels for the scaffold samples there was in fact no significant difference ($p > 0.05$) between the scaffold samples and positive control.

The results obtained from the investigation of cell growth and metabolism of IEC cells seeded on the various polymer samples demonstrated that cell growth occurred over the course of the 21 day study. All polymer samples showed a significant reduction in cell metabolism compared to the positive control (as anticipated, tissue culture plastic being optimal for cell growth). However cell growth occurred on each polymer sample over the whole 21 day period suggesting a slower growth rate compared to tissue culture plastic. There was no significant difference between any of the polymers of different pore sizes or porosities, examined over the time period investigated. No further data was collected after 21 days growth as we believed that this was a reasonable period to demonstrate successful cell growth on the scaffolds and wished to collect samples for SEM analysis at this point. The cells grew at a reasonably steady rate over this time period

and the SEM pictures demonstrate that they were approaching confluence at this point.

These findings however did not testify the belief that higher porosity samples should have better cell proliferation. In this study, the approximate cell size was much smaller than the organoid unit employed in the previously mentioned rat studies. It is assumed that if much larger pore size is used as compared to the cell size, a number of cells may fall through the pores when seeding. In the scaffold of mixed porosity, results of cell growth were not significantly different from the ones with either microporous or macroporous structure alone.

We have developed these porous scaffolds from a relatively new and successful nanocomposite POSS-PCL. In future studies, these scaffolds need to be tested in vivo. One of the options remains using the technique by Vacanti et al where these scaffolds can be seeded with juvenile rats' intestinal epithelial organoid units and then implanted in rats' omentum. The cysts thus generated can then be anastomosed to the intestine. The other option can be a direct anastomosis to an isolated segment of intestine and assess cell growth based mainly on the principles of cell migration from the adjacent native mucosa. This is due to remarkable regenerative capability of intestinal mucosa. However both the above options have their limitations. The entire intestinal length of 40 neonatal rats was required to make

organoid unit-polymer constructs sufficient to implant in 10 adult rats. The question of availability of human neonatal intestine in such large amounts seems to be one of the limiting factors. Moreover, it is not clear whether the absorptive capacity is improved through the anastomosed segment of tissue engineered small intestine (TESI) because of added mucosal surface area or whether it is due to slow transit. In the other option, cell migration is believed to occur only for a short distance and appears not practical when a large absorptive surface is required to compensate for the losses from short bowel syndrome. Furthermore, peristalsis in a neo-intestine will always remain an obstacle, as generation of muscle layer with nerves is unlikely to occur.

Despite these obstacles, tissue engineering of small intestine remains a clinically viable option which can prove to be a life saving promise to the suffering patients with short bowel syndrome. However this would require years of continuing efforts from researchers. One of the feasible options to overcome the main hurdle of cell source will be to isolate stem cell which can be linked with biomolecules or cues towards an intestinal lineage. That can prove to be a holy grail. A better understanding of cell-cell and cell-ECM interactions, specific stem cell markers, trophic growth factors, and bioactive scaffolds is required. We hope to scrutinize porous scaffolds developed in this work from a relatively new nanocomposite as a step forward in this complex field of tissue engineering.

Conclusion and Future Recommendations

Nanocomposite polymers are the new generation polymers which have shown advantages over the conventionally used polymers due to high surface to volume ratio of nanoparticulates resulting in better physical properties and higher performance than the original matrix. After successful applications of nondegradable POSS-PCU developed and patented by our laboratory in vascular tissue engineering, POSS was incorporated in biodegradable polymer PCL to develop relatively new nanocomposite POSS-PCL for investigating tissue engineering soft structures like small intestine. POSS-PCL can be successfully subjected to a novel technique of electrohydrodynamic printing which results in desired pore morphology and fibre diameter, however the optimum thickness of 2-3 mm will be difficult to achieve unless much refined machinery is available to control the flow of polymer solution through the needle in an electric field. The same nanocomposite when fabricated using solvent casting/ particulate leaching results in scaffolds with desired porosity, pore size, and pore morphology. When seeded with rats' intestinal epithelial cells in vitro, POSS-PCL scaffolds allow cells to remain viable and proliferate.

In future POSS-PCL scaffolds needs to be scrutinized in vivo in animal models ideally with stem cells if they can be cued to intestinal lineage. One of the relatively recent advances in successfully identifying stem cells in

small intestine and colon by marker gene Lgr5 may prove to be a vital step in isolating intestinal specific stem cells from the crypts of small intestine (Barker et al. 2007). Lgr5 (leucine-rich-repeat-containing G-protein-coupled receptor 5) is a gene selected from intestinal Wnt target genes.

Tissue engineering of small intestine despite some obstacles remains a clinically viable option which will requires years of research and development. POSS-PCL scaffolds developed in this study can prove to be a vital step forward as a fresh impetus in the complex field of tissue engineering.

References

- Agrawal, C.M. & Ray, R.B. 2001. Biodegradable polymeric scaffolds for musculoskeletal tissue engineering. *J.Biomed.Mater.Res.*, 55, (2) 141-150 available from: PM:11255165
- Ajayan, P.M., Schadler, L.S., & Braun, P.V. 2003. *Nanocomposite Science and Technology* Wiley VCH.
- Akki, R., Desai, P., & Abhiraman, A.S. 1999. A framework for morphological evolution vis-a-vis phase transitions in polymer solutions. *Journal of Applied Polymer Science*, 73, (8) 1343-1355 available from: WOS:000081006900001
- Alison, M.R., Poulsom, R., Jeffery, R., Dhillon, A.P., Quaglia, A., Jacob, J., Novelli, M., Prentice, G., Williamson, J., & Wright, N.A. 2000. Hepatocytes from non-hepatic adult stem cells. *Nature*, 406, (6793) 257 available from: PM:10917519
- Badylak, S., Meurling, S., Chen, M., Spievack, A., & Simmons-Byrd, A. 2000. Resorbable bioscaffold for esophageal repair in a dog model. *J.Pediatr.Surg.*, 35, (7) 1097-1103 available from: PM:10917304
- Bakhshi, R., Eaton-Evans, J., Edirisinghe, M., Derbyshire, A., You, Z., Seifalian, A.M., & Hamilton, G. 2009. A novel nanocomposite polymer for the development of a new aortic stent graft. *British Journal of Surgery*, 96, (Supplement 1) 5-5(1)
- Barker, N., van Es, J.H., Kuipers, J., Kujala, P., van den Born, M., Cozijnsen, M., Haegebarth, A., Korving, J., Begthel, H., Peters, P.J., & Clevers, H. 2007. Identification of stem cells in small intestine and colon by marker gene Lgr5. *Nature*, 449, (7165) 1003-1007
- Beath, S.V., Needham, S.J., Kelly, D.A., Booth, I.W., Raafat, F., Buick, R.G., Buckels, J.A., & Mayer, A.D. 1997. Clinical features and prognosis of children assessed for isolated small bowel or combined small bowel and liver transplantation. *J.Pediatr.Surg.*, 32, (3) 459-461 available from: PM:9094018
- Beaulieu, J.F. 1992. Differential expression of the VLA family of integrins along the crypt-villus axis in the human small intestine. *J.Cell Sci.*, 102 (Pt 3), 427-436 available from: PM:1506425
- Bianchi, A. 1980. Intestinal loop lengthening--a technique for increasing small intestinal length. *J.Pediatr.Surg.*, 15, (2) 145-151 available from: PM:7373489

Bjerknes, M. & Cheng, H. 1999. Clonal analysis of mouse intestinal epithelial progenitors. *Gastroenterology*, 116, (1) 7-14 available from: PM:9869596

Bjerknes, M. & Cheng, H. 2005. Gastrointestinal stem cells. II. Intestinal stem cells. *Am.J.Physiol Gastrointest.Liver Physiol*, 289, (3) G381-G387 available from: PM:16093419

Boccaccini, A.R. & Blaker, J.J. 2005. Bioactive composite materials for tissue engineering scaffolds. *Expert.Rev.Med.Devices.*, 2, (3) 303-317

Bokhari, M.A., Akay, G., Zhang, S., & Birch, M.A. 2005. The enhancement of osteoblast growth and differentiation in vitro on a peptide hydrogel-polyHIPE polymer hybrid material. *Biomaterials*, 26, (25) 5198-5208 available from: PM:15792547

British Association for Parenteral and Enteral Nutrition. Home Parenteral Nutrition in the United Kingdom: A Position Paper. 2003.
Ref Type: Generic

Brittan, M. & Wright, N.A. 2002. Gastrointestinal stem cells. *J.Pathol.*, 197, (4) 492-509 available from: PM:12115865

Brook, G. 1998. Quality of life issues: parenteral nutrition to small bowel transplantation--a review. *Nutrition*, 14, (10) 813-816 available from: PM:9785369

Chen, M.K. & Badylak, S.F. 2001. Small bowel tissue engineering using small intestinal submucosa as a scaffold. *J.Surg.Res.*, 99, (2) 352-358 available from: PM:11469910

Chen, V.J. & Ma, P.X. 2004. Nano-fibrous poly(L-lactic acid) scaffolds with interconnected spherical macropores. *Biomaterials.*, 25, (11) 2065-2073

Chen, Y., Zhang, J., Qu, R., Wang, J., & Xie, Y. 1997. An animal experiment on short gut lengthening. *Chin Med.J.(Engl.)*, 110, (5) 354-357 available from: PM:9594302

Choi, R.S., Riegler, M., Pothoulakis, C., Kim, B.S., Mooney, D., Vacanti, M., & Vacanti, J.P. 1998. Studies of brush border enzymes, basement membrane components, and electrophysiology of tissue-engineered neointestine. *J.Pediatr.Surg.*, 33, (7) 991-996 available from: PM:9694083

Choi, R.S. & Vacanti, J.P. 1997. Preliminary studies of tissue-engineered intestine using isolated epithelial organoid units on tubular synthetic biodegradable scaffolds. *Transplant.Proc.*, 29, (1-2) 848-851 available from: PM:9123551

Cloupeau, M. & Prunetfoch, B. 1990. Electrostatic Spraying of Liquids - Main

Functioning Modes. *Journal of Electrostatics*, 25, (2) 165-184 available from: ISI:A1990EK86900004

Croll, T.I., O'Connor, A.J., Stevens, G.W., & Cooper-White, J.J. 2006. A blank slate? Layer-by-layer deposition of hyaluronic acid and chitosan onto various surfaces. *Biomacromolecules.*, 7, (5) 1610-1622 available from: PM:16677046

Demirbilek, S., Kanmaz, T., Ozardali, I., Edali, M.N., & Yucesan, S. 2003. Using porcine small intestinal submucosa in intestinal regeneration. *Pediatr.Surg.Int.*, 19, (8) 588-592 available from: PM:14551711

Doshi, J. & Reneker, D.H. 1995. Electrospinning Process and Applications of Electrospun Fibers. *Journal of Electrostatics*, 35, (2-3) 151-160 available from: WOS:A1995RP03900002

Draghi, L., Resta, S., Pirozzolo, M.G., & Tanzi, M.C. 2005. Microspheres leaching for scaffold porosity control. *J.Mater.Sci.Mater.Med.*, 16, (12) 1093-1097 available from: PM:16362206

Duxbury, M.S., Grikscheit, T.C., Gardner-Thorpe, J., Rocha, F.G., Ito, H., Perez, A., Ashley, S.W., Vacanti, J.P., & Whang, E.E. 2004. Lymphangiogenesis in tissue-engineered small intestine. *Transplantation*, 77, (8) 1162-1166 available from: PM:15114078

Edirisinghe, M.J. & Jayasinghe, S.N. 2004. Electrohydrodynamic atomization of a concentrated nano-suspension. *International Journal of Applied Ceramic Technology*, 1, (2) 140-145 available from: ISI:000228239800004

Ellis-Behnke, R.G., Liang, Y.X., You, S.W., Tay, D.K., Zhang, S., So, K.F., & Schneider, G.E. 2006. Nano neuro knitting: peptide nanofiber scaffold for brain repair and axon regeneration with functional return of vision. *Proc.Natl.Acad.Sci.U.S.A.*, 103, (13) 5054-5059 available from: PM:16549776

Evans, G.S., Flint, N., Somers, A.S., Eyden, B., & Potten, C.S. 1992. The development of a method for the preparation of rat intestinal epithelial cell primary cultures. *J.Cell Sci.*, 101 (Pt 1), 219-231 available from: PM:1569126

Ferrari, G., Cusella-De, A.G., Coletta, M., Paolucci, E., Stornaiuolo, A., Cossu, G., & Mavilio, F. 1998. Muscle regeneration by bone marrow-derived myogenic progenitors. *Science*, 279, (5356) 1528-1530 available from: PM:9488650

Filmon, R., Retailleau-Gaborit, N., Grizon, F., Galloyer, M., Cincu, C., Basle, M.F., & Chappard, D. 2002. Non-connected versus interconnected macroporosity in poly(2-hydroxyethyl methacrylate) polymers. An X-ray

microtomographic and histomorphometric study. *J.Biomater.Sci.Polym.Ed*, 13, (10) 1105-1117 available from: PM:12484487

Fong, H., Dickens, S.H., & Flaim, G.M. 2005. Evaluation of dental restorative composites containing polyhedral oligomeric silsesquioxane methacrylate. *Dent.Mater.*, 21, (6) 520-529 available from: PM:15904694

GananCalvo, A.M., Davila, J., & Barrero, A. 1997. Current and droplet size in the electrospraying of liquids. Scaling laws. *Journal of Aerosol Science*, 28, (2) 249-275 available from: ISI:A1997WC08100006

Gardner-Thorpe, J., Grikscheit, T.C., Ito, H., Perez, A., Ashley, S.W., Vacanti, J.P., & Whang, E.E. 2003. Angiogenesis in tissue-engineered small intestine. *Tissue Eng*, 9, (6) 1255-1261 available from: PM:14670113

Geng, L., Feng, W., Hutmacher, D.W., Wong, Y.S., Loh, H.T., & Fuh, J.Y.H. 2005. Direct writing of chitosan scaffolds using a robotic system. *Rapid Prototyping Journal*, 11, (2) 90-97

Georgeson, K., Halpin, D., Figueroa, R., Vincente, Y., & Hardin, W., Jr. 1994. Sequential intestinal lengthening procedures for refractory short bowel syndrome. *J.Pediatr.Surg.*, 29, (2) 316-320 available from: PM:8176611

Giordano, R.A., Wu, B.M., Borland, S.W., Cima, L.G., Sachs, E.M., & Cima, M.J. 1996. Mechanical properties of dense polylactic acid structures fabricated by three dimensional printing. *J.Biomater.Sci.Polym.Ed.*, 8, (1) 63-75

Grikscheit, T.C., Siddique, A., Ochoa, E.R., Srinivasan, A., Alsberg, E., Hodin, R.A., & Vacanti, J.P. 2004. Tissue-engineered small intestine improves recovery after massive small bowel resection. *Ann.Surg.*, 240, (5) 748-754 available from: PM:15492554

Gupta, A., Dixit, A., Sales, K.M., Winslet, M.C., & Seifalian, A.M. 2006. Tissue engineering of small intestine--current status. *Biomacromolecules.*, 7, (10) 2701-2709 available from: PM:17025341

Gupta, A., Seifalian, A.M., Ahmad, Z., Edirisinghe, M.J., & Winslet, M.C. 2007. Novel electrohydrodynamic printing of nanocomposite biopolymer scaffolds. *Journal of Bioactive and Compatible Polymers*, 22, (3) 265-280 available from: WOS:000247780500002

Hartman, R.P.A., Borra, J.P., Brunner, D.J., Marijnissen, J.C.M., & Scarlett, B. 1999. The evolution of electrohydrodynamic sprays produced in the cone-jet mode, a physical model. *Journal of Electrostatics*, 47, (3) 143-170 available from: ISI:000082571500004

Hartman, R.P.A., Brunner, D.J., Camelot, D.M.A., Marijnissen, J.C.M., &

Scarlett, B. 2000. Jet break-up in electrohydrodynamic atomization in the cone-jet mode. *Journal of Aerosol Science*, 31, (1) 65-95 available from: ISI:000084135400005

Hing, K.A., Annaz, B., Saeed, S., Revell, P.A., & Buckland, T. 2005. Microporosity enhances bioactivity of synthetic bone graft substitutes. *J.Mater.Sci.Mater.Med.*, 16, (5) 467-475 available from: ISI:000228973700015

Hodde, J. 2002. Naturally occurring scaffolds for soft tissue repair and regeneration. *Tissue Eng*, 8, (2) 295-308 available from: PM:12031118

Hollister, S.J. 2005. Porous scaffold design for tissue engineering. *Nature Materials*, 4, (7) 518-524 available from: ISI:000230190900013

Holmes, T.C., de Lacalle, S., Su, X., Liu, G., Rich, A., & Zhang, S. 2000. Extensive neurite outgrowth and active synapse formation on self-assembling peptide scaffolds. *Proc.Natl.Acad.Sci.U.S.A*, 97, (12) 6728-6733 available from: PM:10841570

Hori, Y., Nakamura, T., Kimura, D., Kaino, K., Kurokawa, Y., Satomi, S., & Shimizu, Y. 2002. Experimental study on tissue engineering of the small intestine by mesenchymal stem cell seeding. *J.Surg.Res.*, 102, (2) 156-160 available from: PM:11796013

Hori, Y., Nakamura, T., Matsumoto, K., Kurokawa, Y., Satomi, S., & Shimizu, Y. 2001. Tissue engineering of the small intestine by acellular collagen sponge scaffold grafting. *Int.J.Artif.Organs*, 24, (1) 50-54 available from: PM:11266043

Hou, Q., Grijpma, D.W., & Feijen, J. 2003. Preparation of interconnected highly porous polymeric structures by a replication and freeze-drying process. *J.Biomed.Mater.Res.B Appl.Biomater.*, 67, (2) 732-740 available from: PM:14598400

Hulbert, S.F., Young, F.A., Mathews, R.S., Klawitter, J.J., Talbert, C.D., & Stelling, F.H. 1970. Potential of ceramic materials as permanently implantable skeletal prostheses. *J.Biomed.Mater.Res.*, 4, (3) 433-456 available from: PM:5469185

Hutmacher, D.W., Schantz, T., Zein, I., Ng, K.W., Teoh, S.H., & Tan, K.C. 2001. Mechanical properties and cell cultural response of polycaprolactone scaffolds designed and fabricated via fused deposition modeling. *J.Biomed.Mater.Res.*, 55, (2) 203-216

Hutmacher, D.W., Sittinger, M., & Risbud, M.V. 2004. Scaffold-based tissue engineering: rationale for computer-aided design and solid free-form fabrication systems. *Trends Biotechnol.*, 22, (7) 354-362 available from:

PM:15245908

Jackson, C. & Buchman, A.L. 2005. Advances in the management of short bowel syndrome. *Curr.Gastroenterol.Rep.*, 7, (5) 373-378 available from: PM:16168235

Janson, D.D. 2002. Commentary on "three years clinical experience with intestinal transplantation" and the nutritional implications. *Nutr.Clin.Pract.*, 17, (6) 361-364 available from: PM:16215012

Jaworek, A. & Krupa, A. 1999. Classification of the modes of EHD spraying. *Journal of Aerosol Science*, 30, (7) 873-893 available from: ISI:000081015400005

Jayasinghe, S.N., Edirisinghe, M.J., & De Wilde, T. 2002. A novel ceramic printing technique based on electrostatic atomization of a suspension. *Materials Research Innovations*, 6, (3) 92-95 available from: ISI:000178842300002

Jiang, Y., Jahagirdar, B.N., Reinhardt, R.L., Schwartz, R.E., Keene, C.D., Ortiz-Gonzalez, X.R., Reyes, M., Lenvik, T., Lund, T., Blackstad, M., Du, J., Aldrich, S., Lisberg, A., Low, W.C., Largaespada, D.A., & Verfaillie, C.M. 2002. Pluripotency of mesenchymal stem cells derived from adult marrow. *Nature*, 418, (6893) 41-49 available from: PM:12077603

Kaihara, S., Kim, S., Benvenuto, M., Kim, B.S., Mooney, D.J., Tanaka, K., & Vacanti, J.P. 1999. End-to-end anastomosis between tissue-engineered intestine and native small bowel. *Tissue Eng*, 5, (4) 339-346 available from: PM:10477856

Kannan, R.Y., Salacinski, H.J., Butler, P.E., & Seifalian, A.M. 2005. Polyhedral oligomeric silsesquioxane nanocomposites: the next generation material for biomedical applications. *Acc.Chem.Res.*, 38, (11) 879-884

Kannan, R.Y., Salacinski, H.J., De, G.J., Clatworthy, I., Bozec, L., Horton, M., Butler, P.E., & Seifalian, A.M. 2006a. The antithrombogenic potential of a polyhedral oligomeric silsesquioxane (POSS) nanocomposite. *Biomacromolecules.*, 7, (1) 215-223

Kannan, R.Y., Salacinski, H.J., Ghanavi, J.E., Narula, A., Odlyha, M., Peirovi, H., Butler, P.E., & Seifalian, A.M. 2007. Silsesquioxane nanocomposites as tissue implants. *Plast.Reconstr.Surg.*, 119, (6) 1653-1662 available from: PM:17440337

Kannan, R.Y., Salacinski, H.J., Sales, K.M., Butler, P.E., & Seifalian, A.M. 2006b. The endothelialization of polyhedral oligomeric silsesquioxane nanocomposites: an in vitro study. *Cell Biochem.Biophys.*, 45, (2) 129-136 available from: PM:16757813

Karageorgiou, V. & Kaplan, D. 2005. Porosity of 3D biomaterial scaffolds and osteogenesis. *Biomaterials*, 26, (27) 5474-5491 available from: PM:15860204

Kato, T., Ruiz, P., Thompson, J.F., Eskin, L.B., Weppler, D., Khan, F.A., Pinna, A.D., Nery, J.R., & Tzakis, A.G. 2002. Intestinal and multivisceral transplantation. *World J.Surg.*, 26, (2) 226-237 available from: PM:11865353

Kayahara, T., Sawada, M., Takaishi, S., Fukui, H., Seno, H., Fukuzawa, H., Suzuki, K., Hiai, H., Kageyama, R., Okano, H., & Chiba, T. 2003. Candidate markers for stem and early progenitor cells, Musashi-1 and Hes1, are expressed in crypt base columnar cells of mouse small intestine. *FEBS Lett.*, 535, (1-3) 131-135 available from: PM:12560091

Kelly, D.A. & Buckels, J.A. 1995. The future of small bowel transplantation. *Arch.Dis.Child*, 72, (5) 447-451 available from: PM:7618918

Kidane, A.G., Burriesci, G., Edirisinghe, M., Ghanbari, H., Bonhoeffer, P., & Seifalian, A.M. 2009. A novel nanocomposite polymer for development of synthetic heart valve leaflets. *Acta Biomater.* available from: PM:19497802

Kim, S.S., Kaihara, S., Benvenuto, M., Choi, R.S., Kim, B.S., Mooney, D.J., Taylor, G.A., & Vacanti, J.P. 1999a. Regenerative signals for tissue-engineered small intestine. *Transplant.Proc.*, 31, (1-2) 657-660 available from: PM:10083283

Kim, S.S., Kaihara, S., Benvenuto, M.S., Choi, R.S., Kim, B.S., Mooney, D.J., Taylor, G.A., & Vacanti, J.P. 1999b. Regenerative signals for intestinal epithelial organoid units transplanted on biodegradable polymer scaffolds for tissue engineering of small intestine. *Transplantation*, 67, (2) 227-233 available from: PM:10075585

Kim, S.S., Kaihara, S., Benvenuto, M.S., Choi, R.S., Kim, B.S., Mooney, D.J., & Vacanti, J.P. 1999c. Effects of anastomosis of tissue-engineered neointestine to native small bowel. *J.Surg.Res.*, 87, (1) 6-13 available from: PM:10527698

Kisiday, J., Jin, M., Kurz, B., Hung, H., Semino, C., Zhang, S., & Grodzinsky, A.J. 2002. Self-assembling peptide hydrogel fosters chondrocyte extracellular matrix production and cell division: implications for cartilage tissue repair. *Proc.Natl.Acad.Sci.U.S.A*, 99, (15) 9996-10001 available from: PM:12119393

Korbling, M., Estrov, Z., & Champlin, R. 2003. Adult stem cells and tissue repair. *Bone Marrow Transplant.*, 32 Suppl 1, S23-S24 available from: PM:12931235

Korbling, M., Katz, R.L., Khanna, A., Ruifrok, A.C., Rondon, G., Albitar, M.,

Champlin, R.E., & Estrov, Z. 2002. Hepatocytes and epithelial cells of donor origin in recipients of peripheral-blood stem cells. *N.Engl.J.Med.*, 346, (10) 738-746 available from: PM:11882729

Krause, D.S., Theise, N.D., Collector, M.I., Henegariu, O., Hwang, S., Gardner, R., Neutzel, S., & Sharkis, S.J. 2001. Multi-organ, multi-lineage engraftment by a single bone marrow-derived stem cell. *Cell*, 105, (3) 369-377 available from: PM:11348593

Lee, S.J., Lee, I.W., Lee, Y.M., Lee, H.B., & Khang, G. 2004. Macroporous biodegradable natural/synthetic hybrid scaffolds as small intestine submucosa impregnated poly(D,L-lactide-co-glycolide) for tissue-engineered bone. *J.Biomater.Sci.Polym.Ed*, 15, (8) 1003-1017 available from: PM:15461186

Leong, K.F., Cheah, C.M., & Chua, C.K. 2003. Solid freeform fabrication of three-dimensional scaffolds for engineering replacement tissues and organs. *Biomaterials*, 24, (13) 2363-2378

Liao, C.J., Chen, C.F., Chen, J.H., Chiang, S.F., Lin, Y.J., & Chang, K.Y. 2002. Fabrication of porous biodegradable polymer scaffolds using a solvent merging/particulate leaching method. *J.Biomed.Mater.Res.*, 59, (4) 676-681 available from: PM:11774329

Mao, J.S., Liu, H.F., Yin, Y.J., & Yao, K.D. 2003. The properties of chitosan-gelatin membranes and scaffolds modified with hyaluronic acid by different methods. *Biomaterials*, 24, (9) 1621-1629 available from: PM:12559822

Mayr, J.M., Schober, P.H., Weissensteiner, U., & Hollwarth, M.E. 1999. Morbidity and mortality of the short-bowel syndrome. *Eur.J.Pediatr.Surg.*, 9, (4) 231-235 available from: PM:10532264

McGlohorn, J.B., Holder, W.D., Grimes, L.W., Thomas, C.B., & Burg, K.J.L. 2004. Evaluation of smooth muscle cell response using two types of porous polylactide scaffolds with differing pore topography. *Tissue Engineering*, 10, (3-4) 505-514 available from: WOS:000221105000020

McIntire, L. V., Greisler, H. P., Griffith, L., Johnson, P. C., Mooney, D. J., Mrksich, M., Parenteau, N. L., & Smith, D. 2002, *WTEC panel report on Tissue Engineering Research*.

Messing, B., Crenn, P., Beau, P., Boutron-Ruault, M.C., Rambaud, J.C., & Matuchansky, C. 1999. Long-term survival and parenteral nutrition dependence in adult patients with the short bowel syndrome. *Gastroenterology*, 117, (5) 1043-1050 available from: PM:10535866

Michna, S., Wu, W., & Lewis, J.A. 2005. Concentrated hydroxyapatite inks for direct-write assembly of 3-D periodic scaffolds. *Biomaterials*, 26, (28)

5632-5639 available from: WOS:000229492200007

Mikos, A.G., Bao, Y., Cima, L.G., Ingber, D.E., Vacanti, J.P., & Langer, R. 1993. Preparation of poly(glycolic acid) bonded fiber structures for cell attachment and transplantation. *J.Biomed.Mater.Res.*, 27, (2) 183-189 available from: PM:8382203

Mikos, A.G. & Temenoff, J.S. 2002. Formation of highly porous biodegradable scaffolds for tissue engineering. *Electronic Journal of Biotechnology*, 3, (2)

Mikos, A.G., Thorsen, A.J., Czerwonka, L.A., Bao, Y., Langer, R., Winslow, D.N., & Vacanti, J.P. 1994. Preparation and Characterization of Poly(L-Lactic Acid) Foams. *Polymer*, 35, (5) 1068-1077 available from: WOS:A1994MZ99700023

Mooney, D.J., Baldwin, D.F., Suh, N.P., Vacanti, J.P., & Langer, R. 1996a. Novel approach to fabricate porous sponges of poly(D,L-lactic-co-glycolic acid) without the use of organic solvents. *Biomaterials*, 17, (14) 1417-1422 available from: PM:8830969

Mooney, D.J., Mazzoni, C.L., Breuer, C., McNamara, K., Hern, D., Vacanti, J.P., & Langer, R. 1996b. Stabilized polyglycolic acid fibre-based tubes for tissue engineering. *Biomaterials*, 17, (2) 115-124 available from: PM:8624388

Moore, M.J., Jabbari, E., Ritman, E.L., Lu, L., Currier, B.L., Windebank, A.J., & Yaszemski, M.J. 2004. Quantitative analysis of interconnectivity of porous biodegradable scaffolds with micro-computed tomography. *J.Biomed.Mater.Res.A*, 71, (2) 258-267 available from: PM:15376269

Moreno, J.M., Planas, M., Lecha, M., Virgili, N., Gomez-Enterria, P., Ordóñez, J., de la, C.C., Apezetxea, A., Marti, E., Garcia Luna, P.P., Forga, M.T., Perez de la, C.A., Munoz, A., Bayo, P., Rodriguez, A., Chamorro, J., Bonada, A., Luengo, L.M., Pedron, C., & Pares, R.M. 2005. [The year 2002 national register on home-based parenteral nutrition]. *Nutr.Hosp.*, 20, (4) 249-253 available from: PM:16045126

Murphy, W.L., Dennis, R.G., Kileny, J.L., & Mooney, D.J. 2002. Salt fusion: an approach to improve pore interconnectivity within tissue engineering scaffolds. *Tissue Eng.*, 8, (1) 43-52

Nam, Y.S., Yoon, J.J., & Park, T.G. 2000. A novel fabrication method of macroporous biodegradable polymer scaffolds using gas foaming salt as a porogen additive. *J.Biomed.Mater.Res.*, 53, (1) 1-7

Narmoneva, D.A., Oni, O., Sieminski, A.L., Zhang, S., Gertler, J.P., Kamm, R.D., & Lee, R.T. 2005. Self-assembling short oligopeptides and the

promotion of angiogenesis. *Biomaterials*, 26, (23) 4837-4846 available from: PM:15763263

Okamoto, R., Yajima, T., Yamazaki, M., Kanai, T., Mukai, M., Okamoto, S., Ikeda, Y., Hibi, T., Inazawa, J., & Watanabe, M. 2002. Damaged epithelia regenerated by bone marrow-derived cells in the human gastrointestinal tract. *Nat.Med.*, 8, (9) 1011-1017 available from: PM:12195435

Organ, G.M., Mooney, D.J., Hansen, L.K., Schloo, B., & Vacanti, J.P. 1992. Transplantation of enterocytes utilizing polymer-cell constructs to produce a neointestine. *Transplant.Proc.*, 24, (6) 3009-3011 available from: PM:1334603

Organ, G.M., Mooney, D.J., Hansen, L.K., Schloo, B., & Vacanti, J.P. 1993. Enterocyte transplantation using cell-polymer devices to create intestinal epithelial-lined tubes. *Transplant.Proc.*, 25, (1 Pt 2) 998-1001 available from: PM:8442297

Perez, A., Grikscheit, T.C., Blumberg, R.S., Ashley, S.W., Vacanti, J.P., & Whang, E.E. 2002. Tissue-engineered small intestine: ontogeny of the immune system. *Transplantation.*, 74, (5) 619-623

Petersen, B.E., Bowen, W.C., Patrene, K.D., Mars, W.M., Sullivan, A.K., Murase, N., Boggs, S.S., Greenberger, J.S., & Goff, J.P. 1999. Bone marrow as a potential source of hepatic oval cells. *Science*, 284, (5417) 1168-1170 available from: PM:10325227

Phongying, S., Aiba, S.I., & Chirachanchai, S. 2006. A novel soft and cotton-like chitosan-sugar nanoscaffold. *Biopolymers* available from: PM:16794997

Pittenger, M.F., Mackay, A.M., Beck, S.C., Jaiswal, R.K., Douglas, R., Mosca, J.D., Moorman, M.A., Simonetti, D.W., Craig, S., & Marshak, D.R. 1999. Multilineage potential of adult human mesenchymal stem cells. *Science*, 284, (5411) 143-147 available from: PM:10102814

Poulsom, R., Forbes, S.J., Hodivala-Dilke, K., Ryan, E., Wyles, S., Navaratnarajah, S., Jeffery, R., Hunt, T., Alison, M., Cook, T., Pusey, C., & Wright, N.A. 2001. Bone marrow contributes to renal parenchymal turnover and regeneration. *J.Pathol.*, 195, (2) 229-235 available from: PM:11592103

Puntis, J.W. 1998. The economics of home parenteral nutrition. *Nutrition*, 14, (10) 809-812 available from: PM:9785368

Putnam, A.J. & Mooney, D.J. 1996. Tissue engineering using synthetic extracellular matrices. *Nat.Med.*, 2, (7) 824-826 available from: PM:8673932

Quaroni, A., Wands, J., Trelstad, R., & Isselbacher, K. 1979. Epithelioid cell cultures from rat small intestine. Characterization by morphologic and

immunologic criteria. *J Cell Biol*, 80, (2) 248-265

Raghunath, J., Georgiou, G., Armitage, D., Nazhat, S.N., Sales, K.M., Butler, P.E., & Seifalian, A.M. 2008. Degradation studies on biodegradable nanocomposite based on polycaprolactone/polycarbonate (80:20%) polyhedral oligomeric silsesquioxane. *J.Biomed.Mater.Res.A* available from: PM:19051308

Ramsanahie, A., Duxbury, M.S., Grikscheit, T.C., Perez, A., Rhoads, D.B., Gardner-Thorpe, J., Ogilvie, J., Ashley, S.W., Vacanti, J.P., & Whang, E.E. 2003. Effect of GLP-2 on mucosal morphology and SGLT1 expression in tissue-engineered neointestine. *Am.J.Physiol Gastrointest.Liver Physiol*, 285, (6) G1345-G1352 available from: PM:12919941

Ray, E.C., Avissar, N.E., Vukcevic, D., Toia, L., Ryan, C.K., Berlanga-Acosta, J., & Sax, H.C. 2003. Growth hormone and epidermal growth factor together enhance amino acid transport systems B(0,+) and A in remnant small intestine after massive enterectomy. *J.Surg.Res.*, 113, (2) 257-263 available from: PM:12957138

Rayleigh, L. 1878. On the instability of jets. *Proc.London Math Soc*, s1-10, 4-13

Reya, T. & Clevers, H. 2005. Wnt signalling in stem cells and cancer. *Nature*, 434, (7035) 843-850 available from: PM:15829953

Rosso, F., Giordano, A., Barbarisi, M., & Barbarisi, A. 2004. From cell-ECM interactions to tissue engineering. *J.Cell Physiol*, 199, (2) 174-180 available from: PM:15039999

Safford, S.D., Freemerman, A.J., Safford, K.M., Bentley, R., & Skinner, M.A. 2005. Longitudinal mechanical tension induces growth in the small bowel of juvenile rats. *Gut*, 54, (8) 1085-1090 available from: PM:15840689

Sander, E.A., Alb, A.M., Nauman, E.A., Reed, W.F., & Dee, K.C. 2004. Solvent effects on the microstructure and properties of 75/25 poly(D,L-lactide-co-glycolide) tissue scaffolds
1. *Journal of Biomedical Materials Research Part A*, 70A, (3) 506-513 available from: ISI:000223281100017

Santiago, L.Y., Nowak, R.W., Peter, R.J., & Marra, K.G. 2006. Peptide-surface modification of poly(caprolactone) with laminin-derived sequences for adipose-derived stem cell applications. *Biomaterials*, 27, (15) 2962-2969 available from: PM:16445976

Sarkar, S., Burriesci, G., Wojcik, A., Aresti, N., Hamilton, G., & Seifalian, A.M. 2009a. Manufacture of small calibre quadruple lamina vascular bypass grafts using a novel automated extrusion-phase-inversion method and

nanocomposite polymer. *J.Biomech.*, 42, (6) 722-730 available from: PM:19249786

Sarkar, S., Burriesci, G., Wojcik, A., Aresti, N., Hamilton, G., & Seifalian, A.M. 2009b. Manufacture of small calibre quadruple lamina vascular bypass grafts using a novel automated extrusion-phase-inversion method and nanocomposite polymer. *J.Biomech.*, 42, (6) 722-730 available from: PM:19249786

Schleicher, I., Parker, A., Leavesley, D., Crawford, R., Upton, Z., & Xiao, Y. 2005. Surface modification by complexes of vitronectin and growth factors for serum-free culture of human osteoblasts. *Tissue Eng*, 11, (11-12) 1688-1698 available from: PM:16411814

Shastri, V.P., Martin, I., & Langer, R. 2000. Macroporous polymer foams by hydrocarbon templating. *Proceedings of the National Academy of Sciences of the United States of America*, 97, (5) 1970-1975 available from: WOS:000085633200005

Shieh, S.J. & Vacanti, J.P. 2005. State-of-the-art tissue engineering: from tissue engineering to organ building. *Surgery*, 137, (1) 1-7 available from: PM:15614274

Shin, M., Hohman, M.M., Brenner, G.C., & Rutledge, A. 2001. A whipping fluid jet generates submicron polymer fibres. *Appl.Phys.Lett.*, 78, 1149-1151

Sigmund, W., Yuh, J., Park, H., Maneeratana, V., Pyrgiotakis, G., Daga, A., Taylor, J., & Nino, J.C. 2006. Processing and structure relationships in electrospinning of ceramic fiber systems. *Journal of the American Ceramic Society*, 89, (2) 395-407 available from: ISI:000234740600001

Stappenbeck, T.S., Mills, J.C., & Gordon, J.I. 2003. Molecular features of adult mouse small intestinal epithelial progenitors. *Proc.Natl.Acad.Sci.U.S.A*, 100, (3) 1004-1009 available from: PM:12552106

Taipale, J. & Keski-Oja, J. 1997. Growth factors in the extracellular matrix. *FASEB J.*, 11, (1) 51-59 available from: PM:9034166

Takezawa, T. 2003. A strategy for the development of tissue engineering scaffolds that regulate cell behavior. *Biomaterials.*, 24, (13) 2267-2275

Tavakkolizadeh, A., Berger, U.V., Stephen, A.E., Kim, B.S., Mooney, D., Hediger, M.A., Ashley, S.W., Vacanti, J.P., & Whang, E.E. 2003. Tissue-engineered neomucosa: morphology, enterocyte dynamics, and SGLT1 expression topography. *Transplantation*, 75, (2) 181-185 available from: PM:12548119

Taylor, G.I. 1964. Disintegration of Water Droplets in an Electric Field.

Proc.Roy.Soc, 280, 383-397

Teng, W.D., Huneiti, Z.A., Machowski, W., Evans, J.R.G., Edirisinghe, M.J., & Balachandran, W. 1997. Towards particle-by-particle deposition of ceramics using using electrostatic atomization. *J.Mater.Sci.Lett.*, 16, 1017-1019

Theise, N.D., Nimmakayalu, M., Gardner, R., Illei, P.B., Morgan, G., Teperman, L., Henegariu, O., & Krause, D.S. 2000. Liver from bone marrow in humans. *Hepatology*, 32, (1) 11-16 available from: PM:10869283

Thompson, J.S., DiBaise, J.K., Iyer, K.R., Yeats, M., & Sudan, D.L. 2005. Postoperative short bowel syndrome. *J.Am.Coll.Surg.*, 201, (1) 85-89 available from: PM:15978448

Thomson, R.C., Yaszemski, M.J., Powers, J.M., & Mikos, A.G. 1998. Hydroxyapatite fiber reinforced poly(alpha-hydroxy ester) foams for bone regeneration. *Biomaterials*, 19, (21) 1935-1943 available from: PM:9863527

Vacanti, J.P., Morse, M.A., Saltzman, W.M., Domb, A.J., Perez-Atayde, A., & Langer, R. 1988. Selective cell transplantation using bioabsorbable artificial polymers as matrices. *J.Pediatr.Surg.*, 23, (1 Pt 2) 3-9 available from: PM:2895175

Voytik-Harbin, S.L., Brightman, A.O., Kraine, M.R., Waisner, B., & Badylak, S.F. 1997. Identification of extractable growth factors from small intestinal submucosa. *J.Cell Biochem.*, 67, (4) 478-491 available from: PM:9383707

Wake, M.C., Gupta, P.K., & Mikos, A.G. 1996. Fabrication of pliable biodegradable polymer foams to engineer soft tissues. *Cell Transplant.*, 5, (4) 465-473 available from: PM:8800514

Wales, P.W., de, S.N., Kim, J.H., Lecce, L., Sandhu, A., & Moore, A.M. 2005. Neonatal short bowel syndrome: a cohort study. *J.Pediatr.Surg.*, 40, (5) 755-762 available from: PM:15937809

Wang, D.Z., Jayasinghe, S.N., & Edirisinghe, M.J. 2005a. High resolution print-patterning of a nano-suspension. *Journal of Nanoparticle Research*, 7, (2) 301-306 available from: ISI:000230141900017

Wang, D.Z., Jayasinghe, S.N., & Edirisinghe, M.J. 2005b. Instrument for electrohydrodynamic print-patterning three-dimensional complex structures. *Review of Scientific Instruments*, 76, (7) available from: ISI:000230436600051

Wang, S., Cui, W., & Bei, J. 2005c. Bulk and surface modifications of polylactide. *Anal.Bioanal.Chem.*, 381, (3) 547-556 available from: PM:15672238

- Wang, Z.Q., Watanabe, Y., & Toki, A. 2003. Experimental assessment of small intestinal submucosa as a small bowel graft in a rat model. *J.Pediatr.Surg.*, 38, (11) 1596-1601 available from: PM:14614707
- Weiser, M.M. 1973. Intestinal epithelial cell surface membrane glycoprotein synthesis. I. An indicator of cellular differentiation. *J.Biol.Chem.*, 248, (7) 2536-2541 available from: PM:4698230
- Whang, K., Thomas, C.H., Healy, K.E., & Nuber, G. 1995. A Novel Method to Fabricate Bioabsorbable Scaffolds. *Polymer*, 36, (4) 837-842 available from: WOS:A1995QK67100021
- Woodard, J.R., Hildore, A.J., Lan, S.K., Park, C.J., Morgan, A.W., Eurell, J.A.C., Clark, S.G., Wheeler, M.B., Jamison, R.D., & Johnson, A.J.W. 2007. The mechanical properties and osteoconductivity of hydroxyapatite bone scaffolds with multi-scale porosity. *Biomaterials*, 28, (1) 45-54 available from: ISI:000242424900006
- Yamamoto, Y., Nakamura, T., Shimizu, Y., Matsumoto, K., Takimoto, Y., Kiyotani, T., Sekine, T., Ueda, H., Liu, Y., & Tamura, N. 1999. Intrathoracic esophageal replacement in the dog with the use of an artificial esophagus composed of a collagen sponge with a double-layered silicone tube. *J.Thorac.Cardiovasc.Surg.*, 118, (2) 276-286 available from: PM:10425001
- Yang, S., Leong, K.F., Du, Z., & Chua, C.K. 2001. The design of scaffolds for use in tissue engineering. Part I. Traditional factors. *Tissue Eng.*, 7, (6) 679-689
- Young, T.-H. & Chen, L.-W. 1995. Pore formation mechanism of membranes from phase inversion process. *Desalination*, 103, 233-247
- Zein, I., Hutmacher, D.W., Tan, K.C., & Teoh, S.H. 2002. Fused deposition modeling of novel scaffold architectures for tissue engineering applications. *Biomaterials*, 23, (4) 1169-1185 available from: PM:11791921
- Zeleny, B.J. 1917. Instability of electrified liquid surfaces. *Phys Rev*, 10, 1-6
- Zhang, H.B. & Edirisinghe, M.J. 2006. Electrospinning zirconia fiber from a suspension. *Journal of the American Ceramic Society*, 89, (6) 1870-1875 available from: WOS:000237812100015
- Zhang, H.B., Edirisinghe, M.J., & Jayasinghe, S.N. 2006a. Flow behaviour of dielectric liquids in an electric field. *Journal of Fluid Mechanics*, 558, 103-111 available from: WOS:000239377300006
- Zhang, H.B., Jayasinghe, S.N., & Edirisinghe, M.J. 2006b. Electrically forced microthreading of highly viscous dielectric liquids. *Journal of Electrostatics*, 64, (6) 355-360 available from: WOS:000237752900002

Zhang, S. 2002. Emerging biological materials through molecular self-assembly. *Biotechnol.Adv.*, 20, (5-6) 321-339 available from: PM:14550019

Zhao, Y., Glesne, D., & Huberman, E. 2003. A human peripheral blood monocyte-derived subset acts as pluripotent stem cells. *Proc.Natl.Acad.Sci.U.S.A*, 100, (5) 2426-2431 available from: PM:12606720

Zhu, Y., Chian, K.S., Chan-Park, M.B., Mhaisalkar, P.S., & Ratner, B.D. 2006. Protein bonding on biodegradable poly(L-lactide-co-caprolactone) membrane for esophageal tissue engineering. *Biomaterials*, 27, (1) 68-78 available from: PM:16005962

Publications

1. Gupta A, Dixit A, Sales KM, Winslet MC, Seifalian AM. 2006. Tissue engineering of small intestine--current status. *Biomacromolecules* 7:2701-2709.
2. Gupta A, Seifalian AM, Ahmad Z, Edirisinghe MJ, Winslet MC. 2007. Novel electrohydrodynamic printing of nanocomposite biopolymer scaffolds. *Journal of Bioactive and Compatible Polymers* 22:265-280.
3. Gupta A, Vara DS, Punshon G, Sales KM, Winslet MC, Seifalian AM. 2009. In vitro small intestinal epithelial cell growth on a nanocomposite polycaprolactone scaffold. *Biotechnol Appl Biochem* 54:221-229.